



**SIMULATIVE AND REAL TIME STABILIZATION AND CONTROL OF  
THE CART-PENDULUM SYSTEM**

**FIDEN TAHSEEN SEDEEQ**

**AUGUST 2016**

**SIMULATIVE AND REAL TIME STABILIZATION AND CONTROL OF  
THE CART-PENDULUM SYSTEM**

**A THESIS SUBMITTED TO  
THE GRADUATE SCHOOL OF NATURAL AND APPLIED  
SCIENCES OF  
ÇANKAYA UNIVERSITY**

**BY  
FIDEN TAHSEEN SEDEEQ**

**IN PARTIAL FULFILLMENT OF THE REQUIREMENTS FOR THE  
DEGREE OF  
MASTER OF SCIENCE  
IN  
THE DEPARTMENT OF  
ELECTRONIC AND COMMUNICATION ENGINEERING**

**AUGUST 2016**

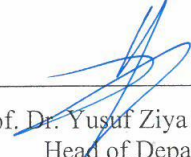
Title of the Thesis: **SIMULATIVE AND REAL TIME STABILIZATION AND CONTROL OF THE CART-PENDULUM SYSTEM**

Submitted by **FIDAN TAHSEEN SEDEEQ**


Approval of the Graduate School of Natural and Applied Sciences, Çankaya University.

  
Prof. Dr. Halil Tanyer EYYUBOĞLU  
Director

I certify that this thesis satisfies all the requirements as a thesis for the degree of Master of Science.

  
Prof. Dr. Yusuf Ziya UMUL  
Head of Department

This is to certify that we have read this thesis and that in our opinion it is fully adequate, in scope and quality, as a thesis for the degree of Master of Science.

  
Asst. Prof. Dr. Ulaş BELDEK  
Supervisor

**Examination Date: 19.08.2016**

**Examining Committee Members**

Assoc. Prof. Dr. Orhan GAZI

(Çankaya Univ.)

Asst. Prof. Dr. Ulaş BELDEK

(Çankaya Univ.)

Asst. Prof. Dr. Tolga İNAN

(TED Univ.)



## STATEMENT OF NON-PLAGIARISM PAGE

I hereby declare that all information in this document has been obtained and presented in accordance with academic rules and ethical conduct. I also declare that, as required by these rules and conduct, I have fully cited and referenced all material and results that are not original to this work.

Name, Last Name : Fidan Tahseen SEDEEQ

Signature :



Date : 19.08.2016

## ABSTRACT

### SIMULATIVE AND REAL TIME STABILIZATION AND ONTROL OF THE CART-PENDULUM SYSTEM

Fidan, Tahseen SEDEEQ

M.Sc., Department of ELECTRONIC AND COMUNICATION ENGINEERING

Supervisor: Asst. Prof. Dr. Ulaş BELDEK

AUGUST 2016,81 pages

The cart-pendulum system has a non-linear dynamics and its mathematical model is expressed by differential equations with high order. Besides, at some control applications this system should be stabilized and controlled around unstable equilibrium points. Due to these characteristics, the cart pendulum system is a good test-bed to design and implement different control algorithms in both simulation and real time applications. In this thesis, applicability of different control algorithms to stabilize and control the cart-pendulum system in inverted pendulum mode is analyzed. Primarily the system structure is simulated and a state feedback control strategy is implemented for this mission. However, the state feedback control strategy is unsuccessful in the real time application. For this reason, in the real time application, a system identification step is required as it is observed that there is a dissonance in the real system dynamics and mathematical model of the system. The system identification step has specified the valuable information about the approximate linearized system structure and this information is used to design new and competent controllers to accomplish the stabilization and control missions in real time. The controllers are designed based on root locus plots of the identified system. After the controllers are designed, their capabilities are tested in various real time applications.

**Key Words** : Cart-pendulum System, System Identification, Proportional-integral-derivative Controllers, Root Locus, State Feedback, Linearization.

## ÖZ

### ARABALI SARKAÇ SİSTEMİNİN BENZETİMSSEL VE GERÇEK ZAMANLI DENGELENMESİ VE KONTROLÜ

Fidan Tahseen SEDEEQ

Yüksek Lisans, Makine Mühendisliği Anabilim Dalı

Tez Yöneticisi: Asst. Prof. Dr. Ulaş BELDEK

AĞUSTOS 2016, 81 sayfa

Arabalı sarkaç sisteminin doğrusal olmayan bir dinamiği bulunmaktadır ve matematiksel modeli yüksek dereceli türevsel denklemlerle ifade edilmektedir. Ayrıca bu sistemin, bazı kontrol uygulamalarında kararsız denge noktalarında dengelenmesi ve kontrol edilmesi gerekmektedir. Bu özelliklerinden dolayı, arabalı ters sarkaç sistemi hem benzetimlerde hem de gerçek zamanlı uygulamalarda kontrol algoritmalarının tasarlanması ve uygulanması için iyi bir sınamaya ortamıdır. Bu tezde, arabalı sarkaç sisteminin ters sarkaç kipinde dengelenmesi ve kontrol edilmesi için farklı kontrol algoritmalarının uygulanabilirliği analiz edilmiştir. Bu amaç doğrultusunda, ilk olarak, sistemin yapısının benzetimi yapılmış ve durum geri beslemesi kontrol stratejisi benzetimde uygulanmıştır. Buna karşın, durum geri beslemesi kontrol stratejisi gerçek zamanlı uygulamada başarısız olmuştur. Bu nedenle, gerçek zamanlı sistemin dinamiği ve sistemin matematiksel modelinin arasındaki uyumsuzluktan dolayı, gerçek zamanlı uygulamada bir sistem tanımlama adımına ihtiyaç duyulmuştur. Sistem tanımlama adımı yaklaşık doğrusal sistem yapısı hakkında değerli bilgileri tayin etmiş ve bu bilgiler gerçek zamanlı uygulamalarda dengeleme ve kontrol görevlerinin başarıyla sonuçlandırması amacıyla yeni ve yetkin denetleyicilerin tasarlanması için kullanılmıştır. Denetleyiciler, tanımlanan sistemin kök yer eğrisi çizimlerine dayanarak tasarlanmıştır. Denetleyiciler tasarlandıktan sonra kabiliyetleri farklı gerçek zamanlı uygulamalarda sınanmıştır.

**Anahtar Kelimeler:** Arabalı Sarkaç Sistemi, Sistem Tanımlama, Oransal-İntegral-Türevsel Denetleyiciler, Kök Yer Eğrisi, Durum Geri Beslemesi, Doğru sallaştırma.

## **ACKNOWLEDGEMENTS**

I would like to express my sincere gratitude to Asst. Prof. Dr. Ulaş BELDEK for his supervision, special guidance, suggestions, and encouragement through the development of this thesis.

It is a pleasure to express my special thanks to my family for their valuable support.

## TABLE OF CONTENTS

STATEMENT OF NON PLAGIARISM.....	iii
ABSTRACT.....	v
ÖZ.....	iv
ACKNOWLEDGEMENTS.....	vi
TABLE OF CONTENTS.....	vii
LIST OF FIGURES.....	ix
LIST OF TABLES.....	xiii
LIST OF ABBREVIATIONS.....	xiv

### CHAPTERS

1. INTRODUCTION.....	1
2. SYSTEM DSCRIPTION .....	5
2.1. System Description.....	5
2.2. The Pendulum- Cart System Components.....	6
2.3. System Dynamics.....	7
2.4. The System Parametes .....	11
3. LINEARIZATION, EQUILIBRIUM POINTS AND CONTROL STRATEGIES.....	12
3.1. System Structure .....	12
3.2. Equilibrium Points.....	12
3.3. Linearization of the Model.....	13
3.4. Transfer Functions.....	14
3.5. State-Space Representation of the Linearized Model.....	16
3.6. Control Strategies.....	17
3.6.1. Swing-Up Control.....	18
3.6.2. Stabilization Control.....	19
4. SIMULATION MODEL.....	20
4.1. Design Strategy.....	20



4.2.	Simulation Sub-Blocks.....	20
4.2.1.	Non-linear Mathematical Model of the Cart-Pendulum System Sub-Block.....	20
4.2.2.	Stabilization with State Feedback Sub-Block.....	22
4.2.3.	Set Point Selection Sub-Block.....	29
4.2.4.	Swing Up Control with Extra PI Position Control Sub-Block.....	30
4.2.4.1.	Applied force direction Function.....	31
4.2.4.2.	Lower Zone Upper Zone Function.....	33
4.2.4.3.	Upright Position Detection Function.....	33
4.2.4.4.	Extra PI Control for Cart Position.....	34
4.2.4.5.	Swing up Stage Strategy.....	34
4.3.	Complete Control Strategy.....	35
5.	REAL- TIME SYSTEM IDENTIFICATION AND CONTROLLER DESIGN.....	39
5.1.	Running Real Time Model.....	39
5.2.	System Identification.....	46
5.3.	Controller Design.....	51
5.2.1.	Controller Design for Pendulum Angle Control.....	52
5.2.2.	Controller Design for Cart Position Control.....	55
5.4.	Test and Comparison of the Controllers.....	60
5.4.1.	Comparison of Performances of Controllers for no Load Condition.....	60
5.4.2.	Reference tracking capability.....	64
5.4.3.	Effect of Disturbances.....	74
6.	CONCLUSION.....	80
	REFERENCES.....	R1
	APPENDICES.....	A1
	A. CURRICULUM VITAE.....	A3

## FIGURES

<b>Figure 2.1</b>	The pendulum mechanical unit .....	6
<b>Figure 2.2</b>	Pendulum control unit .....	7
<b>Figure 2.3</b>	Pendulum phenomenological model.....	8
<b>Figure 3.1</b>	Pendulum stabilization and swing up zones.....	17
<b>Figure 3.2</b>	Pendulum swing-up principle.....	19
<b>Figure 4.1</b>	Sub-block for non-linear mathematical model of cart-pendulum system.....	21
<b>Figure 4.2</b>	Root locus for $G_1(s)$ .....	22
<b>Figure 4.3</b>	Root locus for $G_2(s)$ .....	24
<b>Figure 4.4</b>	Root locus for $G_3(s)$ .....	24
<b>Figure 4.5</b>	Root locus for $G_4(s)$ .....	25
<b>Figure 4.6</b>	Cart-pendulum system stabilization using state feedback.....	25
<b>Figure 4.7</b>	Stabilization with state feedback sub-block.....	28
<b>Figure 4.8</b>	Set Point Selection Sub-Block.....	28
<b>Figure 4.9</b>	Expanded view of swing up control with extra PI.position control Sub-Block.....	29
<b>Figure 4.10</b>	Applied force direction function sub-block .....	30
<b>Figure 4.11</b>	Expanded view of swing up control with extra PI position control Sub-block.....	31
<b>Figure 4.12</b>	Upright position detection function sub-block.....	31
<b>Figure 4.13</b>	Lower zone-upper zone function sub-block.....	32
<b>Figure 4.14</b>	Upright position detection function sub-block	33
<b>Figure 4.15</b>	Complete Control Strategy.....	35
<b>Figure 4.16</b>	Cart position, pendulum angle and control voltage plotted versus time.....	36
<b>Figure 4.17</b>	Cart velocity and pendulum angular velocity plotted versus time.....	36
<b>Figure 4.18</b>	Cart position and pendulum angle and control voltage plotted versus time for reference tracking.....	37

<b>Figure 4.19</b>	Cart velocity and pendulum angular velocity plotted versus time for reference tracking.....	38
<b>Figure 4.20</b>	Cart position (green) and reference cart position (blue) plotted versus time for reference tracking.....	38
<b>Figure 5.1</b>	Magnitude and Phase characteristics of the low-pass filter used in the derivative control part of PID controllers.....	41
<b>Figure 5.2</b>	Control strategy coupled with system identification.....	42
<b>Figure 4.3</b>	Pendulum angle, cart position and extra excitation signals in the identification step.....	43
<b>Figure 5.4</b>	Unfiltered pendulum angular velocity and the cart velocity signals in the identification step.....	44
<b>Figure 5.5</b>	Filtered (green) and unfiltered (blue) pendulum angular velocity versus time in the identification step.....	45
<b>Figure 5.6</b>	Filtered (green) and unfiltered (blue) cart velocity versus time in the identification step.....	45
<b>Figure 5.7</b>	Identification controller for closed-loop control model.....	47
<b>Figure 5.8</b>	Identification controller for closed-loop control model.....	47
<b>Figure 5.9</b>	The root locus plot of $G_{\text{cart\_position}}(s)$ .....	50
<b>Figure 5.10</b>	The root locus plot of $G_{\text{pend\_angle}}(s)$ .....	51
<b>Figure 5.11</b>	The root locus plot of $G_{\text{pend\_angle\_open}}(s)$ .....	54
<b>Figure 5.12</b>	The complementary root locus root of $G_{\text{cart\_position}}(s)$ (root locus of $-G_{\text{cart\_position}}(s)$ ).....	56
<b>Figure 5.13</b>	The root locus of $G_{\text{cart\_position\_open}}(s)$ .....	58
<b>Figure 5.14</b>	The block diagram of control strategy for no load condition.....	61
<b>Figure 5.15</b>	The cart position, pendulum angle and control signal plotted versus time with no extra excitation signals using controllers given in Equation (5.1) and Equation (5.2).....	62
<b>Figure 5.16</b>	The cart position, pendulum angle and control signal plotted versus time. The plots are obtained employing the $C_{\text{cart\_position}}(s)$ and $C_{\text{pend\_angle}}(s)$ controllers given in Equation (5.29) and Equation (5.20).....	63
<b>Figure 5.17</b>	The cart position, pendulum angle and control signal plotted versus time in case of pulse type reference tracking for cart position. The plots are obtained employing the $C_{\text{cart\_position}}(s)$ and $C_{\text{pend\_angle}}(s)$ controllers given in Equation (5.1) and Equation (5.2).....	64

<b>Figure 5.18</b>	The cart position (green) plotted versus time in case of pulse type reference (blue) tracking for cart position. The plots are obtained employing the $C_{cart\_position}(s)$ and $C_{pend\_angle}(s)$ controllers given in Equation (5.1) and Equation (5.2).....	65
<b>Figure 5.19</b>	The cart position, pendulum angle and control signal plotted versus time in case of pulse type reference tracking for cart position. The plots are obtained employing the $C_{cart\_position}(s)$ and $C_{pend\_angle}(s)$ controllers given in Equation (5.29) and Equation (5.20).....	66
<b>Figure 5.20</b>	The cart position (blue) plotted versus time in case of pulse type reference (green) tracking for cart position. The plots are obtained employing the $C_{cart\_position}(s)$ and $C_{pend\_angle}(s)$ controllers given in Equation (5.29) and Equation (5.20).....	67
<b>Figure 5.21</b>	The cart position, pendulum angle and control signal plotted versus time in case of sinusoidal type reference tracking for cart position. The plots are obtained employing the $C_{cart\_position}(s)$ and $C_{pend\_angle}(s)$ controllers given in Equation (5.1) and Equation (5.2).....	68
<b>Figure 5.22</b>	The cart position (green) plotted versus time in case of sinusoidal type reference (blue) tracking for cart position. The plots are obtained employing the $C_{cart\_position}(s)$ and $C_{pend\_angle}(s)$ controllers given in Equation (5.1) and Equation (5.2).....	69
<b>Figure 5.23</b>	The cart position, pendulum angle and control signal plotted versus time in case of sinusoidal type reference tracking for cart position. The plots are obtained employing the $C_{cart\_position}(s)$ and $C_{pend\_angle}(s)$ controllers given in Equation (5.29) and Equation (5.20).....	70
<b>Figure 5.24</b>	The cart position (blue) plotted versus time in case of sinusoidal type reference (green) tracking for cart position. The plots are obtained employing the $C_{cart\_position}(s)$ and $C_{pend\_angle}(s)$ controllers given in Equation (5.29) and Equation (5.20).....	71
<b>Figure 5.25</b>	The cart position, pendulum angle and control signal plotted versus time in case of sinusoidal type reference tracking for cart position. The plots are obtained employing the $C_{cart\_position}(s)$ and $C_{pend\_angle}(s)$ controllers given in Equation (5.29) and Equation (5.20). Amplitude of the reference signal is 0.25.....	72
<b>Figure 5.26</b>	The cart position (blue) plotted versus time in case of sinusoidal type reference (green) tracking for cart position. The plot is obtained employing the $C_{cart\_position}(s)$ and $C_{pend\_angle}(s)$ controllers given in Equation (5.29) and Equation (5.20). Amplitude of the reference signal is 0.25.....	73

<b>Figure 5.27</b>	The cart position, pendulum angle and control signal plotted versus time in case of a mass disturbance of 1246.35 gram. The plots are obtained employing the $C_{cart\_position}(s)$ and $C_{pend\_angle}(s)$ controllers given in Equation (5.29) and Equation (5.20).....	75
<b>Figure 5.28</b>	The cart position, pendulum angle and control signal plotted versus time in case of a mass of 1246.35 gram. The plots are obtained employing the $C_{cart\_position}(s)$ and $C_{pend\_angle}(s)$ controllers given in Equation (5.1) and Equation (5.2).....	76
<b>Figure 5.29</b>	The cart position (green) plotted versus time in case of a mass of 894.63 gram and reference (blue) pulse change of 0.05 units for the cart position. The plots are obtained employing the $C_{cart\_position}(s)$ and $C_{pend\_angle}(s)$ controllers given in Equation (5.1) and Equation (5.2).....	78
<b>Figure 5.30</b>	The cart position (blue) plotted versus time in case of a mass of 894.63 gram and reference (green) pulse change of 0.05 units for the cart position. The plots are obtained employing the $C_{cart\_position}(s)$ and $C_{pend\_angle}(s)$ controllers given in Equation (5.29) and Equation (5.20).....	79

## LIST OF TABLES

### TABLES

<b>Table 2.1</b>	The pendulum parameters.....	11
<b>Table 4.1</b>	Poles and zeros of the transfer functions $G_1(s)$ , $G_2(s)$ , $G_3(s)$ , $G_4(s)$ .....	23
<b>Table 4.2</b>	Evaluation of force direction depending on angular_velocity and zone_signal inputs.....	32
<b>Table 5.1</b>	Poles and zeros of the transfer functions $T_1(s)$ and $T_2(s)$ .....	49
<b>Table 5.2</b>	Poles and zeros of $G_{\text{cart\_position}}(s)$ and $G_{\text{pend\_angle}}(s)$ .....	50
<b>Table 5.3</b>	Poles and zeros of $G_{\text{pend\_angle\_open}}(s)$ .....	54
<b>Table 5.4</b>	Poles and zeros of $G_{\text{cart\_position\_open}}(s)$ .....	59

## LIST OF ABBREVIATIONS

PID Proportional-Integral-Derivative

PI Proportional-Integral

P Proportional

I Integral

D Derivative

## CHAPTER 1

### INTRODUCTION

The Cart-Pendulum system is a good example for non-linear dynamical systems and it is also an important and useful control laboratory experimental set-up to let analysis of unstable mechanical system as well [1]. Due to its non-linear and unstable characteristics, it constitutes a perfect environment to design and implement modern linear and non-linear control techniques and methods. To give an example in [2] Bettayeb et al used PI state feedback to control this system at the stabilization stage, Udhayakumar and Lakshmi [3] implemented an energy based control strategy in the swing up part and used a pole placement strategy in the stabilization stage. Adhikary and Mahanta [4] used sliding mode control in order to mainly deal with the uncertainties in the system structure to obtain robust controller structures. Kai and Bito [5] used discrete mechanics to cope with cart-pendulum problem. Das and Paul [6] in simulation used the cascade model of the cart pendulum system in their feedback control structure that contains two feedback loops. The inner feedback loop contains a feedback controller to control the pendulum angle whereas the outer feedback loop is used to control the cart position. In [7], Lee et al focused on uncertainties on the cart pendulum system and they designed observers to estimate the unmeasured states. Uncertainties play an important role in real time applications and sometimes it is better to surpass this problem through different methods as explained in [7].

Cart pendulum system is an excellent tool and test-bed for a wide range application to design, test and implement control strategies that can be used for various concepts ranging from robotics to space rocket guidance system as well as systems having similar structures such as cart flexible pendulum system [8]. The ideas and experiences gained from non-linear systems can also be implemented for other



control theory applications, but mostly for the control of non-linear unstable system. However, at some occasions, in order to design competent controller structures and ease the burden of dealing with non-linear dynamics, the non-linear system to be controlled is linearized. Linearization [9-10] is generally carried out for the cases when it is intended to control the system around unstable or stable equilibrium point [11].

Any controller structure consists of two vital components. The first component is means of knowledge representation used to indicate the controller structure and the second component is the method it computes its outputs or makes inferences (the decision-making mechanism). The conventional controller structures such as Proportional-Integral-Derivative (PID) controllers represent the knowledge using a mathematical model [12-13]. Differential equations or transfer functions can be used for this purpose. The decision-making mechanism for PIDs is solely the evaluation of the mathematical model embodied in the controllers structure depending on the imminent input(s) to the controller. For the same task, non-conventional structures (i.e. neural-networks, rule-bases, decision trees) and suitable inference mechanisms coherent with these structures (i.e. fuzzy logic, mathematical interpolation) [14-15] can also be employed. Especially these structures and techniques can be fruitful to control non-linear systems. However, still some information should be available about the system characteristics in order to train and realize these structures and mechanism in simulations efficiently. Unluckily training and realization of these structures in real time applications in case the system has unstable characteristics is extremely difficult. Generally, one should implement properly working conventional controllers for these systems first and then mimic the working principle of conventional controller by an extra training step, which is not an easy task. Designing proper controllers most of the time necessitates some extra steps (system identification steps, robust controller design strategies) [8-16] for non-linear and unstable systems as their mathematical model in majority of the cases turn out to be insufficient to represent the dynamical model due to the impurities in system dynamics and uncertainties in the system parameters. Particularly for the cart-pendulum system, if we want to stabilize and control it around one of its unstable

equilibrium points using a neural network in real time application, the system should primarily be carried to a state close to the unstable equilibrium point. Then by different inputs the system should be identified. Finally, depending on the identification step a working neural network that stabilizes and controls the system in dissimilar circumstances such as reference tracking application of disturbances should be trained depending on different scenarios. The scenarios might include cases that threaten the system stability as well. For example, sudden application of reference signal changes can destabilize the system or create increasing oscillations. As a result, these kinds of training scenarios could return to be destructive or at least it causes the controller not to be properly trained. For these reasons, it is better to realize a properly working controller structure using conventional methods instead of the effort to train or implement a non-conventional controller structure primarily. One should not forget that, the critical step to design an unconventional controller also passes from designing a properly working conventional controller.

Particularly for cart-pendulum system, controlling the system around an unstable equilibrium point means keeping the pendulum in upright position (inverted pendulum mode with pendulum angle equal to 0 degree) with the cart position not exceeding dimensions of the rail it is moving along while keeping pendulum angular velocity and cart velocity as small as possible. This control operation is called as stabilization or hold stage. In real time application, precise identification of dynamics of this systems model could be essential for the developing appropriate control algorithms for this stage. Besides, to bring the system close to an unstable equilibrium point one should take the advantage of some non-linear control algorithm first. This operation starts by guiding the system from a stable equilibrium point until it is brought closer to the unstable equilibrium point, which is called as the swing-up stage.

In our thesis, we employed previously defined swing up stage non-linear controllers and previously defined stabilization stage PID controllers to design new controllers in simulation and in real time applications. The designed controllers both for the simulation and the real time application are only for the stabilization stage. In the

simulation part, the mathematical model of the dynamical system is employed to develop state feedback [17-18] control strategy. However, the state feedback control strategy is not able to stabilize the cart-pendulum system in the real time application in the stabilization stage. Hence, a system identification procedure is carried out to realize the system around the unstable equilibrium point. The system identification yields the valuable information (i.e. approximate transfer functions) about the system that is necessary to design new PID controller structures. The design of PID controllers is carried out facilitating from root locus method [17-18]. After design, the controllers are tested and their performances are compared with the previously defined controllers for the stabilization stage with various control applications such as reference signal tracking and durability in case of disturbance. The outputs demonstrate promising results.

The main task and the practical contribution of this thesis is integrating system identification and controller development techniques for a high dimensional non-linear and unstable system altogether in real time application to develop competent PID controller structures. If it is carried out as a simulation, this is a more straightforward task. However, as a real time application the process is not so simple.

The organization of the remaining part of this thesis is as follows: in Chapter 2 the mathematical model of the cart-pendulum system is given. In Chapter 3, the linearization of the mathematical model is carried out around one of the unstable equilibrium points and the linearized model of the system is obtained. In Chapter 4 a simulated model for the system is modified and this modified model is employed to stabilize and control the system around the unstable equilibrium point. In the modified model, state feedback control strategy is employed in the stabilization stage. In Chapter 5, the real time identification and controller design techniques are carried out for the cart-pendulum system. Finally, Chapter 6 summarizes all the thesis work done and it gives concluding remarks and future works.

## CHAPTER TWO

### SYSTEM DESCRIPTION

#### 2.1 System Description

The illustration of an inverted pendulum-cart system is shown in Figure 2.1 [1]. The system is made up of two sub systems. One of the subsystems is a cart moving over a rail horizontally due to a belt connected along its direction of motion. The belt and hence the cart are driven by a DC motor. The voltage applied to the DC motor is proportional with the force exerted to the cart via the belt. Therefore, the value of the force depends on the value of the control voltage. Due to this force, it is possible to move the cart back and forth. The second subsystem is a rigidly connected two-pendulum stick. This stick rotates freely around the cart. In total, the system exhibits non-linear characteristic.

The cart-pendulum system can be represented as a Single Input Multiple Output (SIMO) system where the input is the DC motor Voltage (which is assumed to be directly proportional with the applied force  $F$  to the cart-pendulum system) and the system states and outputs can be assigned as the cart position ( $x_1 = x$ ), cart velocity ( $x_2 = \dot{x} = v$ ), pendulum angle ( $x_3 = \theta$ ) and pendulum angular velocity ( $x_4 = \dot{\theta} = w$ ). This system has infinitely many equilibrium points some of which are unstable. When the system is set to one of these unstable equilibrium points even if a very small and time-limited force is applied to cart, the system directly traverses to one of the equilibrium points, which are all stable. Hence, when there is no type of feedback control (i.e. the system is open loop), it is impossible to stabilize it at unstable equilibrium points in real time applications. To sustain and preserve stability at the unstable equilibrium points the control signal should be achieved due to a closed loop control strategy.

As the system structure is inspected, it is observed that the set of unstable equilibrium points are reached when the pendulum is at upright position ( $\theta = 0$  degree) and the stable equilibrium points are reached when the pendulum is at downright position ( $\theta = 180$  degree). The task of balancing the pendulum vertically at one of the unstable equilibrium points starting from one of the stable equilibrium points is called as Swing Up and Hold (Stabilization) process. In the preceding chapters, we will focus on the Swing Up and Hold Process for the cart-pendulum system after its dynamics is realized and identified.

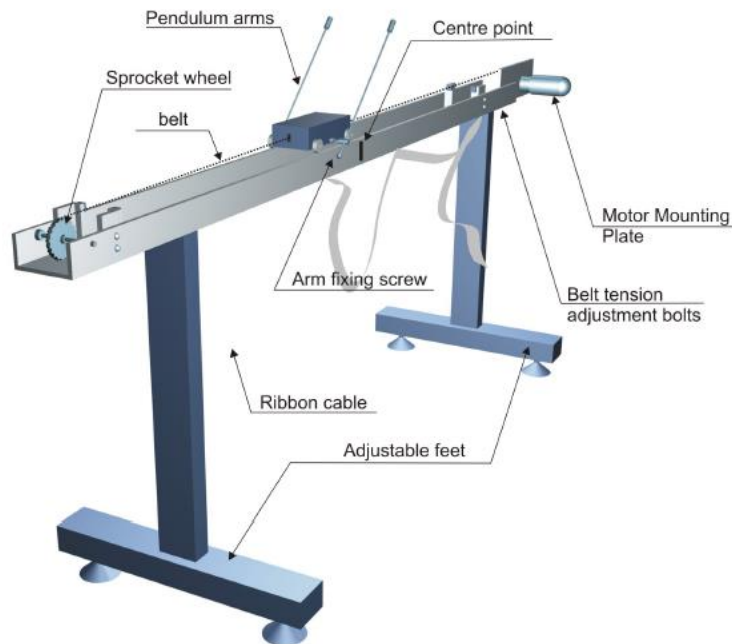


**Figure 2.1:** The pendulum mechanical unit [1].

## 2.2 The Pendulum-Cart System Components

In Figure 2.2 the front profile of the system with its hardware connections is illustrated. The system consists of the following units [1]

- Pentium or AMD based personal computer equipped with RTDAC4/PCI/O board,
- Pendulum and cart mechanical unit,
- Power interface,

- Control software,

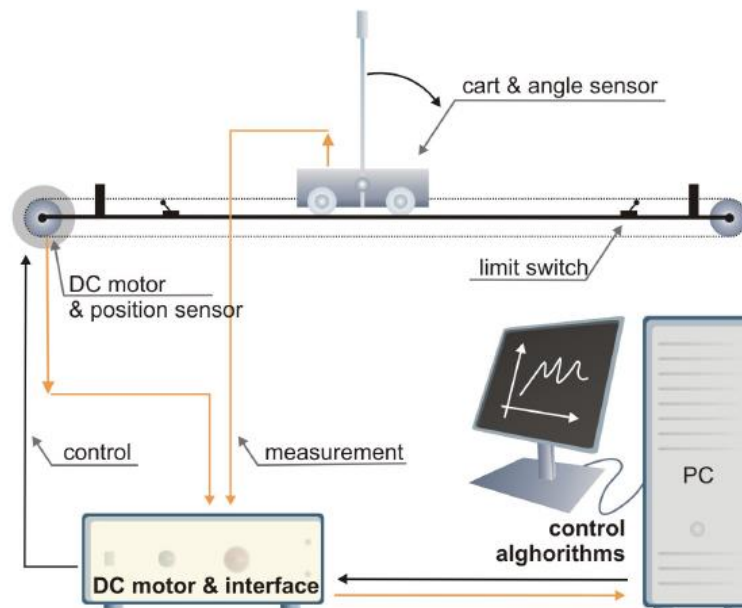


**Figure 2.2:** Pendulum control unit [1]

### 2.3 System Dynamics

The phenomenological model of the system is illustrated in Figure 2.3 [1]. Using this model, the system parameters and variables can be declared as follows:  $M$  is the cart mass,  $m$  is the mass of the pendulum,  $l$  is the pole length (length of the stick),  $I$  is the moment of inertia of the pendulum,  $b$  is the friction coefficient of the cart,  $d$  is the rotational friction coefficient of the pendulum and  $g$  is the gravitational acceleration constant for the earth,  $x$  is the position of the cart and  $\theta$  is the angular position of the pendulum. The dynamic equations of motion of the system can be obtained by summing the forces acting on the pendulum subsystem and cart subsystem. The mathematical equations related to cart-pendulum can be obtained using and modifying the system equations given in [1-2-3-4-5-6]. But, due direction of motion and rotation and declaration of the direction of variables there are sometimes signal and variable differences in these equation.

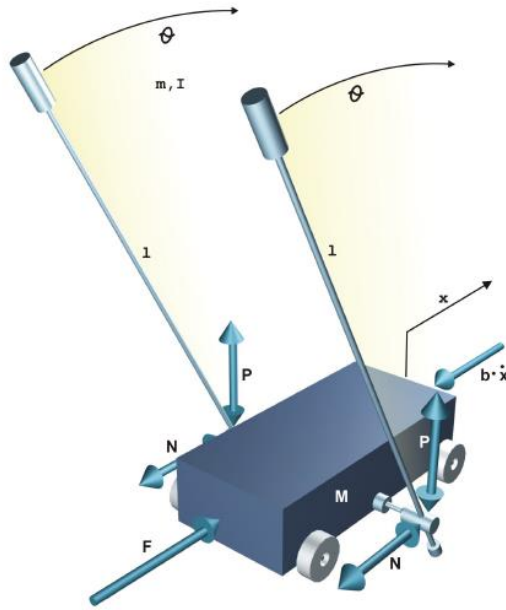


**Figure 2.3:** Pendulum phenomenological model [1].

Based, on the forces in the free body diagram of the cart in horizontal direction we get the following equation of motion

$$F = N + b\dot{x} + M\ddot{x} \quad (2.1)$$

Equation (2.1),  $F$  is the force applied to the system,  $b\dot{x}$  is the friction force,  $N$  is the reaction force in horizontal direction and  $M\ddot{x}$  is the acceleration force achieved for the cart.

To obtain the horizontal reaction force, one can write

$$N = m \frac{d^2}{dt^2} [x + l \sin \theta] = m\ddot{x} + ml\ddot{\theta} \cos \theta - ml\dot{\theta}^2 \sin \theta \quad (2.2)$$

Where  $x + l \sin \theta$  is the center of mass of the pendulum in horizontal direction.

Using Equation (2.1) and Equation (2.2), we get the first equation of motion for the system.

$$F = m\ddot{x} + ml\ddot{\theta} \cos \theta - ml\dot{\theta}^2 \sin \theta + b\dot{x} + M\ddot{x} \quad (2.3)$$

Rearranging the terms at Equation (2.3), we get

$$F = [m + M]\ddot{x} + b\dot{x} + ml\ddot{\theta} \cos \theta - ml\dot{\theta}^2 \sin \theta \quad (2.4)$$

To get the second equation of motion, sum the forces vertically to the pendulum. The vertical components of the forces are obtained from the following equation

$$m \frac{d^2}{dt^2} [l \cos \theta] = P - mg \quad (2.5)$$

Where  $P$  is the reaction force acting on the pole,  $mg$  is the force due to gravitational acceleration acting on pole mass,  $l \cos \theta$  is the center of mass of the pole in vertical direction. Since the length of the pole is constant, we can write

$$ml \frac{d^2}{dt^2} \cos \theta = P - mg \quad (2.6)$$

Taking the first derivative, we obtain

$$ml \left[ \frac{d}{dt} (-\dot{\theta} \sin \theta) \right] = P - mg \quad (2.7)$$

Taking the second derivative, we obtain

$$-ml [\ddot{\theta} \sin \theta + \dot{\theta}^2 \cos \theta] = P - mg \quad (2.8)$$

The total sum of the moments about the centroid of the pendulum gives us the equation

$$Pl \sin \theta - Nl \cos \theta = I\ddot{\theta} + d\dot{\theta} \quad (2.9)$$

Obtaining  $P$  from Equation (2.9).

$$P = \frac{I\ddot{\theta} + Nl \cos \theta + d\dot{\theta}}{l \sin \theta} \quad (2.10)$$

We put Equation (2.10), in Equation (2.8) to solve the second equation of motion, we get

$$-ml [\ddot{\theta} \sin \theta + \dot{\theta}^2 \cos \theta] = \frac{I\ddot{\theta} + Nl \cos \theta + d\dot{\theta}}{l \sin \theta} - mg \quad (2.11)$$

Using Equation (2.2) in Equation (2.11), we obtain

$$-ml^2 \ddot{\theta} \sin^2 \theta - ml \dot{\theta}^2 \cos \theta \sin \theta = I\ddot{\theta} - mgl \sin \theta + l \cos \theta [m\ddot{x} + ml\ddot{\theta} \cos \theta - ml\dot{\theta}^2 \sin \theta] \quad (2.12)$$

Expanding Equation (2.12), we obtain

$$-ml^2 \ddot{\theta} \sin^2 \theta - ml \dot{\theta}^2 \cos \theta \sin \theta = I\ddot{\theta} - mgl \sin \theta + ml \cos \theta \ddot{x} + ml^2 \ddot{\theta} \cos^2 \theta - ml^2 \dot{\theta}^2 \cos \theta \sin \theta \quad (2.13)$$

Reorganizing the terms in Equation (2.13), we obtain

$$-ml^2 \ddot{\theta} [\sin^2 \theta + \cos^2 \theta] = I\ddot{\theta} - mgl \sin \theta + ml \cos \theta \ddot{x} + d\dot{\theta} \quad (2.14)$$

Since,  $(\sin^2 \theta + \cos^2 \theta) = 1$ , the final equation is obtained as



$$(I + ml^2)\ddot{\theta} - mgl \sin \theta + ml \cos \theta \ddot{x} + d\dot{\theta}=0 \quad (2.15)$$

As the result, if we put the states  $x_1$ ,  $x_2$ ,  $x_3$  and  $x_4$  in Equation (2.4) and (2.15) and knowing that the cart velocity is the time derivative of cart position and pendulum angular velocity is the time derivative of the pendulum angle, we obtain the following nonlinear equation of motion

$$(m+M) \dot{x}_2 + b x_2 + ml\dot{x}_4 \cos x_3 - ml x_4^2 \sin x_3 = F \quad (2.16)$$

$$(I + ml^2)\dot{x}_4 - mgl \sin x_3 + ml\dot{x}_2 \cos x_3 + dx_4 = 0 \quad (2.17)$$

$$\dot{x}_1 = x_2 \quad (2.18)$$

$$\dot{x}_3 = x_4 \quad (2.19)$$

## 2.4 The System Parameters

The nominal values of cart-pendulum system parameters are taken from [1]. These parameters are given in Table 2.1.

**Table 2.1:** The pendulum parameters.

<b>Parameter</b>	<b>Value</b>
<i>g</i> -Gravity	9.81 m/s <sup>2</sup>
<i>l</i> -Pole length	0.36 to 0.4 m-depending on the configuration. For the problem we take it as 0.36 m.
<i>M</i> -Cart mass	2.4 kg
<i>m</i> -Pole mass	0.23 kg
<i>I</i> -moment of inertia of the pole	About 0.099 kg.m <sup>2</sup> -depends on the configuration
<i>b</i> - Cart friction coefficient	0.05 Ns/m
<i>d</i> -Pendulum damping coefficient although negligible, necessary in the model -0.005 Nms/rad	Although negligible, necessary in the model-0.005 Nms/rad

## CHAPTER 3

### LINEARIZATION, EQUILIBRIUM POINTS AND CONTROL STRATIGE

#### 3.1 System Structure

The dynamics model of the cart-pendulum system given in Chapter 2 consists of four differential equations (Equation 2.16, Equation 2.17, Equation 2.18 and Equation 2.19) where two of the equations are non-linear (Equation 2.16, Equation 2.17). In order to design controller structures more effectively at and around an operating point, is sometimes necessary to linearize them and used the linearized form of the differential equations. Indeed, there are two important set of equilibrium points depending on the angular position value  $x_3$ . One of the set of equilibrium points has stable characteristics whereas, the other set of equilibrium points exhibits unstable characteristics. The unstable equilibrium points are reached when  $x_3 = 0$  (*inverted pendulum mode*). For this case, the pendulum is in upright position. The stable equilibrium points are achieved when  $x_3 = \pi$  (*crane mode*).

#### 3.2 Equilibrium Points

In a differential equation, in order to achieve the equilibrium points, the derivatives of the states are all equated to 0 ( $\dot{x}_1 = 0, \dot{x}_2 = 0, \dot{x}_3 = 0$  and  $\dot{x}_4 = 0$ ). Putting these values inside Equation (2.16), Equation (2.17), Equation (2.18) and Equation (2.19), we obtain the equilibrium points

$$F = 0, \sin(x_3) = 0, x_1 = \text{arbitrary}, x_2 = 0 \text{ and } x_4 = 0.$$

Hence, to obtain an equilibrium point  $x_3$  can be assigned infinitely many values,

$$x_3 = [\dots, -3\pi, -2\pi, -\pi, 0, \pi, 2\pi, 3\pi, \dots \dots]$$

From these equilibrium points the ones where  $x_3 = [\dots, -4\pi - 2\pi, 0, 2\pi, 4\pi, \dots]$  are the unstable equilibrium points whereas the ones where  $x_3 = [\dots, -3\pi - \pi, \pi, 3\pi, \dots]$  are the stable equilibrium points. We want to focus on particularly two of these equilibrium points. One of them is  $x_1=0, x_2=0, x_3=0, x_4=0$  and  $F=0$  (the pendulum is in upright position with cart position being at the origin) and the other one is  $x_1=0, x_2=\pi, x_3=0, x_4=0$  and  $F=0$  (the pendulum is in downright position with the cart position being at origin).

### 3.3 Linearization of the Model

The equations given in Equation (2.4) and Equation (2.15) are highly non-linear equations and besides they contain some trigonometric functions. The equilibrium points of the system are obtained either when  $x_3 = \theta = 0$  or  $x_3 = \theta = \pi$ . The linearization step starts with the approximation of trigonometric functions around the equilibrium points. If  $\theta = 0$  (*inverted pendulum mode*), the trigonometric functions can be approximated as

$$\sin \theta \approx \theta \quad (3.1)$$

$$\cos \theta \approx 1 \quad (3.2)$$

Besides at the equilibrium point, there should be no translational or rotational motion hence angular velocity of the pendulum should be close to 0. Thus

$$\dot{\theta}^2 \approx 0 \quad (3.3)$$

Using these approximations, the equations of motion given in Equation (2.4) and Equation (2.15) for the inverted pendulum mode take the form

$$(m+M) \ddot{x} + b \dot{x} + ml \ddot{\theta} = F \quad (3.4)$$

$$(I + ml^2) \ddot{\theta} - mgl\theta + ml \ddot{x} + d\dot{\theta} = 0 \quad (3.5)$$

For the linearization of the same system at the stable equilibrium points,  $\pi$  (*crane mode*), following substitutions have to be made

$$\sin \theta \approx -\theta \quad (3.6)$$

$$\cos \theta \approx -1 \quad (3.7)$$

$$\dot{\theta}^2 \approx 0 \quad (3.8)$$

Thus, the equation of motion given in Equation (2.4) and Equation (2.15) for the crane mode can be approximated to take the form

$$(m+M)\ddot{x} + b\dot{x} - ml\ddot{\theta} = F \quad [3.9]$$

$$(I+ ml^2)\ddot{\theta} + mgl\theta - ml\ddot{x} + d\dot{\theta} = 0 \quad [3.10]$$

### 3.4 Transfer Functions

We want to focus on the inverted pendulum linearized model given by the Equation (3.4), and Equation (3.5). Depending on the declaration of the output in the system, we can construct different transfer functions. The first step to obtain these transfer functions is to convert the linearized differential equations to Laplace equations by Laplace transformation assuming all initial conditions of the states are equal to zero. The Laplace transformations of Equation (3.4) and Equation (3.5) gives

$$(m+M)s^2X(s) + bsX(s) + mls^2\theta(s) = F(s) \quad [3.11]$$

$$(I+ ml^2) s^2\theta(s) - mgl\theta(s) + mls^2 X(s) + ds\theta(s) = 0 \quad [3.12]$$

In Equation (3.11) and Equation (3.12), the  $X(s)$ ,  $\theta(s)$  and  $F(s)$  are the Laplace domain representations of  $x$ ,  $\theta$  and  $F$  and  $s$  is the Laplace variable. Recall that transfer function represents the relation between a single input and a single output in Laplace domain. For the system, there is only one input  $F(s)$ , but there might be more than one outputs. If the output is declared as,  $\theta(s)$  we need to eliminate  $X(s)$  from Equation (3.11), and Equation (3.12). Bu before that let's make some new parameter declarations to ease the task

$$h = (m+M) \quad (3.13)$$

$$N = (I+ml^2) \quad (3.14)$$

$$q = hN - m^2l^2 \quad (3.15)$$

From Equation (3.11) using through the parameter change in Equation (3.13), we have

$$X(s) = \frac{F(s) - mls^2\theta(s)}{hs^2 + bs} \quad (3.16)$$

Putting Equation (3.16) in Equation (3.12) with the parameter change in Equation (3.14) and we obtain one of the transfer function their force is the input and the angular position is the output as

$$\frac{\theta(s)}{F(s)} = \frac{-mls^2}{qs^4 + [Nb + hd]s^3 + [bd - mglh]s^2 - mglb} \quad (3.17)$$

As can be seen from Equation (3.17) there is a pole-zero cancellation in this transfer function and it can be written as

$$\frac{\theta(s)}{F(s)} = \frac{-mls}{qs^3 + [Nb + hd]s^2 + [bd - mglh]s - mglb} \quad (3.18)$$

Writing  $\theta(s)$  in terms of  $F(s)$  from Equation (3.18) and putting this equation into Equation (3.16), we can eliminate  $\theta(s)$  and find the transfer function where force is the input and cart position is the output as

$$\frac{X(s)}{F(s)} = \frac{Ns^2 + ds - mgl}{s[qs^3 + [Nb + hd]s^2 + [bd - mglh]s - mglb]} \quad (3.19)$$

It is known that the cart velocity is the time derivative of cart position ( $\dot{x} = v$ ) and pendulum angular velocity is the time derivative of the pendulum angle ( $\dot{\theta} = w$ ). Taking the Laplace transforms of these equations and putting inside Equation (3.18) and Equation (3.19), we reach to new transfer functions.

$$\frac{W(s)}{F(s)} = \frac{-mls^2}{qs^3 + [Nb + hd]s^2 + [bd - mglh]s - mglb} \quad (3.20)$$

and

$$\frac{V(s)}{F(s)} = \frac{Ns^2 + ds - mgl}{[qs^3 + [Nb + hd]s^2 + [bd - mglh]s - mglb]} \quad (3.21)$$

In Equation (3.20) and Equation (3.21),  $W(s)$  and  $V(s)$  are the Laplace transformed forms of  $w$  and  $v$  respectively. All parameters of the original model of the system are given in Table 2.1.

### 3.5 State-Space Representation of the Linearized Model:

Sometimes, in order to design controllers, not the transfer functions but the state space representation of the linearized model is necessary. Equation (3.4) and Equation (3.5) are used to generate the state space representation of the cart-pendulum system around the unstable equilibrium point. To obtain the state space model we used the states defined previously as  $x_1 = x$ ,  $x_2 = \dot{x} = v$ ,  $x_3 = \theta$  and  $x_4 = \dot{\theta} = w$ . With these defined states the state space representation of the system is given by

$$\begin{bmatrix} \dot{x}_1 \\ \dot{x}_2 \\ \dot{x}_3 \\ \dot{x}_4 \end{bmatrix} = \begin{bmatrix} 0 & 1 & 0 & 0 \\ 0 & -\frac{1}{bN} & -\frac{gm^2l^2}{Nh - m^2l^2} & \frac{mld}{Nh - m^2l^2} \\ 0 & 0 & 0 & 1 \\ 0 & \frac{mlh}{Nh - m^2l^2} & \frac{mglh}{Nh - m^2l^2} & -\frac{dh}{Nh - m^2l^2} \end{bmatrix} \begin{bmatrix} x_1 \\ x_2 \\ x_3 \\ x_4 \end{bmatrix} + \begin{bmatrix} 0 \\ N \\ hN - m^2l^2 \\ 0 \\ -ml \\ hN - m^2l^2 \end{bmatrix} F \quad (3.22)$$

### 3.6 Control Strategies

The cart moves in  $x$  or  $-x$  direction along a horizontal rail with limit length, making the pendulum to rotate as shown in Figure 3.1.

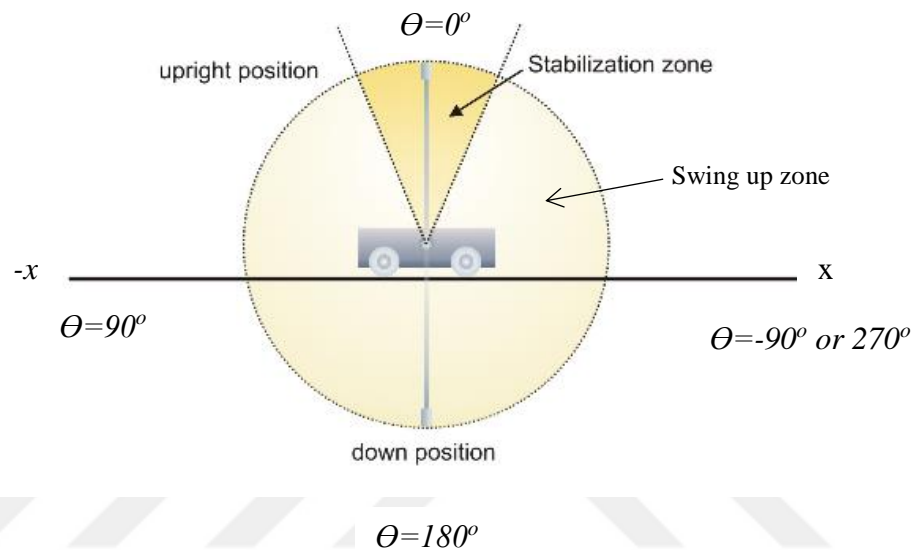


**Figure 3.1:** Pendulum stabilization and swing up zones [1]

In order to stabilize the system around unstable equilibrium point  $\theta = 0^\circ$ , two different control strategies should be accomplished in an order. Initially the pendulum is positioned to the stable equilibrium point  $\theta = 180^\circ$ . Then by application of the first control strategy, the pendulum is carried from stable equilibrium point (downright position of the pendulum) to the close locality of the unstable equilibrium point. This process is called as swing up stage (control) and the region this control strategy is applied is called as swing up region. The second control strategy is utilized at and around the unstable equilibrium point, which is called as the stabilization stage (control) or hold stage. When these two strategies are applied altogether the resulting hybrid control strategy is named as swing up and stabilization (hold) operation. The swing up zone and the stabilization zone are illustrated in Figure 3.1. As can be comprehended the zone depend on pendulum angle variable  $\theta$ . Generally, the stabilization zone in simulations and real time applications is chosen



as  $(-\theta_1 \leq \theta \leq \theta_1)$  where  $\theta_1$  is chosen a value between 0.2 and 0.25 radians. On the other hand, the main purpose of the stabilization stage is to stabilize not only the pendulum but also required to bring the cart to the reference point on the rail.

### 3.6.1 Swing-Up Control

Swing up control technique depends on swinging up the pendulum and obtaining controllable oscillations, while keeping the cart travel on the horizontal rail within verges of the rail (between 0.4 meter and -0.4 meter). However, if the acceleration is unbounded it is possible to bring the pendulum to the upright point in a single swing but this might cause the cart to exceed the limits of the rail. Therefore, it is better to swing up the pendulum in a robust way, which will assure that the pendulum will end up nearly in a vertical position where  $\theta \approx 0$ . There are many methods the swing up control can be accomplished. But, one of the most convenient methods can be described graphically as in Figure 3.2 [1]. The details of this swing up strategy are as follows:

In this strategy, it is assumed that the force magnitude applied to the system is constant. Although, the force magnitude is constant, its direction and duration is changed due to pendulum angle value. Primarily, apply a very short duration starting force to move to the cart. This operation actuates the cart in  $x$  or  $-x$  direction and hence the pendulum also begins to rotate. If pendulum angle  $\theta$  is between  $90^\circ$  and  $270^\circ$ , this means the pendulum is in the lower zone. In the lower zone, apply a force until the pendulum angular velocity reaches 0 rad/sec. When the angular velocity reaches 0 reverse the direction of the force. Continue this procedure as long as the pendulum is at lower zone. If the angle is below  $90^\circ$  or above  $270^\circ$ , this means the pendulum is in now upper zone. When the pendulum crosses from lower zone to upper zone once again change the direction of the force and apply the force until the angular velocity reaches to 0 rad/sec. If the pendulum angular velocity reaches to 0 rad/sec at upper zone, once again the direction of the force is switched. This time the pendulum will move from upper zone to lower zone and when it enters from upper

zone to lower zone once again change the direction of the force. Continue the above procedure until the pendulum reaches and stays within the stabilization zone.

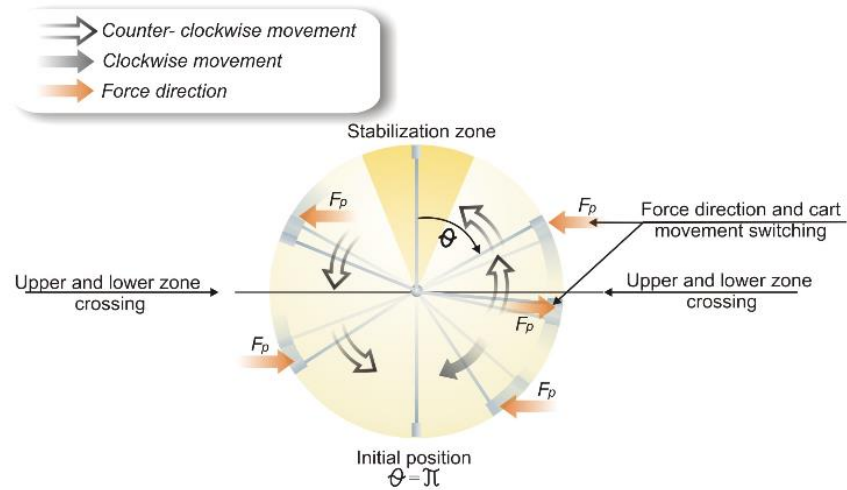


**Figure 3.2:** Pendulum swing-up principle [1].

### 3.6.2 Stabilization Control

There are also many different stabilization stage methods on the literature. These methods mainly use state-space representation design techniques based on the linearized model of the cart-pendulum system. For example, in [3], a kind of pole placement is applied to ensure local stability at the unstable equilibrium point.

## **CHAPTER 4**

### **SIMULATION MODEL**

#### **4.1 Design Strategy**

As previously mentioned in Chapter 2 and Chapter 3 the cart-inverted pendulum system has non-linear characteristics. In order to control the pendulum in upright position generally a swing up and stabilization control is employed. Hence the control strategy consists of two stages. The first stage is the swing up stage where the pendulum is carried from downright position to nearly upright position (approximately the pendulum angle reaches and stays nearly between -11.5 and 11.5 degrees as the result of this stage). In the second stage the pendulum is stabilized around the unstable equilibrium point by a specific controller or set of controllers. The design of this/these controller(s) for simulation models is the main content of this chapter. For the sake of simplicity, the controllers design is handled based on the linearized model of the system. In this chapter primarily the SIMULINK model and implementation of the sub-blocks in the SIMULINK model corresponding to swing-up stage and hold (stabilization) stage is explained in details. Finally, simulation results are monitored.

#### **4.2 Simulation Sub-Blocks**

##### **4.2.1. Non-linear Mathematical Model of the Cart-Pendulum System Sub-Block**

The cart-pendulum system's non-linear mathematical structure is shown in Figure 4.1 [1].



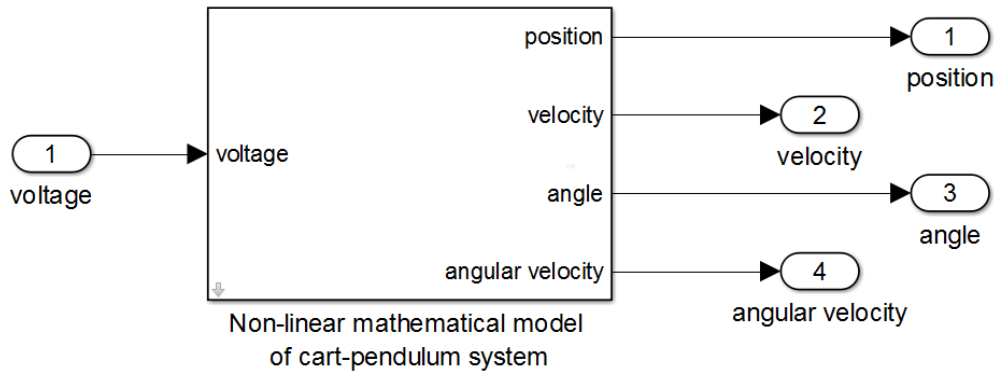


**Figure 4.2:** Sub-block for non-linear mathematical model of cart-pendulum system.

#### 4.2.2. Stabilization with State Feedback Sub-Block

In order to design the controllers, it is better to initially check the dynamic properties of the linearized system. First we want to obtain the dynamical model of the linearized system at the unstable equilibrium point ( $x_3=0$ ). Putting the parameters used for the system that are given in Table 2.1 the state space representation of the linearized system using through Equation (3.22) will be of the form

$$\begin{bmatrix} \dot{x}_1 \\ \dot{x}_2 \\ \dot{x}_3 \\ \dot{x}_4 \end{bmatrix} = \begin{bmatrix} 0 & 1.000 & 0 & 0 \\ 0 & -0.0194 & -0.2026 & 0.0012 \\ 0 & 0 & 0 & 1.000 \\ 0 & 0.0125 & 6.4363 & -0.0396 \end{bmatrix} \begin{bmatrix} x_1 \\ x_2 \\ x_3 \\ x_4 \end{bmatrix} + \begin{bmatrix} 0 \\ 0.3881 \\ 0 \\ -0.2495 \end{bmatrix} F \quad (4.1)$$

In Equation (4.1),  $F$  is the input (applied force) to the system and  $V=k \times F$ , where  $V$  is the voltage applied to the motor with the proportionality constant  $k$  being equal to 1. In Equation (4.1) the system matrix  $A$  and input matrix  $B$  can be written as

$$A = \begin{bmatrix} 0 & 1.000 & 0 & 0 \\ 0 & -0.0194 & -0.2026 & 0.0012 \\ 0 & 0 & 0 & 1.000 \\ 0 & 0.0125 & 6.4363 & -0.0396 \end{bmatrix}, \quad B = \begin{bmatrix} 0 \\ 0.3881 \\ 0 \\ -0.2495 \end{bmatrix} \quad (4.2)$$

The system outputs can be declared as cart position, cart velocity, pendulum angle or the pendulum angular velocity.

To have a better insight of this linearized system, we also found the transfer functions for each output using Equation (3.18) Equation (3.19) Equation (3.20) and Equation (3.21) where  $X_1(s)$ ,  $X_2(s)$ ,  $X_3(s)$  and  $X_4(s)$  stands for  $X(s)$ ,  $V(s)$ ,  $\theta(s)$  and  $W(s)$  respectively

$$G_1(s) = \frac{X_1(s)}{F(s)} = \frac{0.3881s^2+0.01506s-2.447}{s^4+0.05902s^3-6.436s^2-0.1224s} \quad (4.3)$$

$$G_2(s) = \frac{X_2(s)}{F(s)} = \frac{0.3881s^2+0.01506s-2.447}{s^3+0.05902s^2-6.436s-0.1224} \quad (4.4)$$

$$G_3(s) = \frac{X_3(s)}{F(s)} = \frac{-0.2495s+8.114*10^{-19}}{s^3+0.05902s^2-6.436s-0.1224} \quad (4.5)$$

$$G_4(s) = \frac{X_4(s)}{F(s)} = \frac{-0.2495s^2-8.182*10^{-19}s}{s^3+0.05902s^2-6.436s-0.1224} \quad (4.6)$$

The denominators of each transfer function are nearly equal however,  $G_1(s)$  has an extra pole at the origin (the order of  $G_1(s)$  is 4 whereas the order of the other transfer functions is 3). The open loop poles and zeros of each transfer function are given at Table 4.1

**Table 4.1:** Poles and zeros of the transfer functions  $G_1(s)$ ,  $G_2(s)$ ,  $G_3(s)$ ,  $G_4(s)$ .

Transfer Function	Open loop poles	Open loop zeros
$G_1(s)$	0,-2.5571,2.5171,-0.0190	-2.5307, 2.4918
$G_2(s)$	-2.5571,2.5171,-0.0190	-2.5307, 2.4918
$G_3(s)$	-2.5571,2.5171,-0.0190	$3.2526 \times 10^{-18} \approx 0$
$G_4(s)$	-2.5571,2.5171,-0.0190	$0, -3.2526 \times 10^{-18} \approx 0$

From Table 4.1, we can conclude that the system has four eigenvalues at the locations 0, -2.5571, 2.5171, -0.0190. Only in one of the transfer functions, we do not observe a pole zero cancellation, which is  $G_1(s)$ . Besides,  $G_1(s)$  and  $G_2(s)$  has non-minimum phase zero.

The root locus plots for  $G_1(s)$ ,  $G_2(s)$ ,  $G_3(s)$ , and  $G_4$  are shown in Figure 4.3, Figure 4.4, Figure 4.5, and Figure 4.6 respectively.

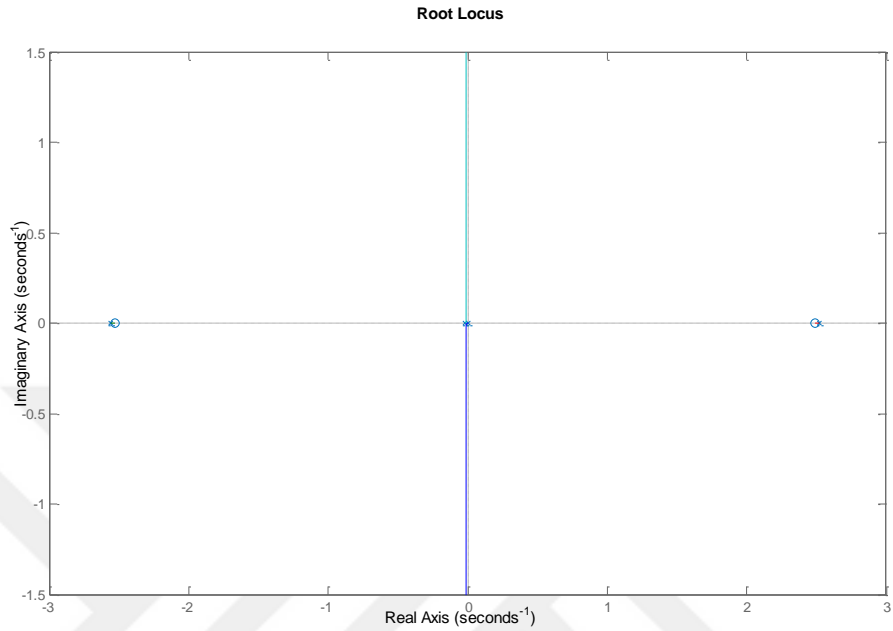


**Figure 4.3:** Root locus for  $G_1(s)$

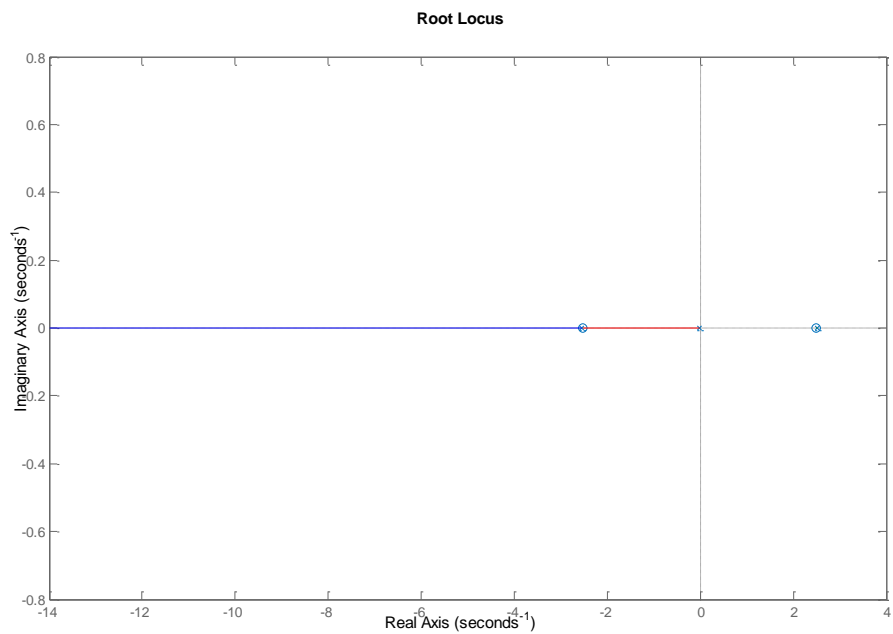


**Figure 4.4:** Root locus for  $G_2(s)$

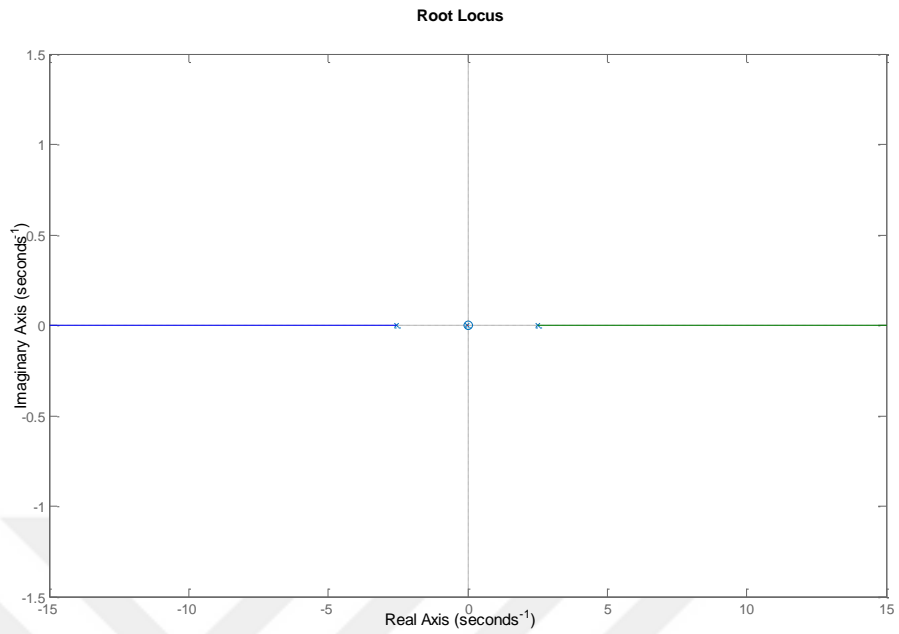


**Figure 4.5:** Root locus for  $G_3(s)$

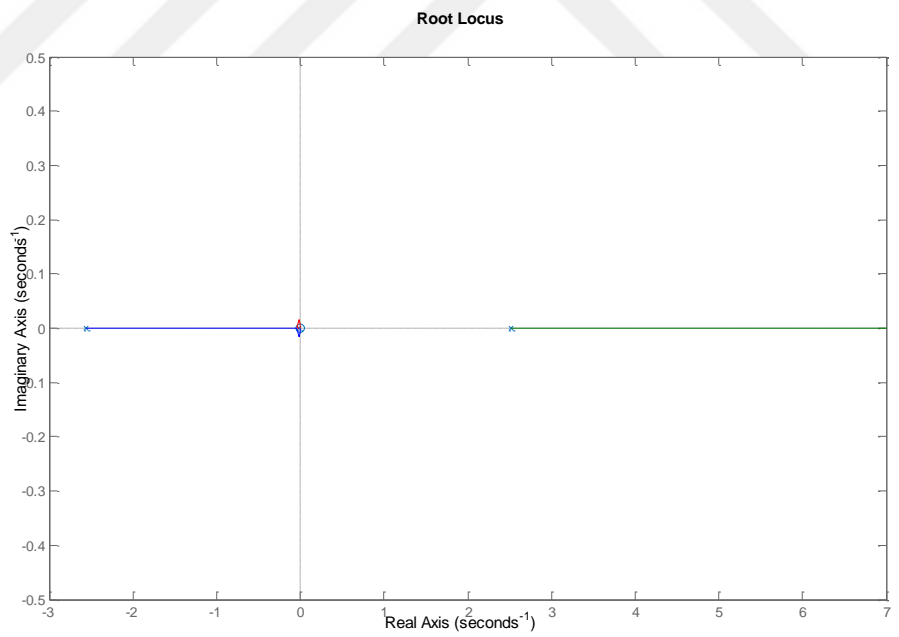


**Figure 4.6:** Root locus for  $G_4(s)$



As seen from root locus plots, the open loop system is unstable for all the states besides it is hard to control all the states at the same time with a feedback control strategy solely from one of the selected outputs. There are many alternatives for solving this control problem. One of them is establishing PID controllers for more than one output (i.e. cart position and pendulum angle together) and combining these controller outputs to carve out the final control signal. Another alternative is using state feedback [17-18]. State feedback is employed in order to relocate all the poles of the closed loop system to desired location. In simulations, employing state feedback is straightforward as not the actual state signals but their imitations in the simulative model are processed. However, to apply state feedback thoroughly in the simulations, we should check whether the system is small time locally controllable or not. If the linearized system is completely controllable at the unstable equilibrium point than the system is small time locally controllable as it is given by the theorem [19]. In general, controllability of non-linear systems is also studies in [20]. For showing the linearized system is controllable, we have to check the controllability matrix  $Q$ .

$$Q = [B \quad AB \quad A^2B \quad A^3B] \quad (4.7)$$

Now  $Q$  matrix can be computed as

$$Q = \begin{bmatrix} 0 & 0.3881 & -0.0078 & 0.0507 \\ 0.3881 & -0.0078 & 0.0507 & -0.0060 \\ 0 & -0.2495 & 0.0147 & -1.6063 \\ -0.2495 & 0.0147 & -1.6063 & 0.1590 \end{bmatrix} \quad (4.8)$$

The determinant of  $Q$  is non-zero ( $\det(Q)=0.3727$ ). Hence, the linearized system is completely controllable that means the non-linear system is small time locally controllable as explained in [19] and state feedback can be applied perfectly around the unstable equilibrium point. For state feedback, the Ackermann formula [17-18] is employed. Primarily the new eigenvalue locations for the system with state feedback should be determined. Checking the pole locations at Table 4.1, we decided to put them to -3, -3, -3, and -3. These values have more negative real parts compared to the eigenvalues of uncontrolled linearized system. Hence, the corresponding closed loop system characteristic polynomial will be

$$P(s) = (s+3)^4 = s^4 + 12s^3 + 54s^2 + 108s + 81 \quad (4.9)$$

The coefficients of the characteristic polynomial are  $p_0=81$ ,  $p_1=108$ ,  $p_2=54$ ,  $p_3=12$  and  $p_4=1$ .

To obtain the coefficients of the state feedback vector  $K$ , we need the vector  $v^T$  where

$$v^T = [0 \ 0 \ 0 \ 1]Q^{-1} \quad (4.10)$$

Taking the inverse of  $Q$ , we get

$$Q^{-1} = \begin{bmatrix} 0.0500 & 2.6300 & -0.0000 & 0.0828 \\ 2.6297 & -0.0079 & 0.00818 & -0.0123 \\ -0.0241 & -0.4088 & -0.0622 & -0.6359 \\ -0.4086 & -0.0025 & -0.6358 & -0.0039 \end{bmatrix} \quad (4.11)$$

Using Equation (4.10) and (4.11),  $v^T$  can be computed

$$v^T = [-0.4086 \quad -0.0025 \quad -0.6358 \quad -0.0039] \quad (4.12)$$

Now it is possible to find the transpose of state feedback vector  $K$

$$K^T = -p_0v^T - p_1v^T A - p_2v^T A^2 - p_3v^T A^3 - p_4v^T A^4 \quad (4.13)$$

Putting the values at of  $A$ ,  $v^T$  and  $p_0$ ,  $p_1$ ,  $p_2$ ,  $p_3$  and  $p_4$  at Equation (4.13) we obtain

$$K^T = [k_1 \ k_2 \ k_3 \ k_4] = [33.0982 \quad 44.3847 \quad 296.4294 \quad 116.9134] \quad (4.14)$$

This state feedback vector is used for stabilization of the pendulum in upright position. The computed SIMULINK model for this operation is given in Figure 4.7

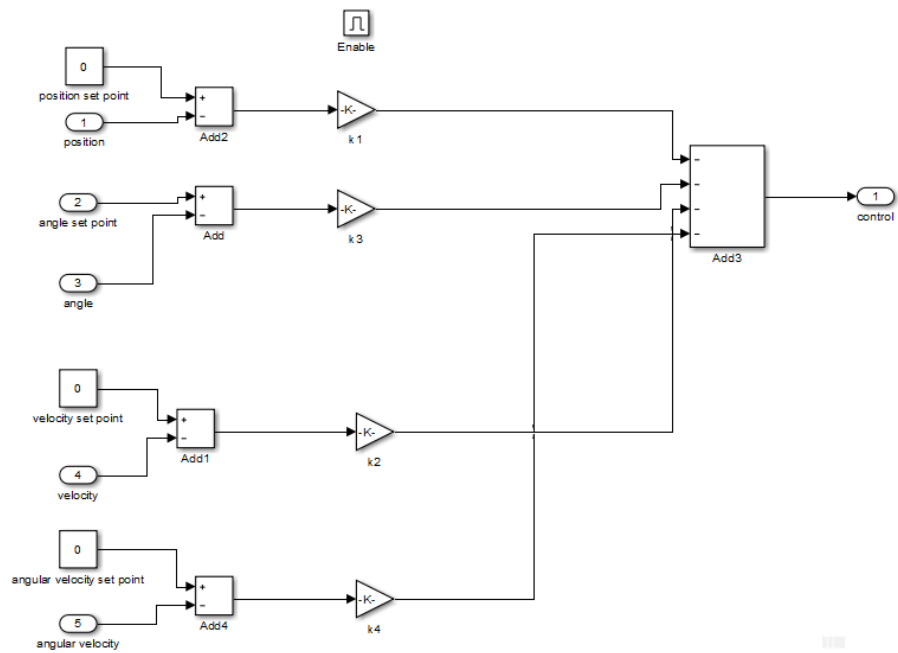


**Figure 4.7:** Cart-pendulum system stabilization using state feedback

In the model shown in Figure 4.7 there are 5 inputs (position, angle set point, angle, velocity and angular velocity) and 3 parameters which are taken to be equal to zero (position set point, velocity set point and angular velocity set point) and a single output (control). The state feedback parameters obtained in Equation (4.15) as  $k_1$ ,  $k_2$ ,  $k_3$  and  $k_4$  are used as the gain values of the gain blocks in Figure 4.7 and as the result state feedback control is implemented. Enable signal in the block activates this control strategy when necessary (If enable is 1 it is activated; this operation is performed in stabilization stage). The activated control strategy generates the control signal (voltage). This SIMULINK model is implemented as a sub-block is in Figure 4.8.

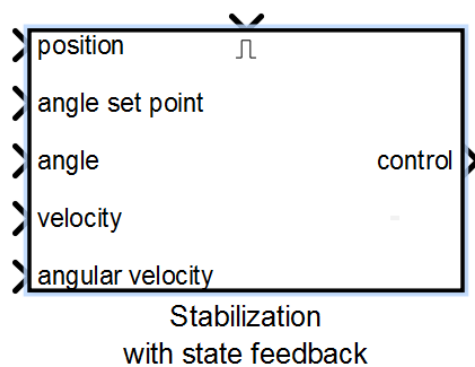


**Figure 4.8:** Stabilization with state feedback sub-block

### 4.2.3 Set Point Selection Sub-Block

In the simulation model, this sub-block is shown in Figure 4.9.

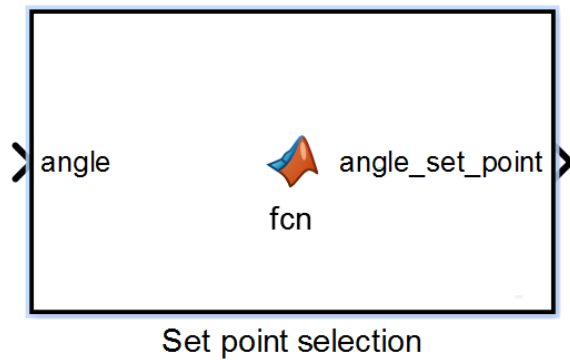


**Figure 4.9:** Set Point Selection Sub-Block

This sub-block is implemented as a MATLAB function. It has a single input (`angle`) and a single output (`angle_set_point`). It determines the angle set point at the stabilization stage (either 0 or  $2\pi$  radian) due to the number of net rotations of the pendulum starting from downright position (180 degrees) to upright position (to 0 or  $2\pi$  radians). If pendulum reaches the final upright position by rotating in clockwise direction (if `angle < radians`) `angle_set_point` is set to 0, otherwise it is set to  $2\pi$ . The code for set point selection is given in Appendix 1.

#### 4.2.4 Swing Up Control with Extra PI Position Control Sub-Block

In the simulation model this sub-block is shown in Figure 4.10

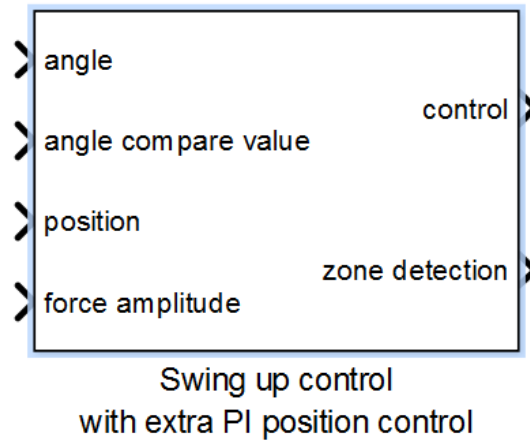


**Figure 4.10:** Swing up control with extra PI position control sub-block

This sub-block has 4 inputs (angle, angle compare value, position and force amplitude) and two outputs (control and zone detection). The expended view of the sub-block is given in Figure 4.11.

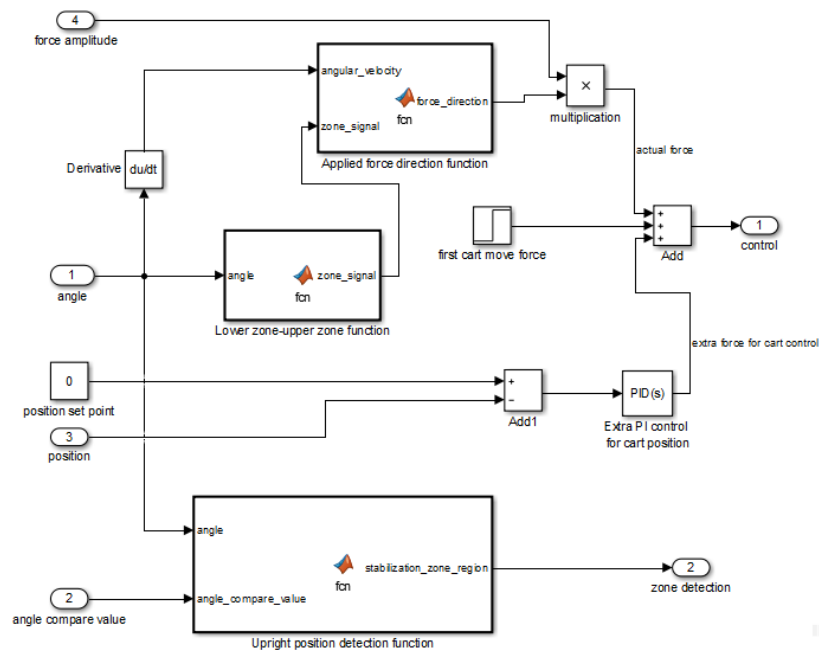


**Figure 4.11:** Expanded view of swing up control with extra PI position control sub-block

In the expended view, new SIMULINK sub-blocks are also implemented: These sub-blocks are ‘Applied force direction function’, ‘Lower zone-upper zone function’, ‘Upright position detection function’ and ‘Extra PI control for cart position’ sub-blocks.

#### 4.2.4.1 Applied Force Direction Function

The SIMULINK sub-block for this function is given in Figure 4.12

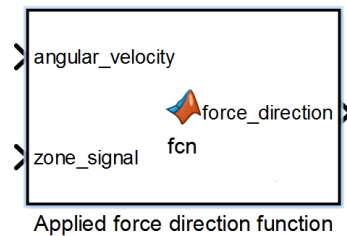


**Figure 4.12:** Applied force direction function sub-block.

This function takes two inputs. The first input is angular\_velocity (pendulum angular velocity). If the angular velocity is in clockwise direction its value is negative if it is in counterclockwise direction, its value is positive. The second input is zone\_signal. This input is equal to 1 when the pendulum is in the upper region, and it is equal to zero when the pendulum is in the lower region. The output of this function is force\_direction which gives the direction of the force that should be applied to swing the pendulum to make it reach to stabilization zone. The implementation of this function is given in Table 4.2

**Table 4.2:** Evaluation of force direction depending on angular\_velocity and zone\_signal inputs.

<b>angular_velocity and zone_signal</b>	<b>force_direction</b>
angular_velocity $\geq 0$ and zone_signal=1 (the pendulum returns in counterclockwise direction and the pendulum is at the upper zone)	-1 (in negative x direction)
angular_velocity $\geq 0$ and zone_signal=0 (the pendulum returns in counterclockwise direction and the pendulum is at the lower zone)	1 (in positive x direction)
angular_velocity $< 0$ and zone_signal=1 (the pendulum returns in counterclockwise direction and the pendulum is at the upper zone)	1 (in positive x direction)
angular_velocity $< 0$ and zone_signal=0 (the pendulum returns in counterclockwise direction and the pendulum is at the lower zone)	-1 (in negative x direction)

The MATLAB code of this function is given in the Appendix 2

#### 4.2.4.2. Lower Zone-Upper Zone Function

The SIMULINK sub-block for this function is given in given in Figure 4.13.

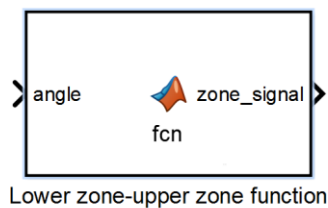


**Figure 4.13:** Lower zone-upper zone function sub-block

This function has one input (angle) and one output (zone\_signal). If the pendulum angle is at the upper zone, (angle value is between 0 and 90 degrees or angle value is between 270 and 360 degrees) the zone\_signal is equal to 1. If the pendulum angle is at the lower zone (the angle is between 90 and 270 degrees), the zone\_signal will be equal to 0. The MATLAB code of this function is given in the Appendix 3.

#### 4.2.4.3 Upright Position Detection Function

The SIMULINK sub-block for this function is given in given in Figure 4.14.

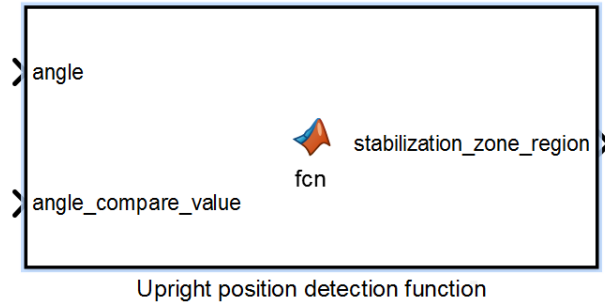


**Figure 4.14:** Upright position detection function sub-block

This function takes two inputs and it has one output. The inputs are angle (pendulum angle) and angle\_compare\_value whereas the output is stabilization\_zone\_region signal, which can be assigned two values (either 0 or 1). The function determines whether the system has reached to stabilization zone or not based on the comparison of the angle with the angle\_compare\_value. Stabilization zone is localized by the angle\_compare\_value in the simulation and it is set to 0.2 radians (11.4592 degrees). If the angle is between 0.2 and -0.2 radians this means the system is in stabilization zone and in this case stabilization\_zone\_region signal becomes 1 and the swing up stage is finalized and the system goes to stabilization stage, otherwise stabilization\_zone\_region signal is always equal to 0 and the system continues to operate in the swing up stage until the stabilization zone is reached. The MATLAB code of this function is given in the Appendix 4.



#### 4.2.4.4 Extra PI Control for Cart Position

This block is indeed realized in order not to let the cart move too close to the end of the rails in the swing up stage. It is a PI controller block that tries to pull the cart to its initial position ( $x_I=0$ ) as it moves away from its initial position. The PI controller parameters should be determined based on the experience in the swing up stage for better performance. The output of the sub-block is the extra control signal that tries to compensate the gap between the actual cart position and initial cart position.

#### 4.2.4.5. Swing up Stage Strategy

Swing up stage strategy is given in Figure 4.11. The explanation of this strategy can be summarized as follows: if the system is not in stabilization zone ( $\text{stabilization\_zone\_region} = 0$ ), based on the Lower zone-upper zone function, the  $\text{zone\_signal}$  is specified. The  $\text{zone\_signal}$  and angular velocity of the pendulum are used in determination of the evaluation strategy given in Table 4.2 to yield the  $\text{force\_direction}$  in swing up stage. Then the  $\text{force\_direction}$  is multiplied by the force amplitude to yield the actual force. The actual force is added with the first cart move force (employed to create the first cart movement from its initial position) and extra force for cart control (the force that intends to pull the cart to its initial position in order not to let it go the boundaries of the rail). The aggregation of these forces creates the control signals (voltage) that govern the system when the system is in swing up stage. Whenever, the system enters to the stabilization zone ( $\text{stabilization\_zone\_region} = 1$ ), the swing up stage finalizes.

### 4.3 Complete Control Strategy

The complete SIMULINK model is given in Figure 4.15.

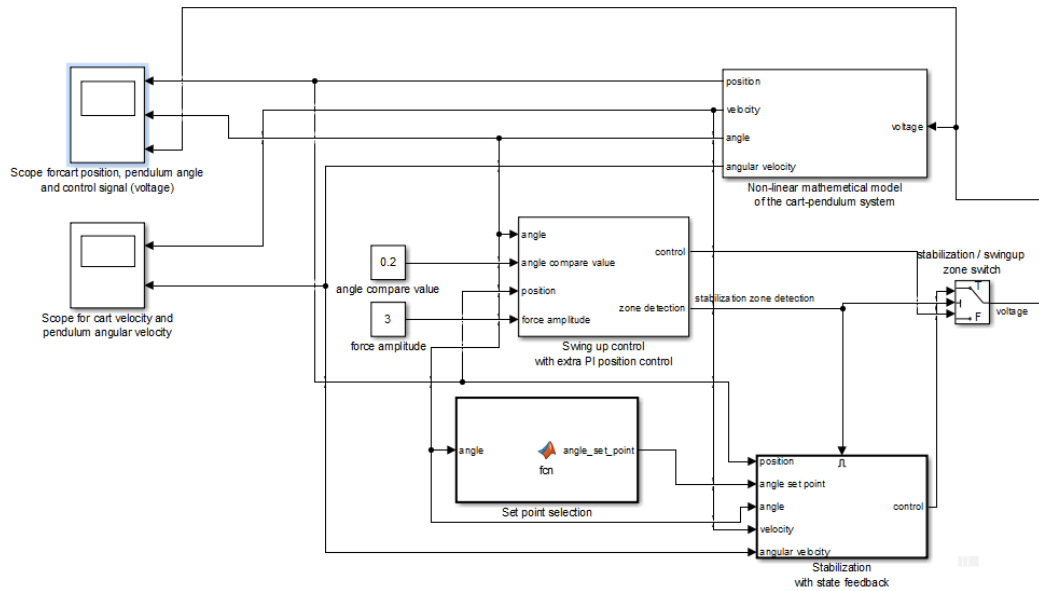


**Figure 4.15:** Complete Control Strategy

The explanation of operation of the complete model is as follows: the pendulum starts its movement from downright position in swing up stage. The non-linear mathematical model or the cart pendulum system is run by the voltage signal generated by the ‘Swing up control with extra PI position control sub-block. In this sub-block, the force amplitude is taken as 3 Newton and angle compare value is set to 0.2 radians. Swing up stage continues until zone detection (stabilization\_zone\_region) signal becomes 1 and the pendulum enters to the stabilization zone. When the pendulum enters the stabilization zone, hold (stabilization) stage takes action. In the stabilization stage ‘Stabilization with state feedback’ block is enabled and it begins to produce the voltage signal that runs the system. During these actions, all states and control signal are recorded in scopes. Using these procedures and parameters and running the simulation model given in Figure 4.15 we have obtained the results given in Figure 4.16 and Figure 4.17.

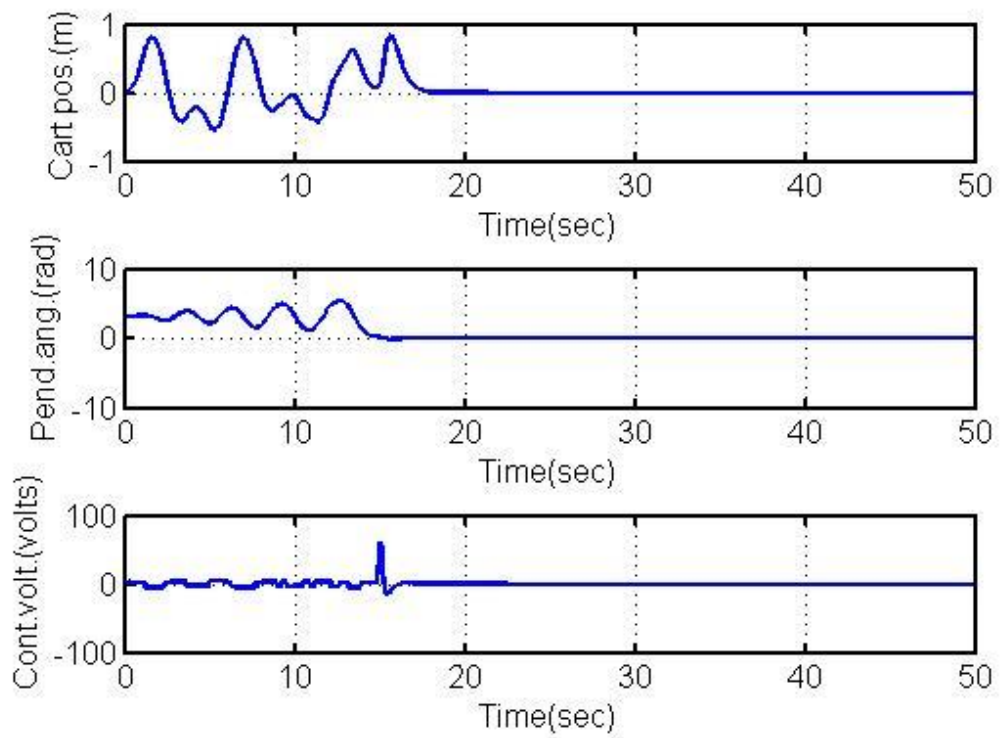


**Figure 4.16:** Cart position, pendulum angle and control voltage plotted versus time.

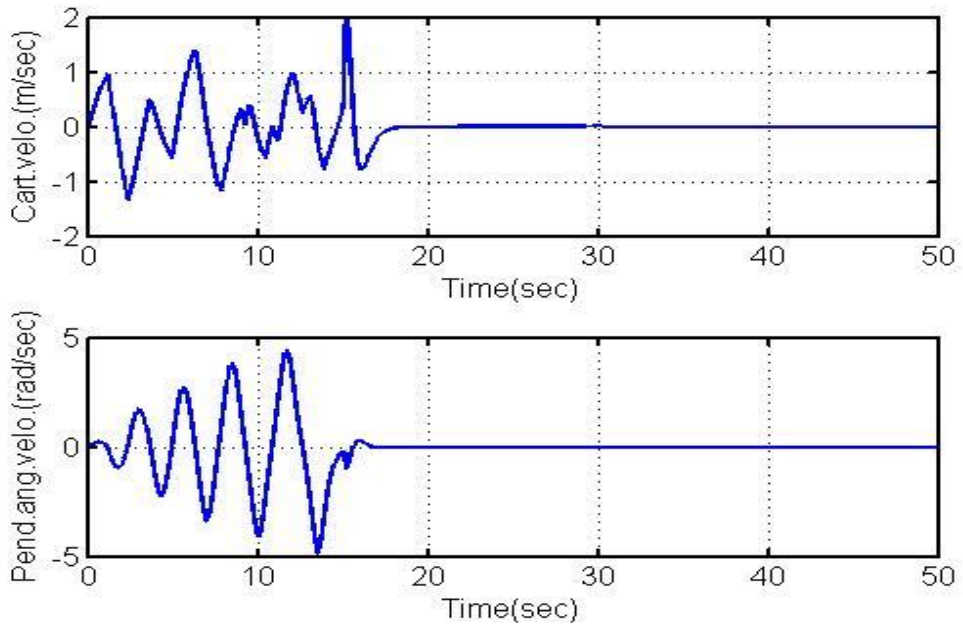


**Figure 4.17:** Cart velocity and pendulum angular velocity plotted versus time.

As seen from Figure 4.16 and 4.17 using state feedback at the stabilization, stage (with the state feedback parameters given in Equation 4.14) stabilizes the system. We also want to see the performance of state feedback for reference signal tracking. For this reason, position set point block in Figure 4.7 is replaced by a pulse train that is activated at the 20<sup>th</sup> second of the simulation. The amplitude of the pulse train is 0.1 and period is 10 seconds with a duty cycle of 50%. With this reference change, we simulate the model given in Figure 4.15 once again and we have obtained the results given in Figure 4.18 Figure 4.19 and Figure 4.20.

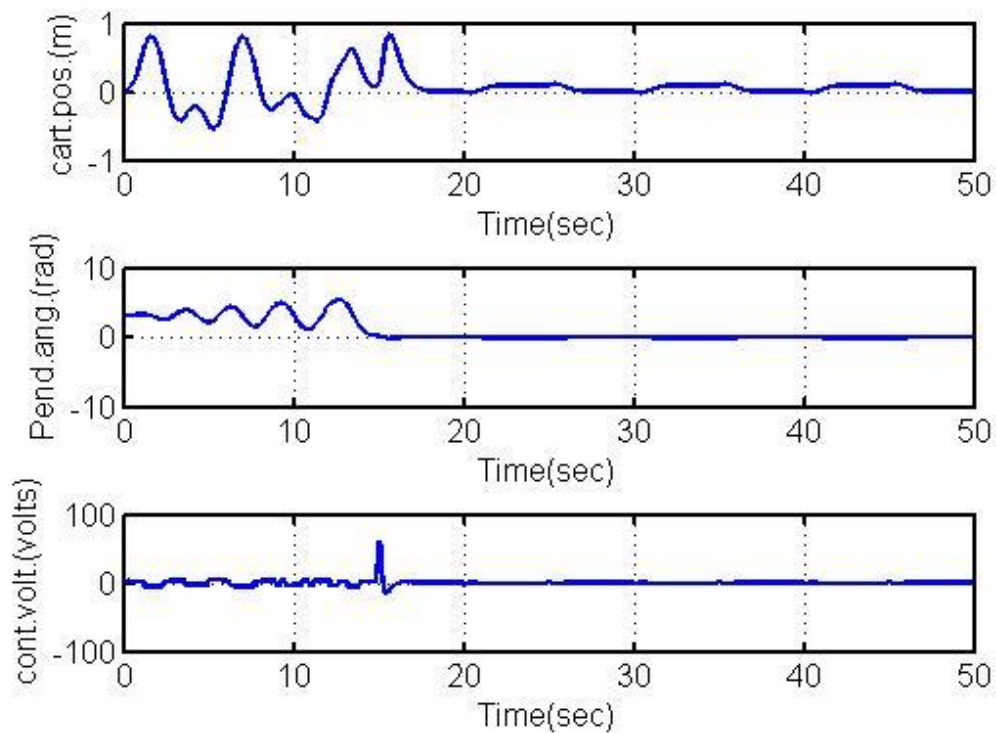


**Figure 4.18:** Cart position and pendulum angle and control voltage plotted versus time for reference tracking.

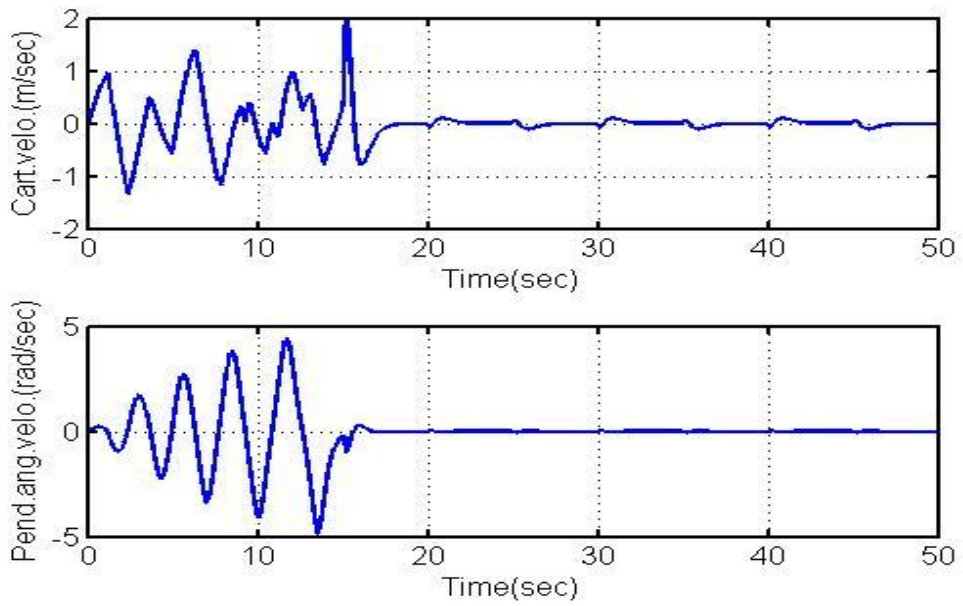


**Figure 4.19:** Cart velocity and pendulum angular velocity plotted versus time for reference tracking.

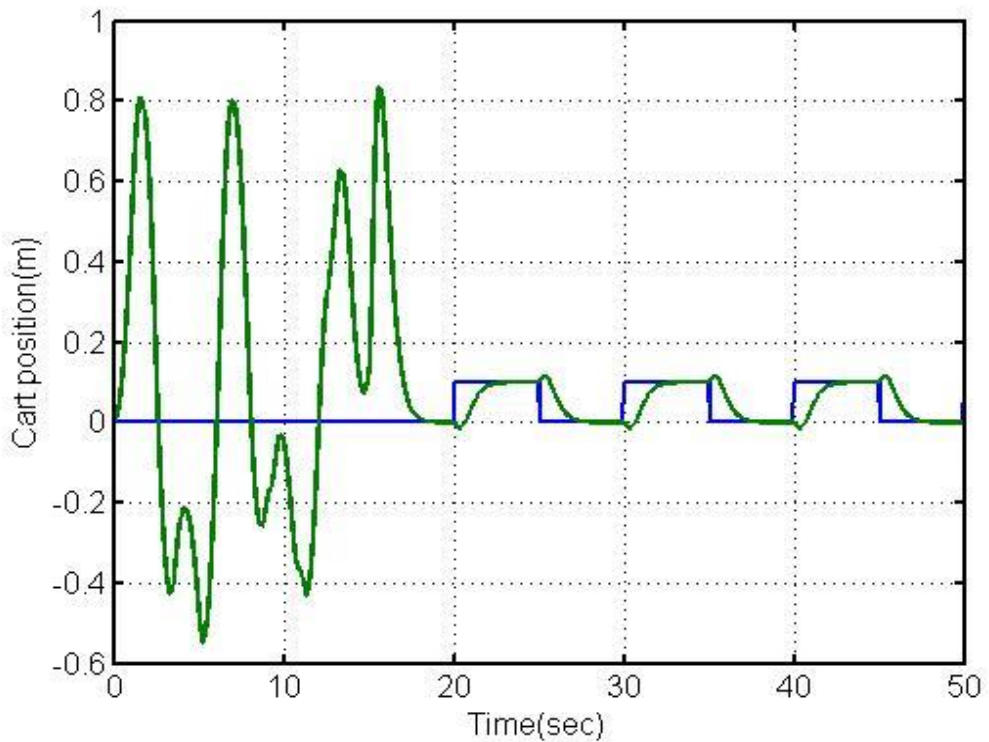


**Figure 4.20:** Cart position (green) and reference cart position (blue) plotted versus time for reference tracking.

As seen from Figure 4.18, Figure 4.19 and Figure 4.20, the state feedback can also fulfill the reference signal-tracking task successfully.

## CHAPTER 5

### REAL- TIME SYSTEM IDENTIFICATION AND CONTROLLER DESIGN

#### 5.1 Running Real Time Model

System identification is an important intermediate stage to realize more successful controller structures for the real time applications. For this reason, we have used the previously established ‘InvPendIdent’ model [1]. This model is a real time application that can be divided into two different stages where the first stage is the swing up stage that is carried out to take the system from the initial state ( $x_1=0, x_2=0, x_3=\pi, x_4=0$ ) to a state where the system is in stabilization zone ( $-0.25 \text{ rad} \leq x_3 \leq 0.25 \text{ rad}$  and  $x_1$  stay in the limits of the rail). The second stage is the use of linear controllers coupled with extra excitation signal to carry out the tasks of stabilizing the cart position  $x_1$  and the pendulum angle  $x_3$  simultaneously with exiting the stabilized system by the extra excitation signal to carry out the identification process. Hence, the data obtained in the swing up stage related with the states and extra excitation signal are not used in the identification process. This stage is indeed just a preliminary step to bring the system to the stabilization stage where the identification process is actually covered.

The details of the swing up stage are as follow: It is initiated by the slow oscillations. The cart-pendulum system is moved from the initial state to states where oscillations are observed both in the cart position and pendulum angle. These oscillations are controlled oscillations such that the cart position does not exceed the limits of the rail it is moving over and besides the pendulum navigates more widespread nearly circular trajectories from one swing to another. This is practiced by increasing the magnitude of the force applied to the cart-pendulum system in each swing in opposite directions by a specific algorithm similar to the one explained in Chapter 4

in the simulation example. This stage is suddenly stopped and stabilization stage is activated whenever, the system states enter the stabilization (hold) zone.

The stabilization stage includes two tasks that are fulfilled simultaneously. One of them is the stabilization of the system at and around an unstable equilibrium point (i.e.  $x_1=0$ ,  $x_2=0$ ,  $x_3=\pi$ ,  $x_4=0$ ) and the other one is the system identification task. Whenever, the system enters the stabilization zone two previously designed PID controllers in [1] (one for cart position control and the other one for pendulum angle control) instantly begin to rule over the system. The mathematical structure of the controllers for cart position and pendulum angle are given in Equation (5.1) and Equation (5.2) respectively

$$C_{cart\_position}(s) = 7 + \frac{0.1}{s} + 2s \quad (5.1)$$

$$C_{pend\_angle}(s) = 20 + \frac{0.1}{s} + 2s \quad (5.2)$$

In these equations, the derivative parts of the controllers are also connected to a previously designed low pass filter [1] in order to get rid of the noise which is amplified due to the differentiation process. This filter is given by

$$C_{filter}(s) = \frac{10^4}{s^2 + 70.4s + 10^4} \quad (5.3)$$

This filter eliminates high frequency noise and yields smother control signals. The filter is also used at the swing up stage in order to manipulate more precise and accurate cart velocity ( $x_2$ ) and pendulum angular velocity ( $x_4$ ) signals. The magnitude and phase characteristics of this filter's frequency response are given in Figure 5.1.

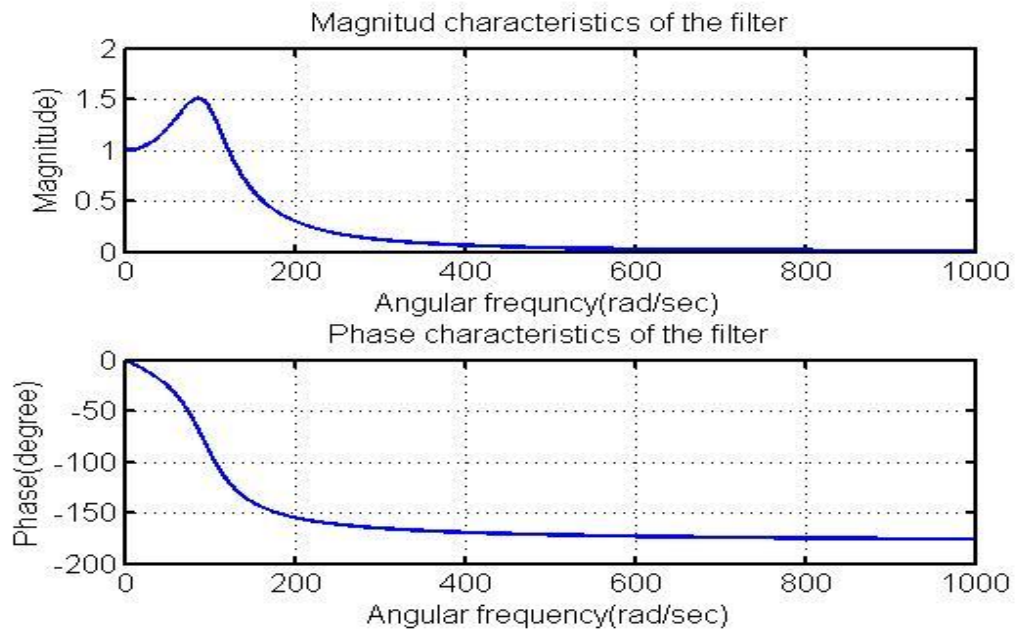


**Figure 5.1:** Magnitude and Phase characteristics of the low-pass filter used in the derivative control part of PID controllers.

The filter passes small angular frequency components (between 0 and 20 rad/sec) with a gain nearly equal to 1. It amplifies the mid-range angular frequencies (20 to 120 rad/sec) slightly and it rejects high-range angular frequencies very sharply (after 130 rad/sec).

Another source of noise is the undesired mechanical vibrations both in swing up and stabilization stage. The states  $x_2$  (cart velocity) and  $x_4$  (pendulum angular velocity) are the time derivatives of the states  $x_1$  (cart position) and  $x_3$  (pendulum angle) respectively. When there are undesired vibrations in the control process the states measured by the sensor ( $x_1$  and  $x_3$ ) are sure to be noisy. Taking the derivatives of these states amplifies the noise in the new states created due the derivatives. Hence, states  $x_2$  and  $x_4$  contains more noise compared to  $x_1$  and  $x_3$ . In order to get rid of the excessive noise  $x_2$  and  $x_4$  are also passed from the filter given in Equation (5.3) for obtaining these states more precisely in both the swing up stage and the stabilization stage coupled with the identification process.

The PID controllers employed in the stabilization stage are assumed to have average performance, however, they are still successful. For identification mission the PID



controllers outputs are coupled with an extra excitation signal that is used at the identification task. The block diagram of control strategy coupled with extra excitation signal for identification purpose is shown in Figure 5.2.

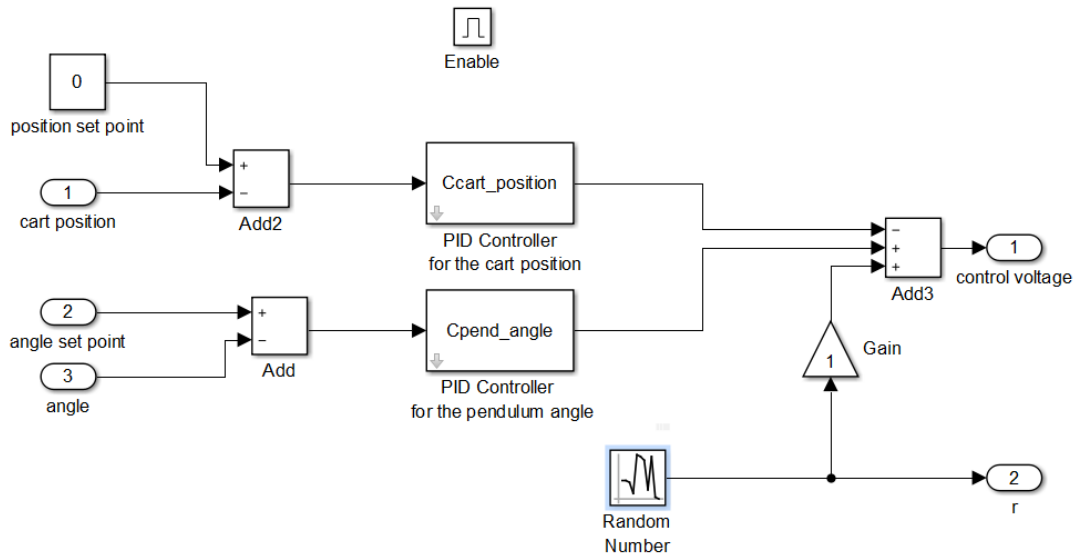


**Figure 5.2:** Control strategy coupled with system identification

As seen from Figure 5.2, the controller structure is activated by an Enable signal when necessary (whenever the system states reach to stabilization zone). There are 3 inputs (cart position, angle set point and angle) and 1 parameter (position set point) which is initialized as 0. The angle set point of the model is either taken to be equal to 0 or  $2\pi$  depending on the number of net rotations of the pendulum. A random number function is inserted to block to generate the extra excitation signal  $r$ . The signals coming from the PID controllers for stabilizing the cart position and pendulum angle and the extra excitation signal are aggregated to obtain the control signal (control voltage). The control voltage drives the system and the system is stabilized and then it is kept stabilized in the stabilization zone while the system is excited with the extra excitation signal. Due to the system configuration and used coordinate frame the positive  $x$  direction for the real time system and the applied force direction are opposite (if  $F$  is positive it causes  $x_1$  to decrease and if  $F$  is

negative it causes the  $x_1$  to increase). This effect is implanted into the control strategy shown in Figure 5.2 in the form of a negative addition in the addition block Add3.

Using this control strategy, the state signals for  $x_1$  and  $x_3$  and the extra excitation signal are recorded throughout the real time application which lasts for 40 seconds. The profile of the signals (cart position, pendulum angle and extra excitation signal) obtained as the result of this application are shown in Figure 5.3 In Figure 5.4 the unfiltered pendulum angular velocity and the cart velocity signals are also given.

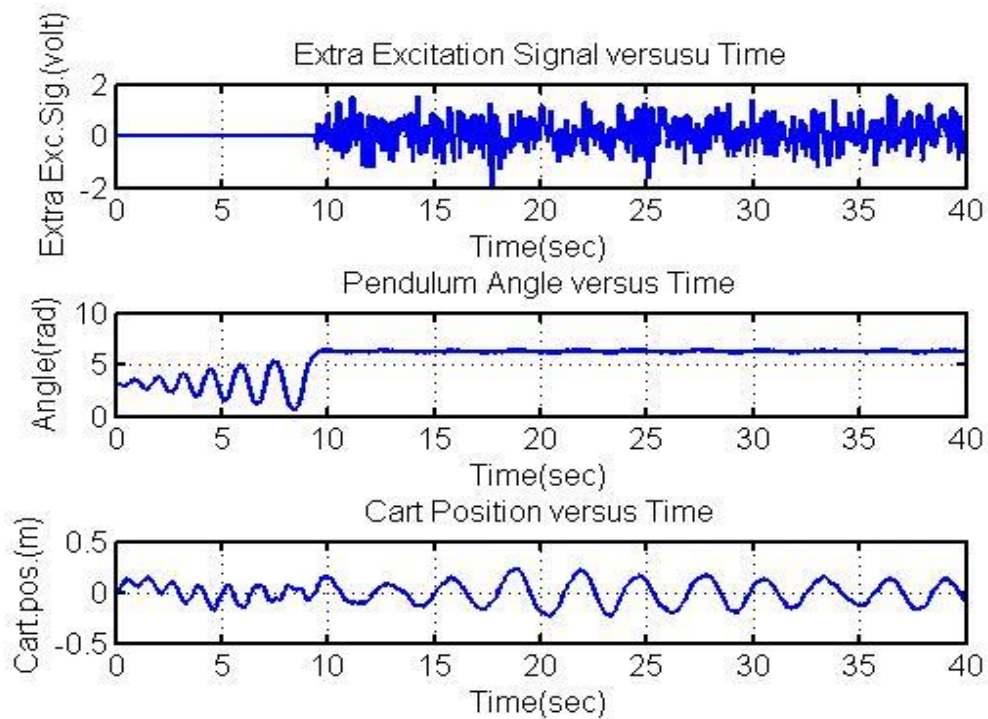


**Figure 5.3:** Pendulum angle, cart position and extra excitation signals in the identification step.

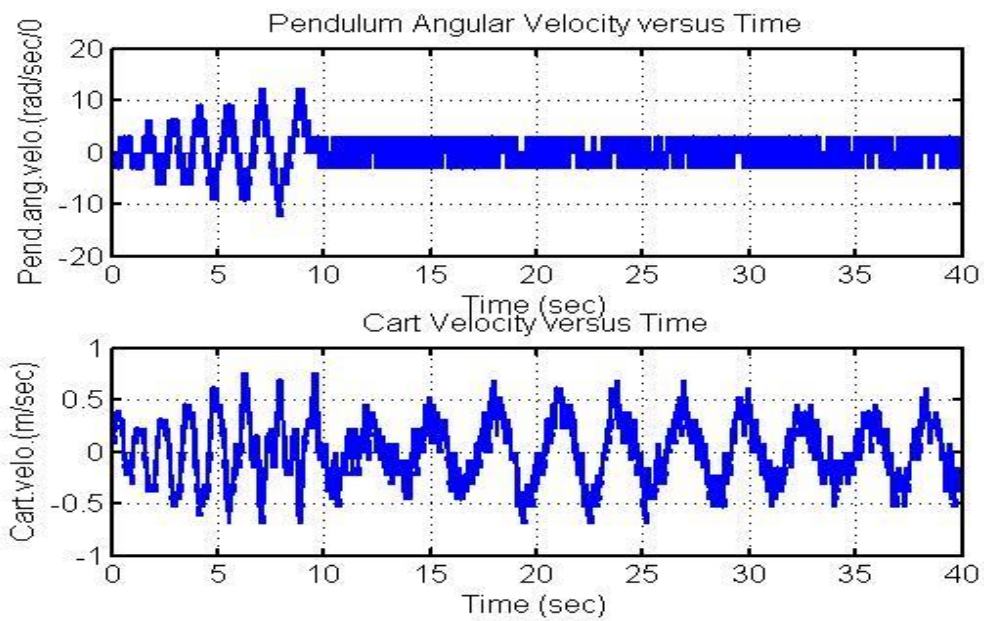


**Figure 5.4:** Unfiltered pendulum angular velocity and the cart velocity signals in the identification step.

As seen from the Figure 5.3, the system is stabilized (the pendulum angle remains nearly constant around  $2\pi$  radians closely after 10 seconds) by the use of these two controllers. As there is some extra excitation signal the cart position  $x_1$  is somewhat oscillatory however these oscillations do not cause a sudden change in the pendulum angle value. From Figure 5.4. it is easy to observe that the unfiltered pendulum angular velocity and the cart velocity signals are very noisy (especially the pendulum angular velocity signal). Besides, the maximum angular velocity value of the pendulum is seen to be around 12-13 rad/sec. Hence, it is convenient to use the filter given in Equation (5.3) both in the PID controllers and in the other processes of the swing up stage to eliminate the noisy components of the states  $x_2$  and  $x_4$ . When the noise is filtered out with the filter used in Equation (5.3). we obtain the following pendulum angular velocity and cart velocity profiles given in Figure 5.5 and Figure 5.6 respectively

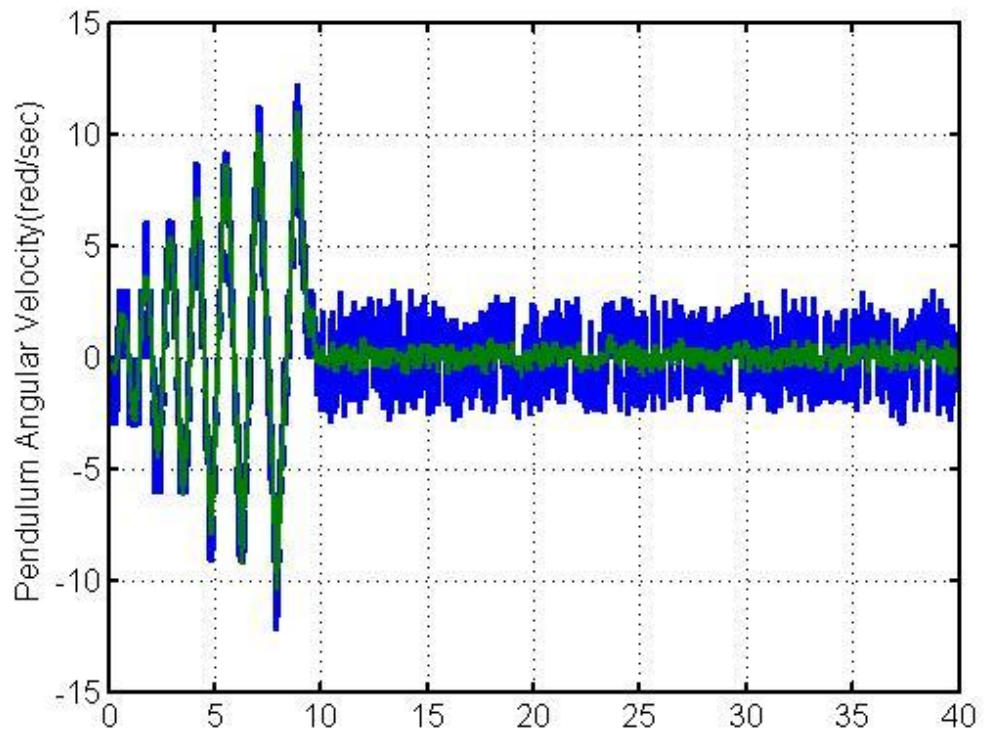


**Figure 5.5:** Filtered (green) and unfiltered (blue) pendulum angular velocity versus time in the identification step.

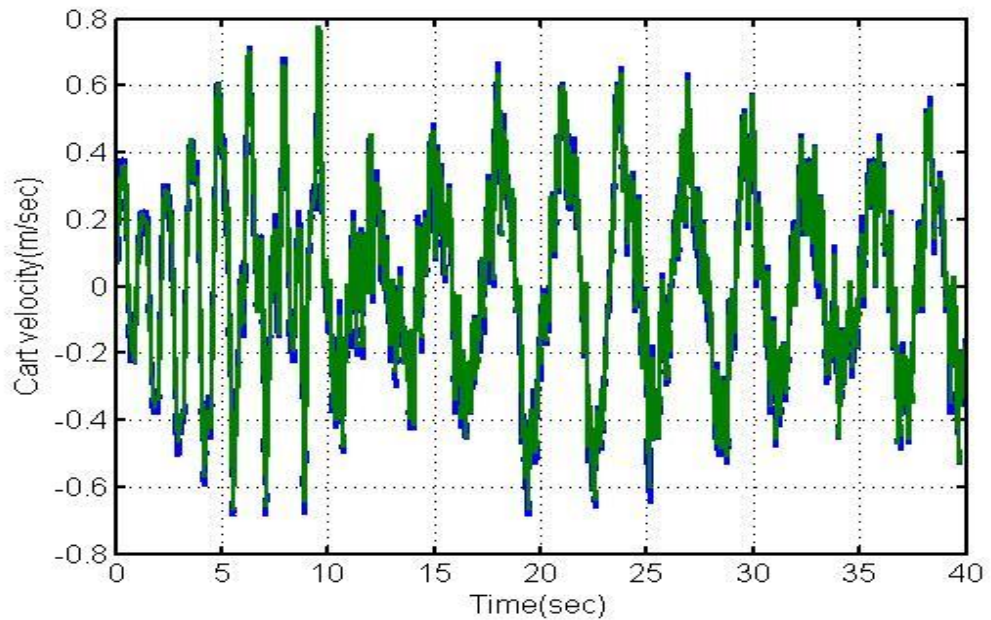


**Figure 5.6:** Filtered (green) and unfiltered (blue) cart velocity versus time in the identification step

As can be seen from Figure 5.5 and Figure 5.6 the filtering of the pendulum angular velocity and the cart velocity signals eliminates most of the components of the noise. The filtering effect is much more significant especially for the pendulum angular velocity signal.

## 5.2. System Identification

In the system identification step we will use the data gathered in Section 5.1. These data are the states  $x_1$  and  $x_3$  and the extra excitation signal  $r$ . As seen from the Figure 5.3 a non-zero extra excitation signal is first observed nearly after 9 seconds (it is the first time the system gets into stabilization zone) and the pendulum angle nearly settles around the unstable equilibrium point ( $x_3 \approx 2\pi$  radians or  $x_3 \approx 0$  radians) when the time is nearly equal to 10 seconds. Thus, to use in the identification process,  $x_1$ ,  $x_3$  and  $r$  values are recorded after the 10<sup>th</sup> second. However, recording them is not enough. In order to start the identification, process these data might require a pre-processing. A pre-processing step is applied to  $x_3$ . If the pendulum rotates a net amount of  $\pi$  radians in counterclockwise direction starting from the initial point ( $x_3 = \pi$  radians initially) it stabilizes around  $2\pi$  and reversely if it rotates a net amount of  $-\pi$  radians in clockwise direction starting from the initial point it stabilizes around 0. Hence, as an extra normalization step, if the pendulum stabilizes around  $2\pi$ , we subtract  $2\pi$  from each  $x_3$  data and use this normalized data as actual  $x_3$  data.

In the identification step the system identification toolbox of MATLAB is used. One should not forget that not the exact mathematical model of the real time system is found but approximated model by system identification is attained. Besides, the data related with states  $x_1$  and  $x_3$  are the data obtained for the stabilized system. Hence, they are not solely the data of the open loop system. There should be some extra effort to identify the open loop system structure.

The identification step starts with determining the structure of the controlled closed loop system. If we want to show them as block diagrams, we can use the following models Figure 5.7 and Figure 5.8

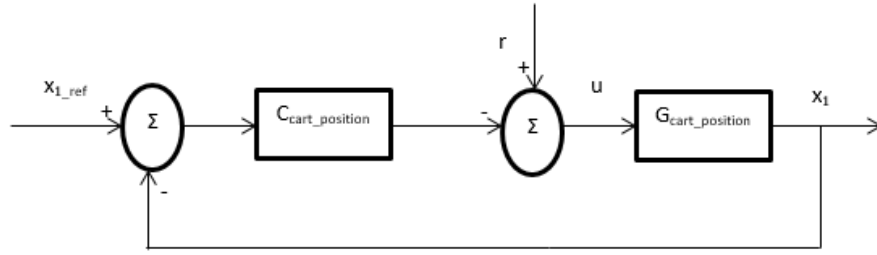


**Figure 5.7:** Identification controller for closed-loop control model.

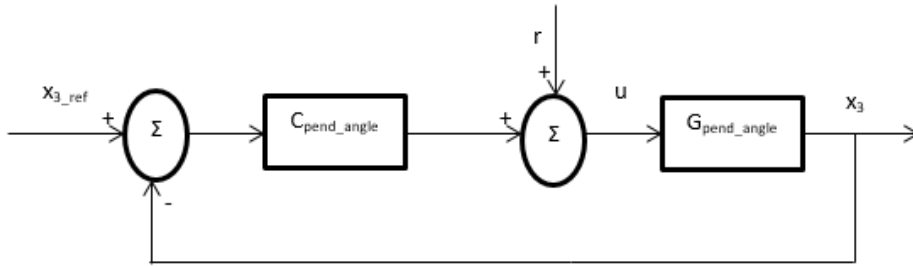


**Figure 5.8:** Identification controller for closed-loop control model.

In Figure 5.7 and Figure 5.8,  $x_{1\_ref}$  is the cart position reference value (position set point),  $x_1$  is the cart position,  $x_{3\_ref}$  is the pendulum angle reference value (angle set point),  $x_3$  is the pendulum angle,  $r$  is the extra excitation signal,  $u$  is the control signal.  $G_{cart\_position}$  is the linearized open loop transfer function for the cart position,  $G_{pend\_angle}$  is the linearized open loop transfer function for the pendulum angle,  $C_{cart\_position}$  is the PID controller for the cart position given in Equation (5.1),  $C_{pend\_angle}$  is the PID controller for the pendulum angle given in Equation (5.2). If we check the signs of the addition blocks where the extra excitation signal is added, in Figure 5.7 the sign is negative since it is coming from the cart position and it is positive in Figure 5.8 since it is coming from the pendulum angle (check the model in Figure 5.2).

For both models the reference values can be taken as 0 ( $x_{1\_ref}=0$  and  $x_{3\_ref}=0$  due to normalization). Hence, we need to find the closed loop linearized mathematical relations where  $r$  is the input and  $x_1$  and  $x_2$  are the outputs. Let's say the closed loop system has the transfer functions  $T_1(s)$  and  $T_2(s)$  where:

$$T_1(s) = \frac{X_1(s)}{R(s)} \quad (5.4)$$

$$T_2(s) = \frac{X_3(s)}{R(s)} \quad (5.5)$$

In Equation (5.4) and Equation (5.5),  $X_1(s)$ ,  $X_2(s)$  and  $R(s)$  are the Laplace transformed forms of signals  $x_1$ ,  $x_2$  and  $r$  respectively. Taking the reference values to be equal to 0, these transfer functions can mathematically be obtained as

$$T_1(s) = \frac{G_{cart\_position}(s)}{1 - G_{cart\_position}(s) \times C_{cart\_position}(s)} \quad (5.6)$$

$$T_2(s) = \frac{G_{pend\_angle}(s)}{1 + G_{pend\_angle}(s) \times C_{pend\_angle}(s)} \quad (5.7)$$

The identification toolbox of MATLAB is used in order to find the closed loop transfer functions of  $T_1(s)$  and  $T_2(s)$ . For this purpose, states  $x_1$  and  $x_2$  and extra excitation signal  $r$  are employed in the identification process where  $r$  is the input and  $x_1$  and  $x_3$  are the outputs. The identification process yields the transfer functions for  $T_1(s)$  and  $T_2(s)$ . The success percentages (fit to estimate to data) of the transfer functions  $T_1(s)$  and  $T_2(s)$  are 85.7% and 81.25% respectively (success percentages are evaluated by the mean square error between the actual state values and the state value calculated using  $T_1(s)$  and  $T_2(s)$ ). In the system identification step, it is assumed that  $T_1(s)$  and  $T_2(s)$  are fourth order transfer functions with 4 poles and 2 zeros in reality by increasing the order of  $T_1(s)$  and  $T_2(s)$  better success rates and better transfer functions can be obtained, however as system order increases, the open loop system transfer function gets more complex structures and it becomes more difficult to design controllers. Due to this reason, the number of poles is selected as 4 and number of zeros is selected as 2 for each transfer function.

The resulting  $T_1(s)$  and  $T_2(s)$  are:

$$T_1(s) = \frac{-0.08784s^2 + 0.4083s - 60.43}{s^4 + 2.87s^3 + 85.04s^2 + 29.45s + 373.4} \quad (5.8)$$

$$T_2(s) = \frac{10.68s^2 - 6.981s + 5.239}{s^4 + 18.67s^3 + 159.1s^2 + 117.7s + 696.5} \quad (5.9)$$

The poles and zeros of the transfer function are shown in Table 5.1.

**Table 5.1:** Poles and zeros of the transfer functions  $T_1(s)$  and  $T_2(s)$ .

$T_1(s)$	-1.3281+8.8333j -1.3281-8.8333j -0.1067+2.1607j -0.1067-2.1607j	2.3242+26.1247j 2.3242-26.1247j
$T_2(s)$	-9.2266+8.0874j -9.2266-8.0874j -0.1073+2.1483j -0.1073-2.1483j	0.3268+0.6195j 0.3268-0.6195j

As seen from the poles of  $T_1(s)$  and  $T_2(s)$ , the closed loop systems are stable (real parts of all the poles are smaller than 0). Now using the identified closed loop systems, we can find the open loop transfer functions by

$$G_{cart\_position}(s) = \frac{T_1(s)}{1+T_1(s) \times C_{cart\_position}(s)} \quad (5.10)$$

$$G_{pend\_angle}(s) = \frac{T_2(s)}{1-T_2(s) \times C_{pend\_angle}(s)} \quad (5.11)$$

Using Equation (5.10), Equation (5.1), Equation (5.11), Equation (5.2) we obtain the minimal realization of  $G_{cart\_position}(s)$  and  $G_{pend\_angle}(s)$  as

$$G_{cart\_position}(s) = \frac{-0.08784s^3 + 0.4083s^2 - 60.43s}{s^5 + 2.694s^4 - 85.24s^3 - 88.566s^2 - 49.54s - 6.043} \quad (5.10)$$

$$G_{pend\_angle}(s) = \frac{10.68s^3 - 6.981s^2 + 5.239s}{s^5 - 2.693s^4 - 40.52s^3 + 245.8s^2 + 592.9s - 0.5239} \quad (5.11)$$

These transfer functions are the outcomes of system identification procedure. Hence, we cannot account them as the actual transfer functions of the linearized system at the unstable equilibrium point. However, they still exhibit a respectable estimate of the functionality of the real time system. The poles and the zeros of the  $G_{cart\_position}(s)$  and  $G_{pend\_angle}(s)$  are given in Table 5.2.



**Table 5.2:** Poles and zeros of  $G_{cart\_position}(s)$  and  $G_{pend\_angle}(s)$

Transfer Function	Poles	Zeros
$G_{cart\_position}(s)$	-1.8309+9.2727j -1.8309-9.2727j 1.3974 -0.2148+0.0478j -0.2148-0.0478j	0.0000 2.3242+26.1247j 2.3242-26.1247j
$G_{pend\_angle}(s)$	5.6923+3.6016j 5.6923-3.6016j -6.7606 -1.9320 0.0009	0.0000 0.3268+0.6195j 0.3268-0.6195j

The root locus plots of  $G_{cart\_position}(s)$  and  $G_{pend\_angle}(s)$  are given in Figure 5.9 and 5.10 respectively.

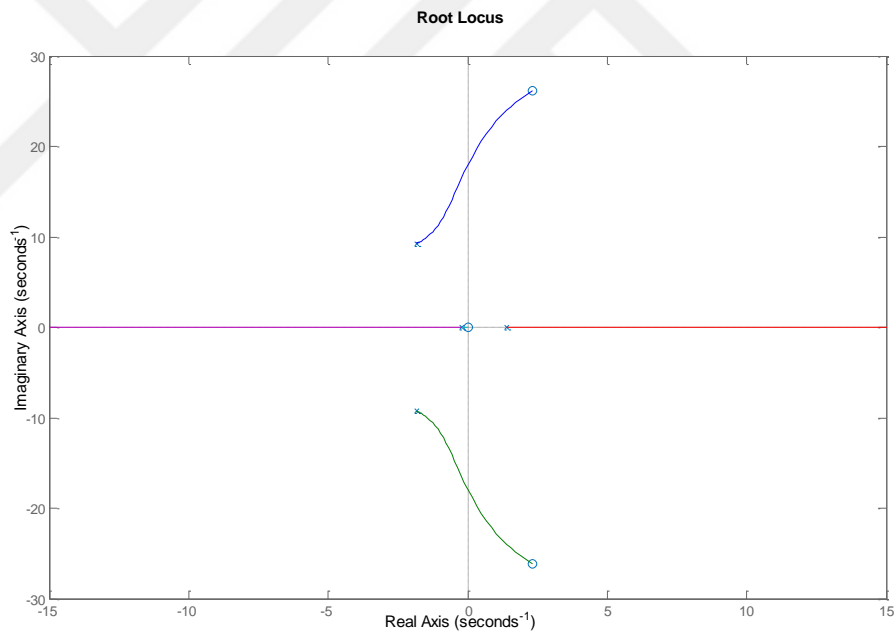


**Figure 5.9:** The root locus plot of  $G_{cart\_position}(s)$

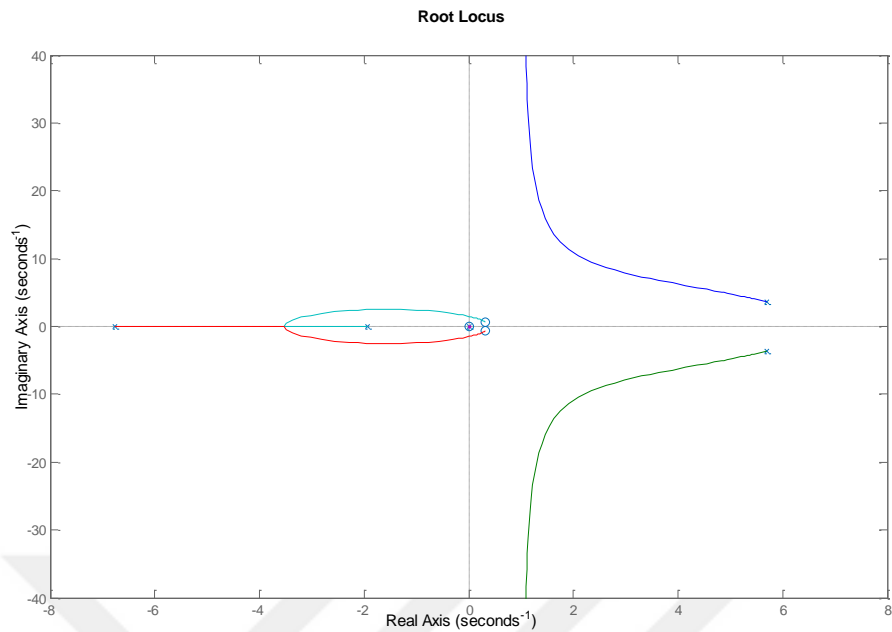


**Figure 5.10:** The root locus plot of  $G_{pend\_angle}(s)$ .

As seen from the Figure 5.9, as we give positive gain for  $G_{cart\_position}(s)$ , one of the roots goes to positive infinity and the other one goes to negative infinity direction along the real axis. Thus, according to this plot there are two asymptotes and one of them is 0 degrees whereas the other one is 180 degrees. In reality for a linear system having 5 poles and 3 zeros, the asymptotes in the root locus plot should be 90 and -90 degrees as it is the case for the root locus plot obtained for  $G_{pend\_angle}(s)$  in Figure 5.10. This difference comes from the sign of the highest order term at the numerator of the transfer function. For  $G_{cart\_position}(s)$  this term is negative while for  $G_{pend\_angle}(s)$  it is positive. Hence, the root locus plot of  $G_{cart\_position}(s)$  resembles a complementary root locus plot.

### 5.3. Controller Design

In order to design more competent and successful controllers, the behavior of the system should be understood properly. This is definitely possible if the root locus plots given in Figure 5.9 and 5.10 are better investigated and attained information from these plots are properly employed for controller design and development procedure. Our aim is to design PID controllers that are functioning altogether in

harmony both to stabilize cart position ( $x_1$ ) and pendulum angle ( $x_3$ ) at the unstable equilibrium point. Initially, it is intended to design a PID controller structure for the pendulum angle then for the cart position and finally these controllers performance will be tested and compared with respect to the controllers given in Equation (5.1) and Equation (5.2).

### 5.3.1. Controller Design for Pendulum Angle Control

The transfer function for  $G_{pend\_angle}(s)$  has 3 unstable poles (locations are  $5.6923+3.6016j$ ,  $5.6923-3.6016j$ ,  $0.0009$ ) and a zero at the origin (location  $0$ ). Besides, one of the unstable poles (location  $0.0009$ ) is very close to the zero at the origin. As a design specification, the most important objective should be getting rid of all of the unstable poles (the real parts of the poles should be negative) while not letting any stable pole to become unstable. After this objective is accomplished, one should also enhance the quality of the stability sustained in the system. For example, another important objective that the system exhibit should be obtaining zero steady state error value for unit step type inputs. For this purpose, we decided to use a PID controller:

$$C_{pend\_angle}(s) = P + \frac{I}{s} + Ds \quad (5.12)$$

The PID controller in Equation (5.12) can also be written in the form

$$C_{pend\_angle}(s) = D \times \left( \frac{s^2 + \frac{P}{D}s + \frac{I}{D}}{s} \right) \quad (5.13)$$

$C_{pend\_angle}(s)$  has a single pole at the origin and two zeros. The zeros of  $C_{pend\_angle}(s)$  can be chosen such that with suitable parameter settings, these two zeros are due to attract and pull the unstable poles of  $G_{pend\_angle}(s)$  located at  $5.6923+3.6016j$ ,  $5.6923-3.6016j$  when  $C_{pend\_angle}(s)$  and  $G_{pend\_angle}(s)$  are multiplied to yield the open loop controller and the identified system total transfer function as:

$$G_{pend\_angle\_open}(s) = D \times \left( \frac{s^2 + \frac{P}{D}s + \frac{I}{D}}{s} \right) \left( \frac{10.68s^3 - 6.981s^2 + 5.239s}{s^5 - 2.693s^4 - 40.52s^3 + 245.8s^2 + 592.9s - 0.5239} \right) \quad (5.13)$$

As there is pole-zero cancellation on Equation (5.13),  $G_{pend\_angle\_open}(s)$  can be reassigned as

$$G_{pend\_angle\_open}(s) = D \times \left( s^2 + \frac{P}{D}s + \frac{I}{D} \right) \left( \frac{10.68s^2 - 6.981s + 5.239}{s^5 - 2.693s^4 - 40.52s^3 + 245.8s^2 + 592.9s - 0.5239} \right) \quad (5.14)$$

The pole-zero cancellation at the origin for the transfer function  $G_{pend\_angle\_open}(s)$  is expected to stabilize the unstable pole located at 0.0009 as this pole will probably traverse to and at the end collide with the pole located at -1.9320 with suitable  $P, I, D$  parameter settings.

Now, as an intermediate step, we want to put two zeros to locations at -3 and -3 to attract the unstable poles at  $5.6923 + 3.6016j$  and  $5.6923 - 3.6016j$ . These two new zeros will have a polynomial equation that should be equal to the zeros of the controller as

$$s^2 + \frac{P}{D}s + \frac{I}{D} = (s + 3)^2 = s^2 + 6s + 9 \quad (5.15)$$

Putting Equation (5.15) in Equation (5.14) we get

$$G_{pend\_angle\_open}(s) = D \frac{(s+3)^2 \times (10.68s^2 - 6.981s + 5.239)}{s^5 - 2.693s^4 - 40.52s^3 + 245.8s^2 + 592.9s - 0.5239} \quad (5.16)$$

And from (5.15) we get

$$\frac{P}{D} = 6 \quad (5.17)$$

$$\frac{I}{D} = 9 \quad (5.18)$$

Hence, there is only one design parameter left for the open loop controller and the identified system total transfer function  $G_{pend\_angle\_open}(s)$ . That parameter is  $D$  parameter governs and sustains the stability of the transfer function  $G_{pend\_angle\_open}(s)$ . Hence, it is better to check the root locus of the  $G_{pend\_angle\_open}(s)$  to specify its value. In Figure 5.11, we observe the root locus of  $G_{pend\_angle\_open}(s)$  given in Equation (5.16) as  $D$  is the free gain parameter for this transfer function.

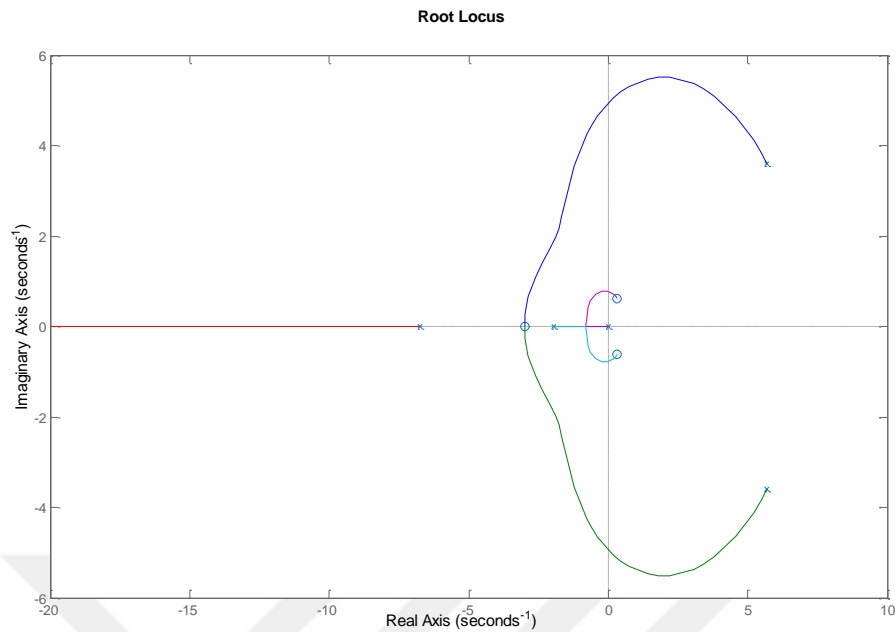


**Figure 5.11:** The root locus plot of  $G_{pend\_angle\_open}(s)$

In Table 5.3 the open loop pole and zero locations of  $G_{pend\_angle\_open}(s)$  are given

**Table 5.3:** Poles and zeros of  $G_{pend\_angle\_open}(s)$

Transfer Function	Poles	Zeros
$G_{pend\_angle\_open}(s)$	$5.6923+3.6016j$	$0.3268+0.6195j$
	$5.6923-3.6016j$	$0.3268-0.6195j$
	$-6.7606$	$-3$
	$-1.9320$	$-3$
	$0.0009$	

Deeply investigating the root locus plot of  $G_{pend\_angle\_open}(s)$ , the pendulum angle is stabilized nearly when  $1.46 \leq D \leq 8.8$ . When  $D \approx 1.46$  the two unstable poles (located at  $5.6923+3.6016j$  and  $5.6923-3.6016j$  initially) crosses the imaginary axis from right to left and thus their real parts become negative and stabilizes the system. Similarly, When  $D \approx 8.8$  the two poles (located at  $-1.9320$  and  $0.0009$  initially) after collusion with each other passes the imaginary axis from left to right and thus their real parts become positive causing instability. Hence, in our design  $D$  value should be between these two bound values. One of the best ways to specify  $D$  is choosing it as the gain value where the poles located at  $-1.9320$  and  $0.0009$  initially collide. These two poles

collide at -0.784 (two overlapping poles at the same location) when the gain value is 3.49. Hence, one of the best alternatives for the choice of  $D$  is 3.49.

If  $D=3.49$  in this case, the closed loop pole locations will be determined by solving the equation

$$G_{pend\_angle\_open}(s) + 1 = 1 + 3.49 \frac{(s+3)^2 \times (10.68s^2 - 6.981s + 5.239)}{s^5 - 2.693s^4 - 40.52s^3 + 245.8s^2 + 592.9s - 0.5239} = 0 \quad (5.19)$$

Which gives the pole locations -29.7373, -1.6383+2.5036j, -1.6383-2.5036j, -0.7838+0.0441j, -0.7838-0.0441j. As seen all the closed loop poles have negative real parts and the closed loop transfer function is stable.

Choosing  $D=3.49$  and using Equation (5.17) and (5.18) we obtain  $P=20.94$  and  $I=31.41$ . Thus design of the controller for stabilizing the pendulum angle is completed where the controller has the following mathematical structure

$$C_{pend\_angle}(s) = 20.94 + \frac{31.41}{s} + 3.19s \quad (5.20)$$

### 5.3.2. Controller Design for Cart Position Control

The transfer function for  $G_{cart\_position}(s)$  has 1 unstable pole (location is 1.3974) and a zero at the origin). The main characteristics of the root locus of  $G_{cart\_position}(s)$  are that it resembles a complementary root locus plot (root locus where the gain is negative). Hence, it is better to check the root locus plot of  $-1 \times G_{cart\_position}(s)$  (complementary root locus of  $G_{cart\_position}(s)$ ) and perform the PID controller design due to this new plot. The complementary root locus root of  $G_{cart\_position}(s)$  is given in Figure 5.12.

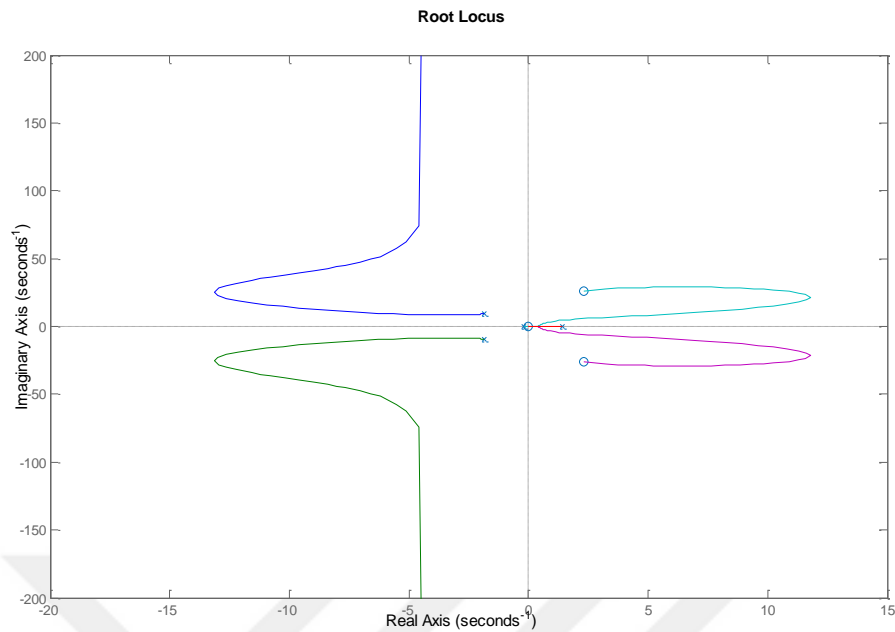


**Figure 5.12:** The complementary root locus root of  $G_{\text{cart\_position}}(s)$  (root locus of  $-G_{\text{cart\_position}}(s)$ ).

The complementary root locus of  $-G_{\text{cart\_position}}(s)$ , illustrates the difficulty of controller design for controlling the cart position. The difficulties can be summarized as follows: primarily, the transfer function  $-G_{\text{cart\_position}}(s)$  has 5 poles and 3 zeros. The complex conjugate poles located at  $-0.2148+0.0478j$  and  $-0.2148-0.0478j$  are very close to the origin and by application of a very small gain value (nearly 0.9), these poles cross the imaginary axis from left to right and hence they become unstable poles in addition to the unstable pole located at 1.3974 initially. Secondly, the pole located at 1.3974 always remains in the open right half plane for any positive gain value. This pole reaches to the zero of the  $-G_{\text{cart\_position}}(s)$  located at the origin when gain value reaches to infinity. These two situations make the controller design extremely difficult. However, by suitable selection of PID controller parameters these difficulties can partially or totally be removed.

As we have done previously for the design of the PID controller in order to stabilize the pendulum angle, the design procedure for the cart position control focuses on eliminating the effect of the unstable pole (located at 1.3974) and not letting any stable pole to become unstable. For other secondary objectives like zero steady state

error one can insert extra serial controllers chained with this primary PID controller structure after the controller is designed. The structure of PID controller is

$$C_{cart\_position}(s) = P + \frac{I}{s} + Ds \quad (5.21)$$

The PID controller in Equation (5.21) can also be written in the form:

$$C_{cart\_position}(s) = D \times \left( \frac{s^2 + \frac{P}{D}s + \frac{I}{D}}{s} \right) \quad (5.22)$$

$C_{cart\_position}(s)$  has a single pole at the origin and two zeros. The pole of  $C_{cart\_position}(s)$  located at the origin cancel the zero of  $-G_{cart\_position}(s)$  at the origin when these two transfer functions are multiplied to yield

$$G_{cart\_position\_open}(s) = D \times \left( \frac{s^2 + \frac{P}{D}s + \frac{I}{D}}{s} \right) \left( \frac{-1 \times (-0.08784s^3 + 0.4083s^2 - 60.43s)}{s^5 + 2.694s^4 - 85.24s^3 - 88.566s^2 - 49.54s - 6.043} \right) \quad (5.23)$$

After pole-zero cancellation at the origin the transfer function in Equation (5.23) can be written as

$$G_{cart\_position\_open}(s) = D \times \left( s^2 + \frac{P}{D}s + \frac{I}{D} \right) \left( \frac{(0.08784s^2 - 0.4083s + 60.43)}{s^5 + 2.694s^4 - 85.24s^3 - 88.566s^2 - 49.54s - 6.043} \right) \quad (5.24)$$

Now open loop controller and identified system transfer function in total is given by Equation (5.24). This transfer function has 5 poles and 4 zeros where two of the zeros are undetermined

Choosing the undetermined zero locations properly gives the opportunity to relocate the unstable pole (located at 1.3974 initially) and two complex conjugate pole pairs (located at -0.2148+0.0478j and -0.2148-0.0478j) to locations, which more negative real parts. For this reason, the zero locations should be chosen such that they have more negative real parts compared to complex conjugate pole pairs (located at -0.2148+0.0478j and -0.2148-0.0478j initially). Hence, we have chosen the zero locations as -2 and -2. In this case, we can write

$$s^2 + \frac{P}{D}s + \frac{I}{D} = (s + 2)^2 = s^2 + 4s + 4 \quad (5.25)$$



From Equation (5.25) we can get:

$$\frac{P}{D} = 4 \quad (5.26)$$

$$\frac{I}{D} = 4 \quad (5.27)$$

Using Equation (5.25) the open loop controller and identified system transfer function can be written as

$$G_{cart\_position\_open}(s) = D \left( \frac{(s+2)^2 \times (0.08784s^2 - 0.4083s + 60.43)}{s^5 + 2.694s^4 - 85.24s^3 - 88.566s^2 - 49.54s - 6.043} \right) \quad (5.28)$$

Hence, there is only one design parameter left for the open loop controller and the identified system total transfer function  $G_{cart\_position\_open}(s)$ . To specify the value of  $D$ , it is better to check the root locus of the  $G_{cart\_position\_open}(s)$ . In Figure 5.13, we observe the root locus of  $G_{cart\_position\_open}(s)$ .

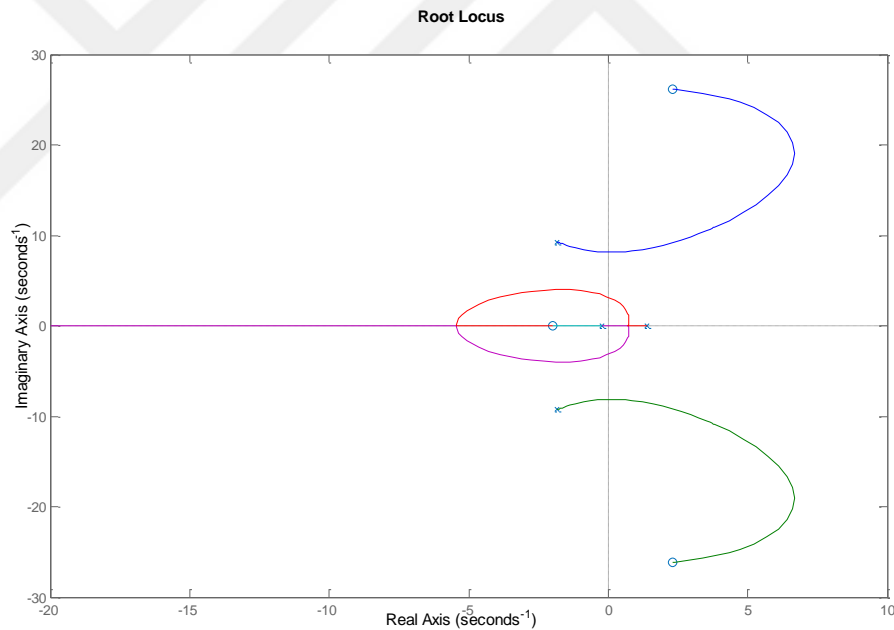


**Figure 5.13:** The root locus of  $G_{cart\_position\_open}(s)$ .

In Table 5.4, the open loop pole and zero locations of  $G_{cart\_position\_open}(s)$  are given.

**Table 5.4:** Poles and zeros of  $G_{\text{cart\_position\_open}}(s)$ 

Transfer Function	Poles	Zeros
$G_{\text{cart\_position\_open}}(s)$	-1.8309+9.2727j -1.8309-9.2727j 1.3974 -0.2148+0.0478j -0.2148-0.0478j	2.3242+26.1247j 2.3242-26.1247j -2 -2

The root locus plot gives the trajectory of roots. Luckily by deeper investigation, it is observed that all the closed loop poles of the system remain in open left half plane (left hand side of the imaginary axis) if the gain value (namely  $D$  value of the controller in Equation 5.22) is chosen nearly between 5.35 and 3.52. The behavior of the closed loop poles due to increasing gain value is as follows. Primarily, the complex conjugate poles located initially at  $-0.2148+0.0478j$  and  $-0.2148-0.0478j$  collide with each other (at break-in break-away point located nearly at  $-0.213$ ) when the gain value is nearly 0.00169. Then one of these poles began to go to one of the zeros located at  $-2$  (reaches there when the gain is increased to infinity) and the other pole began to move towards the unstable pole located initially at  $1.3974$ . The unstable pole and the pole moving towards the unstable pole hit each other at another break-in break-away point when the gain value is 0.123 at the location  $0.716$  (at this gain value both of these poles has unstable characteristics). Later on these two unstable poles began to make a reverse arc towards the imaginary axis and they cut the imaginary axis from right to left at the gain value 3.52 and the poles become stable. After this gain those two poles always produce stable modes. While these three poles are traversing such trajectories, the complex conjugate pole pairs initially located at  $-1.8309+9.2727j$  and  $-1.8309-9.2727j$  trace arc like trajectories and pass the imaginary axis from left to right at the gain value 5.35 and they began to exhibit unstable characteristics after this point. As the gain increases these two closed loop poles try to reach to the zeros located at  $2.3242+26.1247j$  and  $2.3242-26.1247j$ . Hence, the closed loop transfer function exhibits stable characteristics when the gain (namely  $D$  parameter) is between 3.52 and 5.35. It is better to take a value between these two limit values to finish the design of the controller. Hence, we selected  $D=4.5$ .

Using Equation (5.26) and (5.27) we obtain  $P=18$  and  $I=18$ . Thus, the design of the controller for stabilizing the cart position is completed where the controller has the following mathematical structure

$$C_{cart\_position}(s) = 18 + \frac{18}{s} + 4.5s \quad (5.29).$$

If  $D=4.5$  in this case, the closed loop pole locations will be determined by solving the equation

$$G_{cart\_position\_open}(s) + 1 = 1 + 4.5 \left( \frac{(s+2)^2 \times (0.08784s^2 - 0.4083s + 60.43)}{s^5 + 2.694s^4 - 85.24s^3 - 88.566s^2 - 49.54s - 6.043} \right) \quad (5.30)$$

Which gives the pole locations are  $-0.4569 + 8.2374j$ ,  $-0.4569 - 8.2374j$ ,  $-0.5099 + 3.6733j$ ,  $-0.5099 - 3.6733j$ ,  $-1.1555$ . As seen, all the closed loop poles have negative real parts and the closed loop transfer function is stable.

#### 5.4. Test and Comparison of the Controllers

As the design of the controllers (given in Equation 5.20 and 5.29) is completed, we can test them and compare their performance with the performance of the controllers given in Equation (5.1) and Equation (5.2). After the comparison, the designed controllers will also be examined for reference signal tracking and their resilience due to disturbance will be monitored with different real time applications.

##### 5.4.1. Comparison of Performances of Controllers for no Load Condition

For comparison, we have made a variation in the 'InvPendIdent' model [1]. With every other procedure remaining the same, we replaced the extra excitation signal  $r$  used in the identification step with zero signals (a constant value 0 is given as extra excitation signal  $r$ ). Hence, the controllers are only due to stabilize the system with no extra objective of system identification. With this modification, the block diagram of control strategy coupled with extra excitation signal for test and comparison purpose is implemented as the illustrated model in Figure5.14.

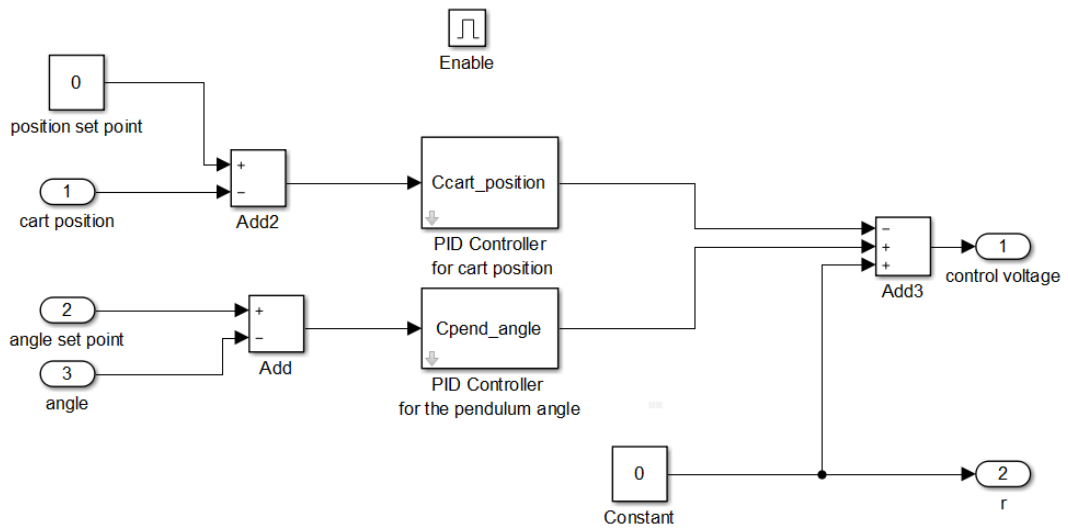


**Figure 5.14:** The block diagram of control strategy for no load condition

We have run this modified real time model primarily using the  $C_{cart\_position}(s)$  and  $C_{pend\_angle}(s)$  controllers given in Equation (5.1) and Equation (5.2). The pendulum angle, cart position and control signal outputs are plotted in Figure 5.15

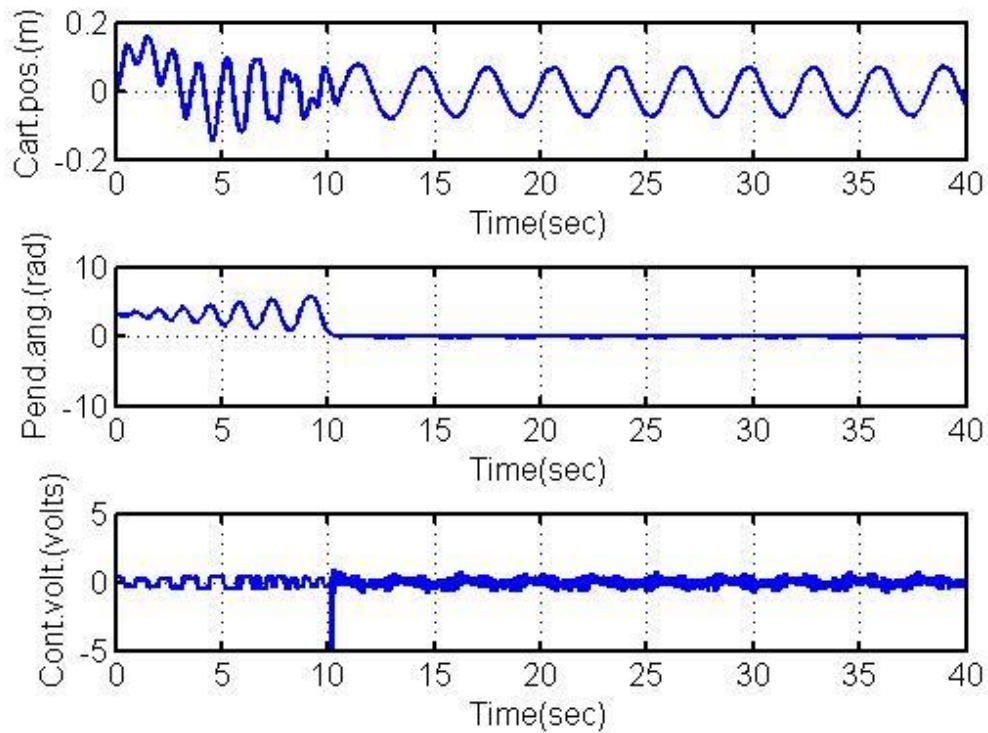


**Figure 5.15:** The cart position, pendulum angle and control signal plotted versus time with no extra excitation signals using controllers given in Equation (5.1) and Equation (5.2).

As we deeply investigate Figure 5.15, we can say that the system stabilized around the equilibrium point  $x_3 = 0$  radians nearly after the 10<sup>th</sup> second. However, there are some oscillations for the state variable  $x_1$ . These oscillations deviate approximately between 70 mm and -75 mm. Hence, there is some controlled oscillation for  $x_1$  (cart position) to better control the state  $x_3$  (pendulum angle). However, the fluctuations (oscillations) for  $x_3$  seem to be limited.  $x_3$  oscillated between 0.03 and -0.03 radians (nearly  $\pm 1.71$  degrees).

Now we want to see the performance of the controllers that are designed at Section 5.3. We have run this modified real time model primarily using the  $C_{\text{cart\_position}}(s)$  and  $C_{\text{pend\_angle}}(s)$  controllers given in Equation (5.29) and Equation (5.20). The pendulum angle, cart position and control signal outputs are plotted in Figure 5.16.

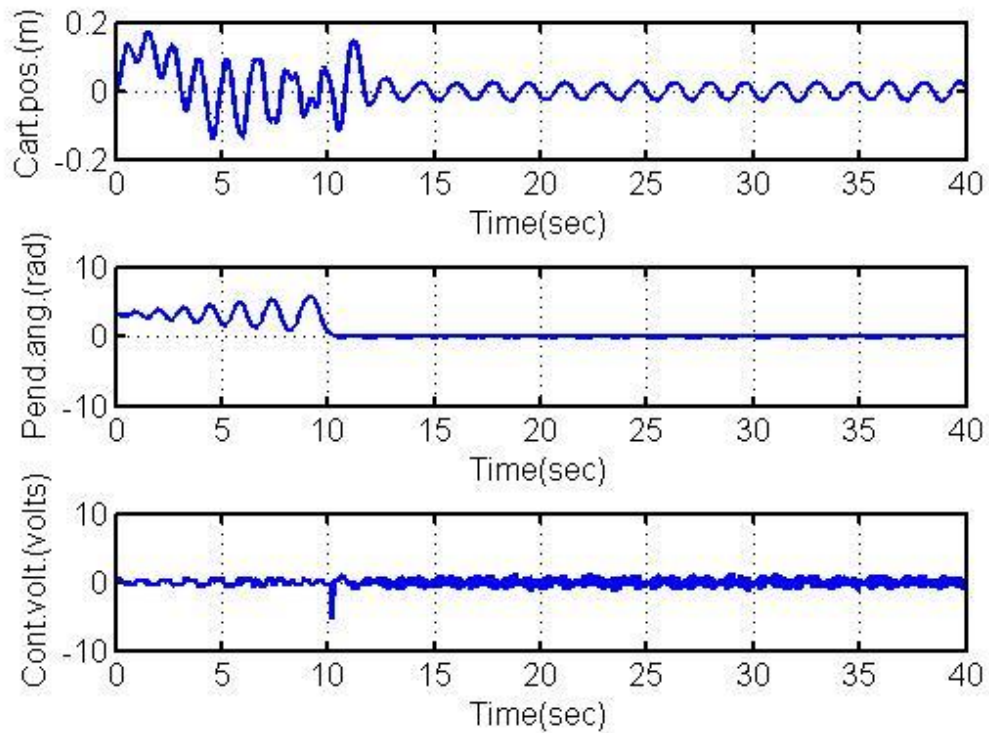


**Figure 5.16:** The cart position, pendulum angle and control signal plotted versus time. The plots are obtained employing the  $C_{cart\_position}(s)$  and  $C_{pend\_angle}(s)$  controllers given in Equation (5.29) and Equation (5.20).

As we deeply investigate Figure 5.16, we can say that the system stabilized around the equilibrium point  $x_3 = 0$  radians nearly after the 10<sup>th</sup> second. Still using the designed controllers, there are some oscillations for the state variable  $x_1$ . But these oscillations are not as high as the ones that we observe in Figure 5.15. The oscillations deviate approximately between 30 mm and -30 mm. The fluctuations (oscillations) for  $x_3$  seem to be also limited.  $x_3$  oscillates between 0.024 and -0.027 radians (nearly  $\pm 1.54$  degrees). Thus the designed controllers seem to work better compared to the controllers given in Equation (5.1) and Equation (5.2).

### 5.4.2 Reference Tracking Capability

The reference tracking capabilities of the controllers is an important identifier for concluding whether the controllers are working properly or not. For this reason, some real time reference tracking applications are devised. In the first application, we want to test the reference tracking for pulse changes. For this reason, the position set point block (which is initially set to zero) in Figure 5.14 is replaced by a pulse of 0.15, which is applied between the 20<sup>th</sup> and 30<sup>th</sup> second of the real time application. In order to limit the control voltage, a saturation block is also inserted before the control voltage that limits the voltage between 3 and -3 volts. The performance of the old controllers (given in Equation 5.1 and 5.2) and the new ones (given in Equation 5.29 and 5.20) are tested. The results for the old controllers are given in Figure 5.17 and Figure 5.18.

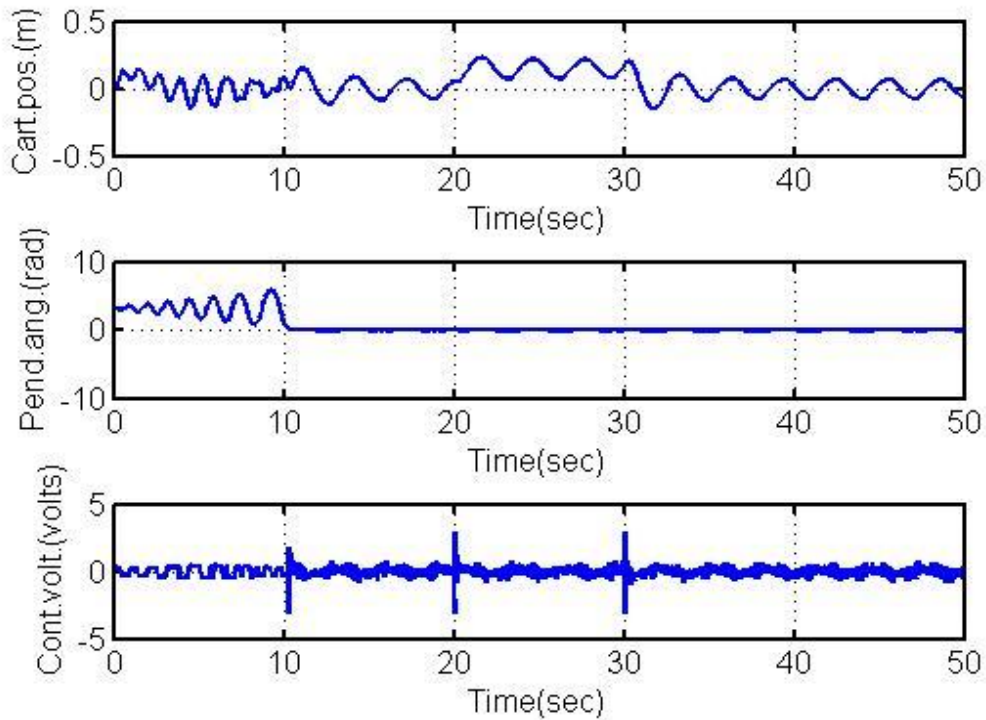


**Figure 5.17:** The cart position, pendulum angle and control signal plotted versus time in case of pulse type reference- tracking for cart position. The plots are obtained employing the  $C_{cart\_position}(s)$  and  $C_{pend\_angle}(s)$  controllers given in Equation (5.1) and Equation (5.2).

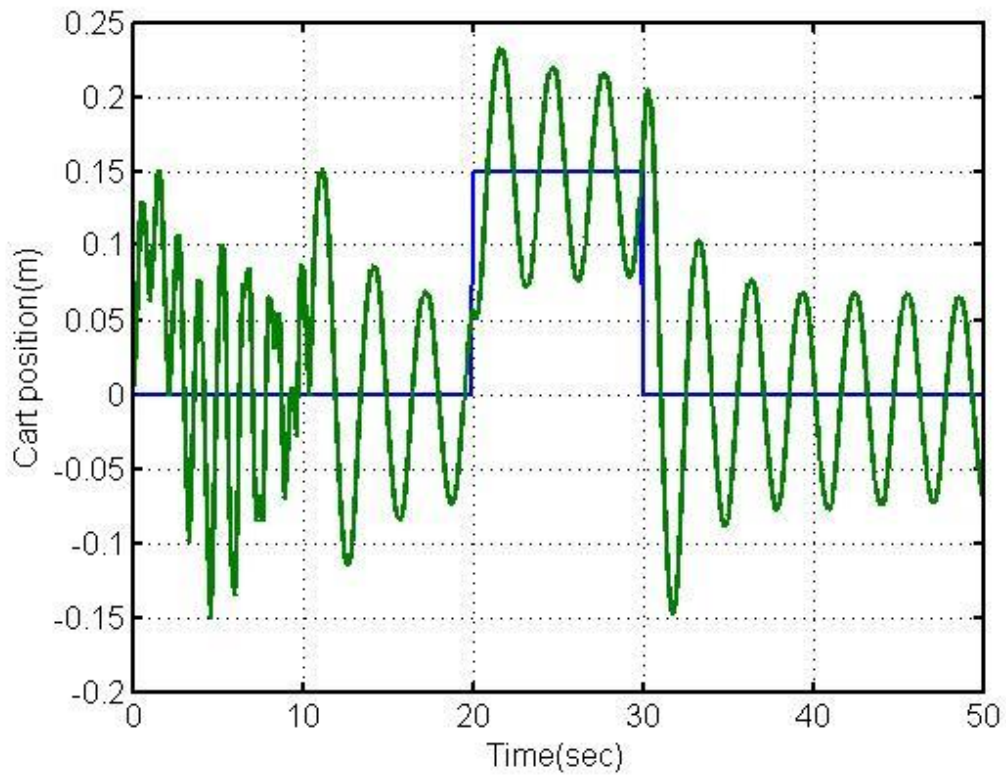


**Figure 5.18:** The cart position (green) plotted versus time in case of pulse type reference (blue) tracking for cart position. The plots are obtained employing the  $C_{cart\_position}(s)$  and  $C_{pend\_angle}(s)$  controllers given in Equation (5.1) and Equation (5.2).

The results for the new controllers are given Figure 5.19 and Figure 5.20.



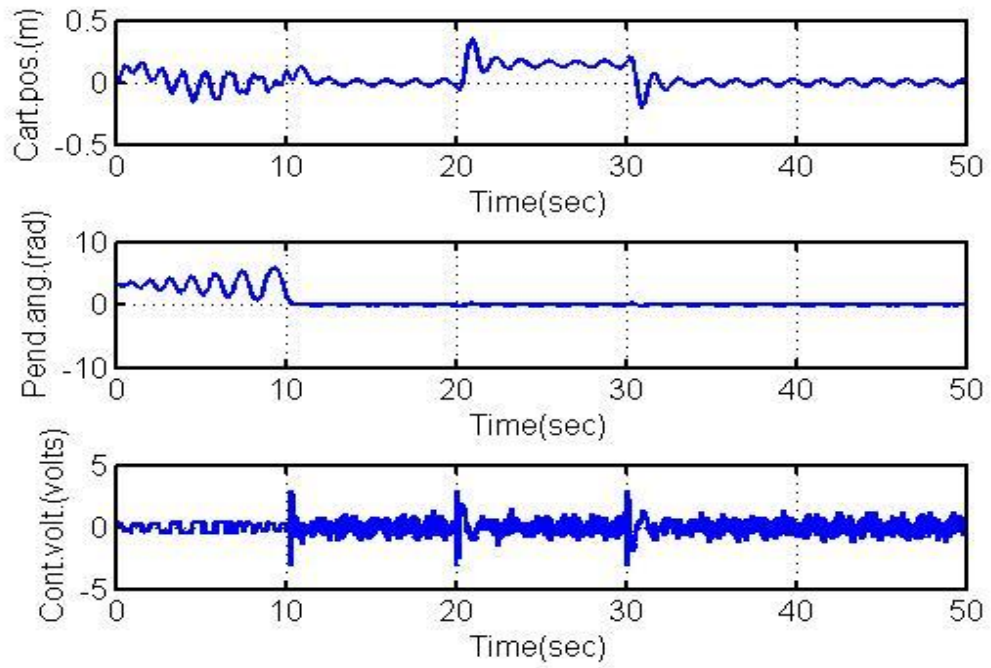


**Figure 5.19:** The cart position, pendulum angle and control signal plotted versus time in case of pulse type reference tracking for cart position. The plots are obtained employing the  $C_{cart\_position}(s)$  and  $C_{pend\_angle}(s)$  controllers given in Equation (5.29) and Equation (5.20).

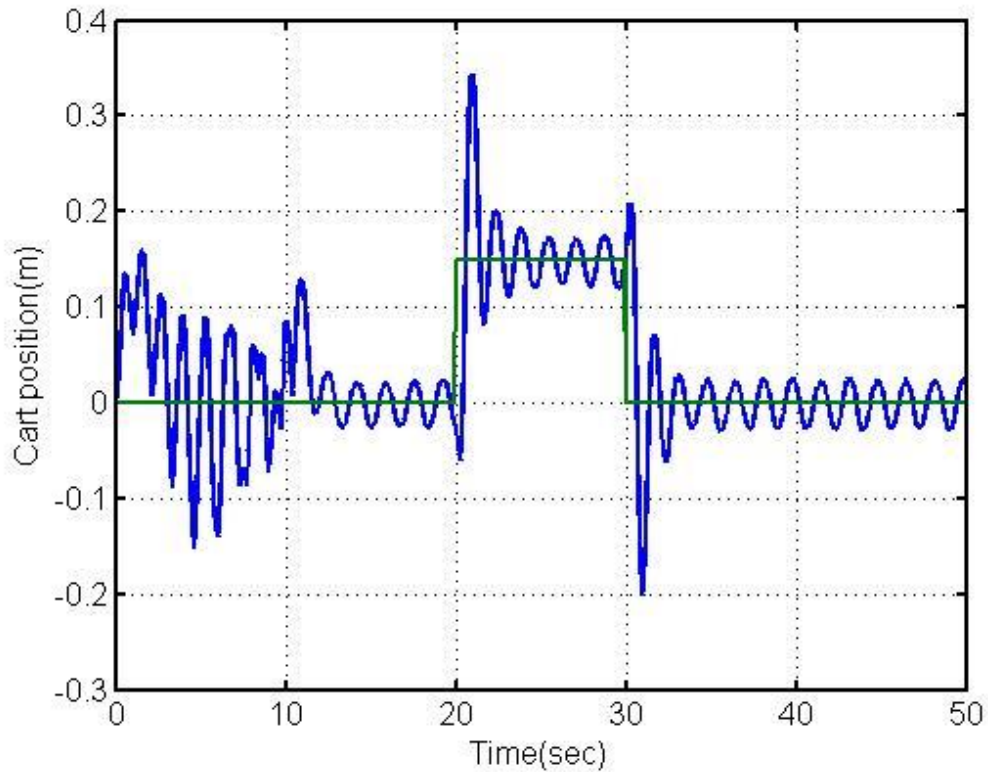


**Figure 5.20:** The cart position (blue) plotted versus time in case of pulse type reference (green) tracking for cart position. The plots are obtained employing the  $C_{cart\_position}(s)$  and  $C_{pend\_angle}(s)$  controllers given in Equation (5.29) and Equation (5.20).

From the Figures 5.17, 5.18, 5.19 and 5.20, one can conclude that for pulse type reference tracking where the reference value changes in a sudden, the new controllers are fast but in total they cause high overshoot (especially for cart position tracking) and the old controllers are slow however they cause less overshoot. On the other hand, the reaction speed of the new controllers is respectable and the settling time for both of the states  $x_1$  (cart position) and  $x_3$  (pendulum angle) is small by use of these new controllers. After the system is settled, the cart position and pendulum angle oscillates in similar levels as explained in section 5.4.1 when new controllers are employed. When old controllers are employed, the reaction of the system is very slow. It takes more time for the system to settle down besides still high oscillations are observed for the cart position even if the system settles down.

As a second reference tracking application, we applied a sinusoidal input as the position reference between the 20<sup>th</sup> and 40<sup>th</sup> seconds of the real time application. The sinusoidal signal has amplitude of 0.15 and frequency of 0.2 Hertz. The performance of the controllers is checked under these circumstances. The results for the old controllers are given in Figure 5.21 and Figure 5.22 and the results for the new controllers are given in Figure 5.23 and Figure 5.24.

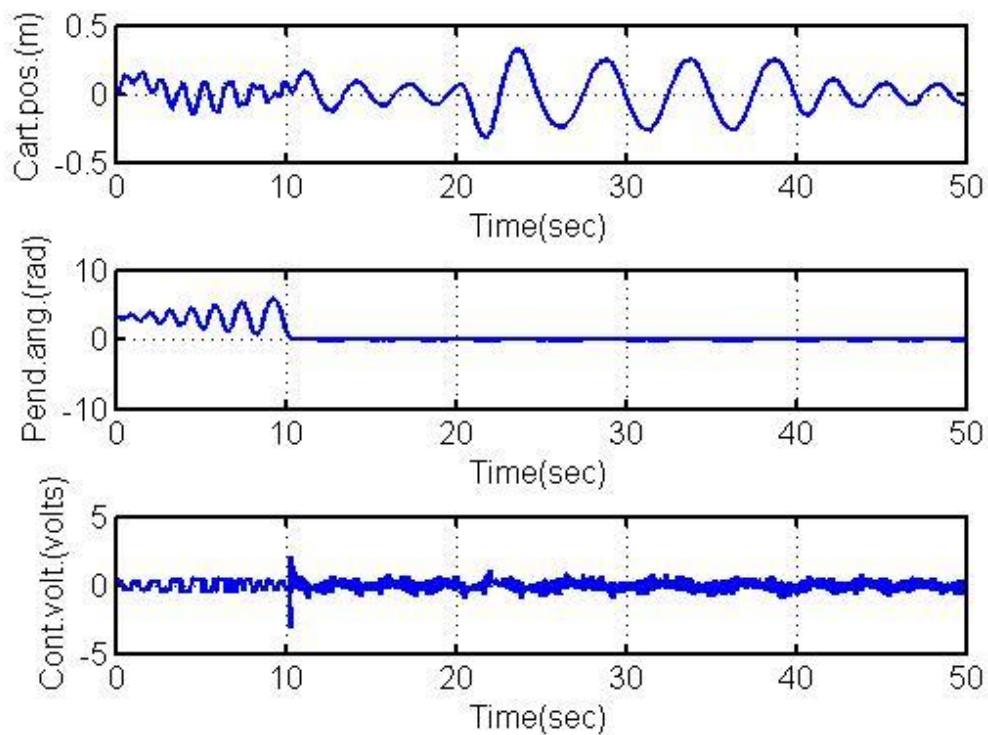


**Figure 5.21:** The cart position, pendulum angle and control signal plotted versus time in case of sinusoidal type reference tracking for cart position. The plots are obtained employing the  $C_{cart\_position}(s)$  and  $C_{pend\_angle}(s)$  controllers given in Equation (5.1) and Equation (5.2).

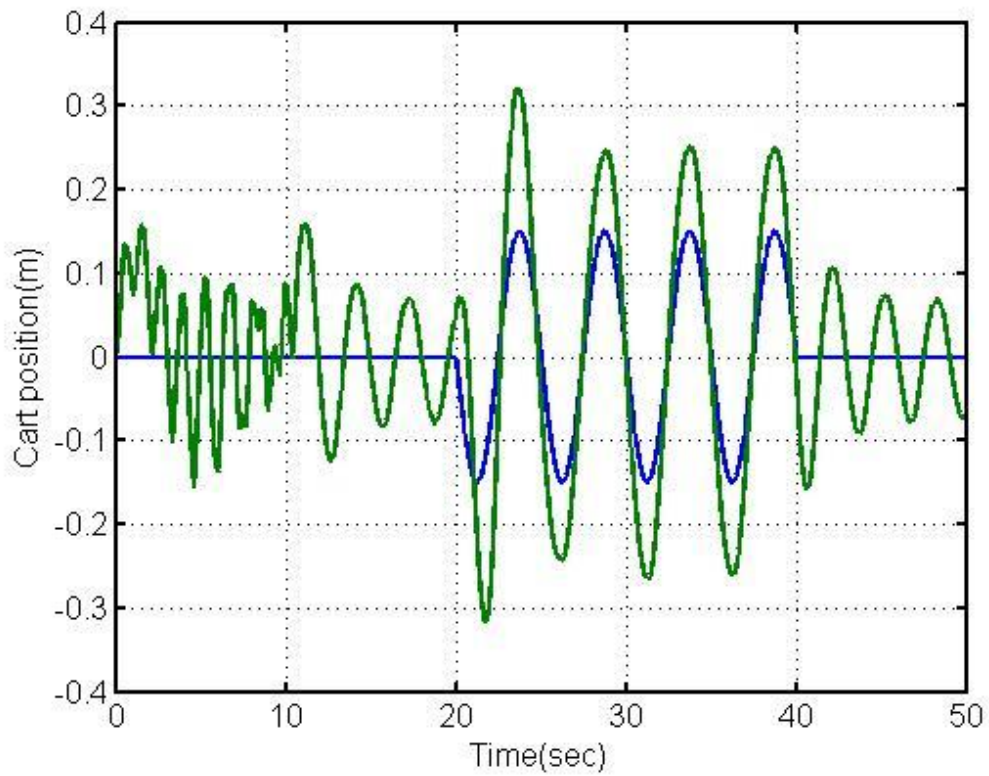


**Figure 5.22:** The cart position (green) plotted versus time in case of sinusoidal type reference (blue) tracking for cart position. The plots are obtained employing the  $C_{cart\_position}(s)$  and  $C_{pend\_angle}(s)$  controllers given in Equation (5.1) and Equation (5.2).

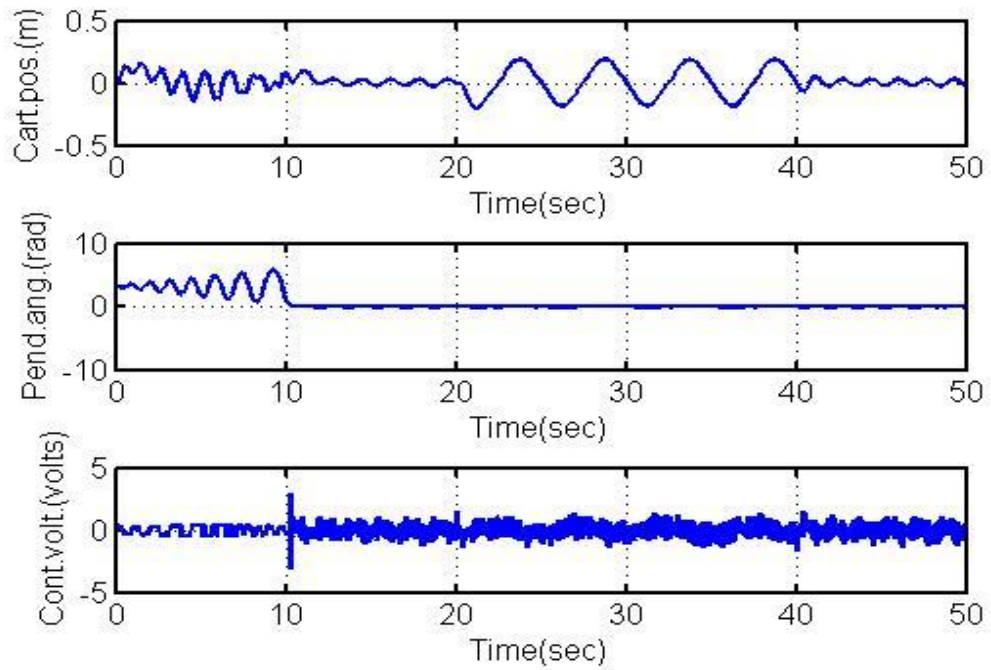


**Figure 5.23:** The cart position, pendulum angle and control signal plotted versus time in case of sinusoidal type reference tracking for cart position. The plots are obtained employing the  $C_{cart\_position}(s)$  and  $C_{pend\_angle}(s)$  controllers given in Equation (5.29) and Equation (5.20).

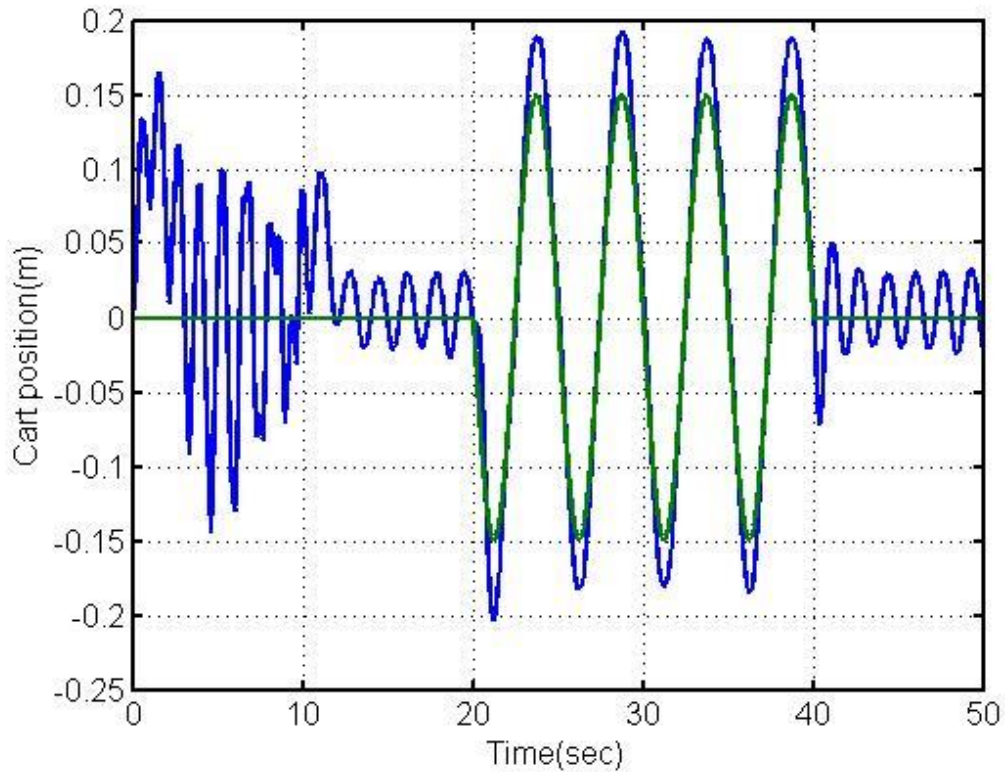


**Figure 5.24:** The cart position (blue) plotted versus time in case of sinusoidal type reference (green) tracking for cart position. The plots are obtained employing the  $C_{cart\_position}(s)$  and  $C_{pend\_angle}(s)$  controllers given in Equation (5.29) and Equation (5.20).

As seen from Figures 5.21, 5.22, 5.23 and 5.24 new controllers are much better than the old ones for sinusoidal reference tracking for cart position. We have also increased the amplitude of the reference signal from 0.15 to 0.25, even in these circumstances, the new controllers are able to track the reference signal however, the old controllers are not able to move the cart-pendulum system regularly and the cart reached the limits of the rail and hence it stopped and the tracking task failed. The results obtained employing the new controllers with this real time application are shown in Figure 5.25 and 5.26.

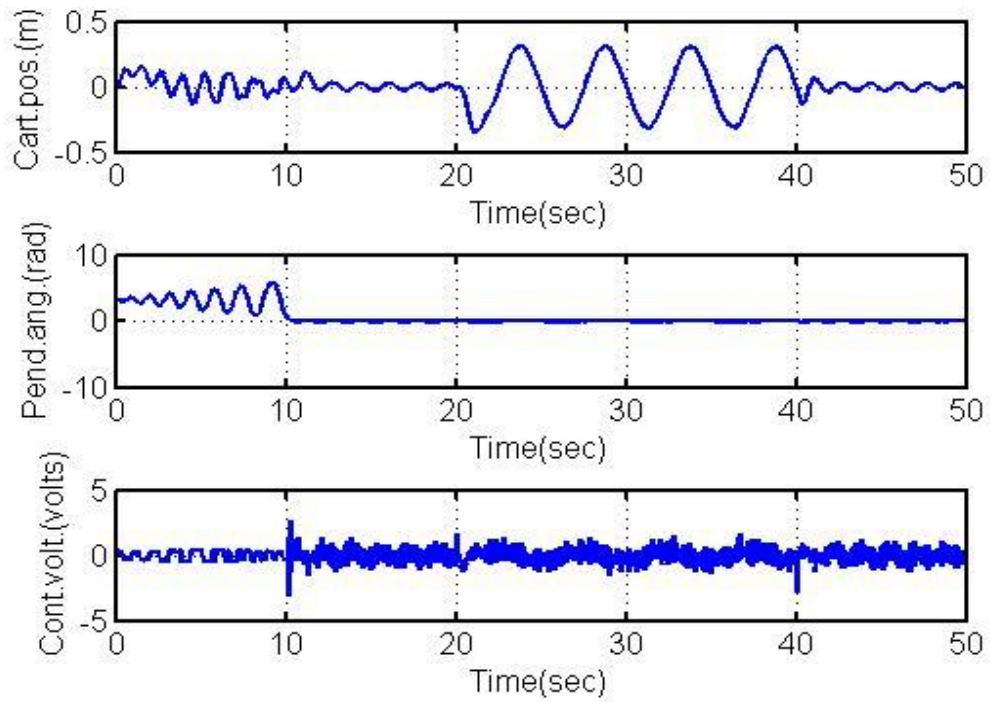


**Figure 5.25:** The cart position, pendulum angle and control signal plotted versus time in case of sinusoidal type reference tracking for cart position. The plots are obtained employing the  $C_{\text{cart\_position}}(s)$  and  $C_{\text{pend\_angle}}(s)$  controllers given in Equation (5.29) and Equation (5.20). Amplitude of the reference signal is 0.25.

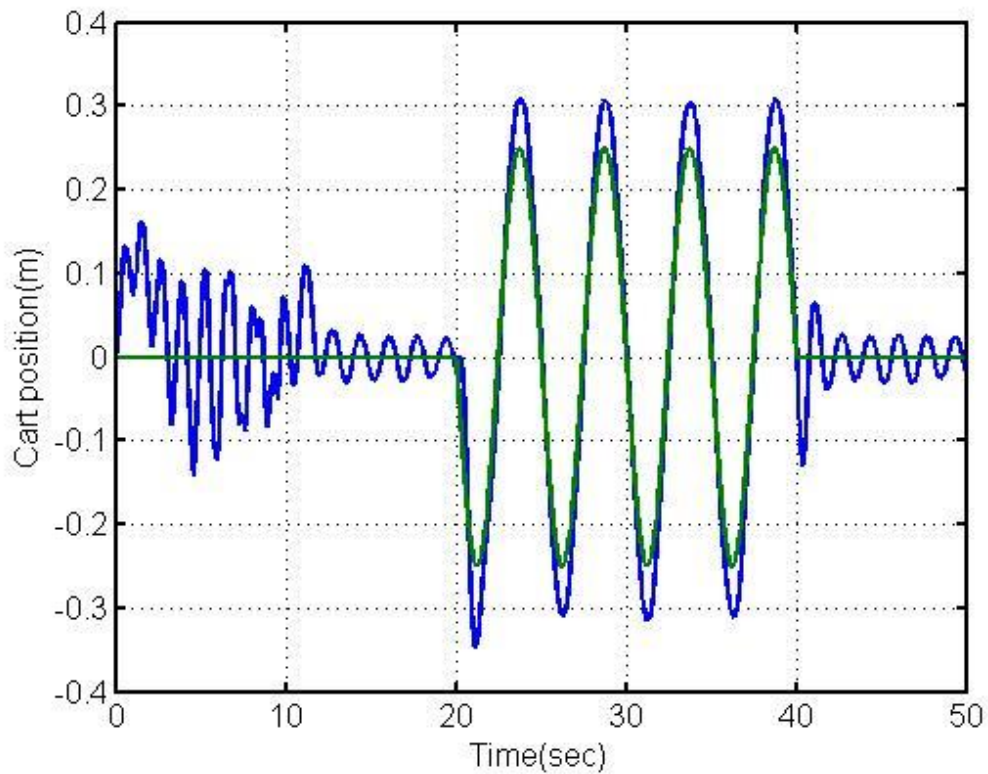


**Figure 5.26:** The cart position (blue) plotted versus time in case of sinusoidal type reference (green) tracking for cart position. The plot is obtained employing the  $C_{\text{cart\_position}}(s)$  and  $C_{\text{pend\_angle}}(s)$  controllers given in Equation (5.29) and Equation (5.20). Amplitude of the reference signal is 0.25.

Nearly all the cart position reference-tracking applications show that, the new controllers demonstrate better performance in terms of speed, steady state error and capacity to stabilize the unstable system around the unstable equilibrium point. There is only one drawback of the new controllers: when the reference signal changes very suddenly (a pulse like reference signal) and besides if the amplitude of this reference signal is high, the new controllers produces very high control signals because of the derivative content they encompass and this causes very sudden movements in the cart besides because of the integral content the system began to exhibit underdamped oscillations and overshoot is observed. Even in these circumstances, the system is



still stabilized however as the amplitude is increased more the system becomes unstable

### **5.4.3 Effect of Disturbances**

In this new real time application, we intend to see the effect of disturbance. The first disturbance is putting an extra mass to the cart when the system is stabilized around the equilibrium point. The second one is giving some force to the pole by a stick by pushing and pulling when the system is stabilized. And combination of both of these disturbances in system performance is also monitored as a third application. First, the real time application is run as in section 5.4.1 using old and new controllers when the position set point in Figure 5.14 is set to 0. At the 20<sup>th</sup> second (after the system is stabilized at the unstable equilibrium point) we put extra mass of 1246.35 gram to the system and the following cart position, pendulum angle and control voltage signals are observed in Figure 5.27 when new controller are used given in Equations (5.29) and Equations (5.20).

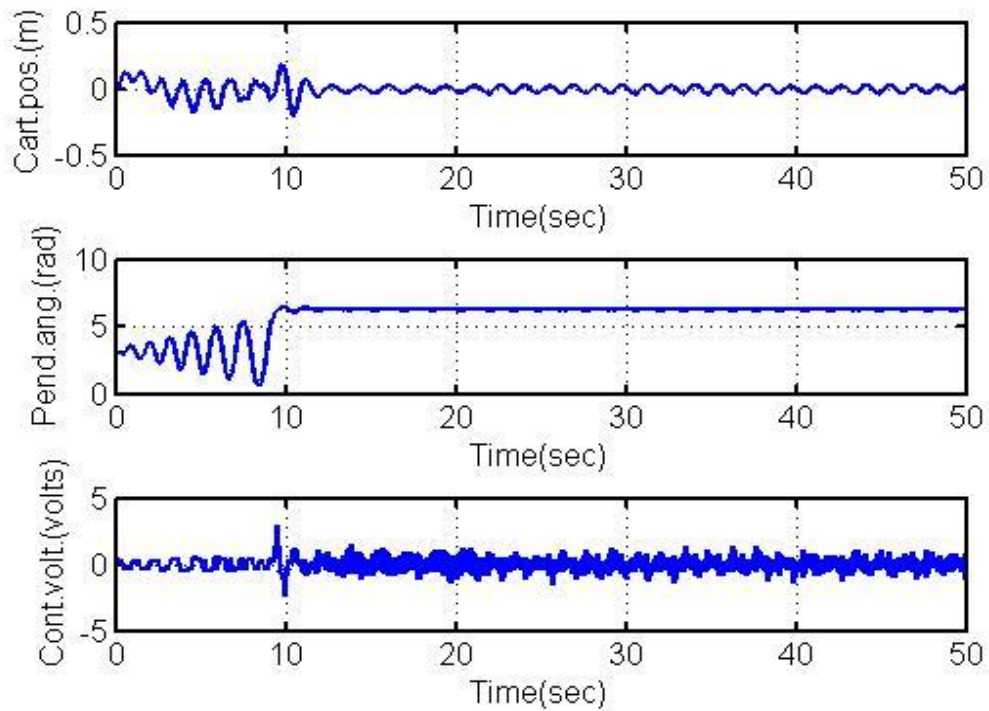


**Figure 5.27:** The cart position, pendulum angle and control signal plotted versus time in case of a mass disturbance of 1246.35 gram. The plots are obtained employing the  $C_{\text{cart\_position}}(s)$  and  $C_{\text{pend\_angle}}(s)$  controllers given in Equation (5.29) and Equation (5.20).

The same mass is also applied for the old controllers given in Equation (5.1) and Equation (5.2) and the following results in Figure 5.28 are obtained.

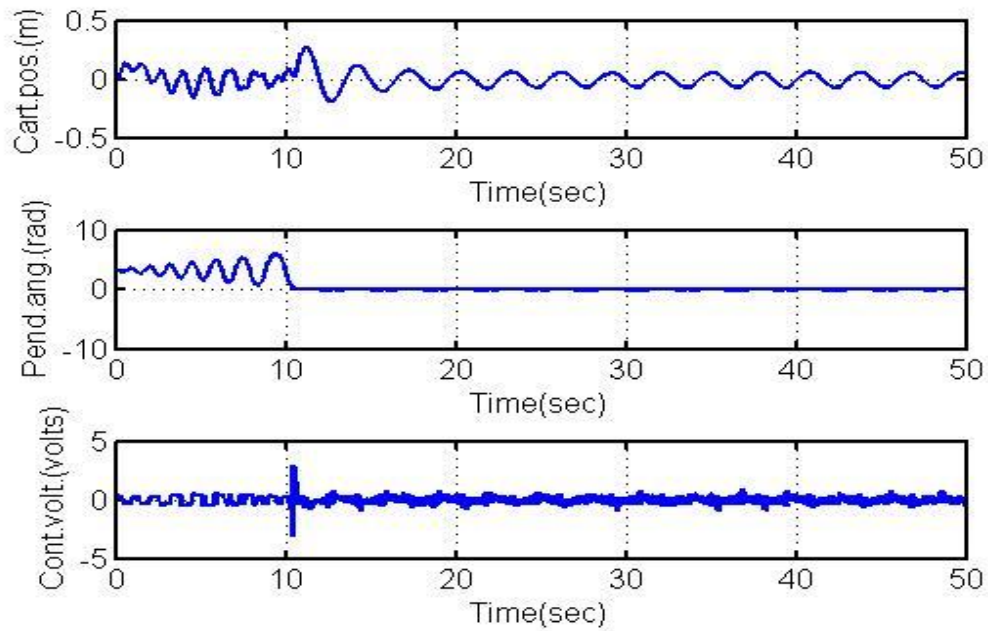


**Figure 5.28:** The cart position, pendulum angle and control signal plotted versus time in case of a mass of 1246.35 gram. The plots are obtained employing the  $C_{\text{cart\_position}}(s)$  and  $C_{\text{pend\_angle}}(s)$  controllers given in Equation (5.1) and Equation (5.2).

We haven't observed much difference between the performances of old and new controllers when we put the extra mass of 1246.35 gram over the cart as a disturbance. However, the cart began to have oscillations with slightly higher frequencies around the cart position set point ( $x_I=0$ ) if the new controllers are employed. Such a disorder is not significantly observed for the old controllers. Hence, the system controlled by new controllers might go to instability earlier compared to the case with old controller in case of application of higher masses. To see this effect, we also applied higher masses to compare the durability of the old and new controllers. When we put a total extra mass of 2140.98 gram to the system, we observed that the old controllers performance is nearly similar compared to the situation when smaller mass of 1246.35 gram is applied. However, as we put the same mass to the system controlled by the new controllers we observed that the system began to oscillate with higher frequency and amplitude around the cart position set point and become unstable at the end. Hence, durability of the system controlled by the old controllers is higher compared to system controlled by the new controllers in case of application of a mass type of disturbance. However, both

systems can resist until masses of nearly 1250 gram and not much performance change is observed.

The second application is applying a force to the pole in order to destabilize it by a stick. We pushed and pulled the pole connected to the pendulum with this stick. In both circumstances, the cart-pendulum system is able to stabilize the system again, hence the performance of the two set of controllers (old controllers and new controllers) is not very different. Besides as, the disturbances are not directly measurable for this application, a one to one comparison cannot be performed soundly.

As a last application, we put the mass and we changed the reference point. First, we used a pulse like reference point change in the cart position of 0.05 units between the 30<sup>th</sup> and 40<sup>th</sup> seconds of the real time application besides we put 894.63 gram of mass nearly at the 20<sup>th</sup> second over the cart. Primarily, the old controllers are employed. The result about the cart position are shown in Figure 5.29.

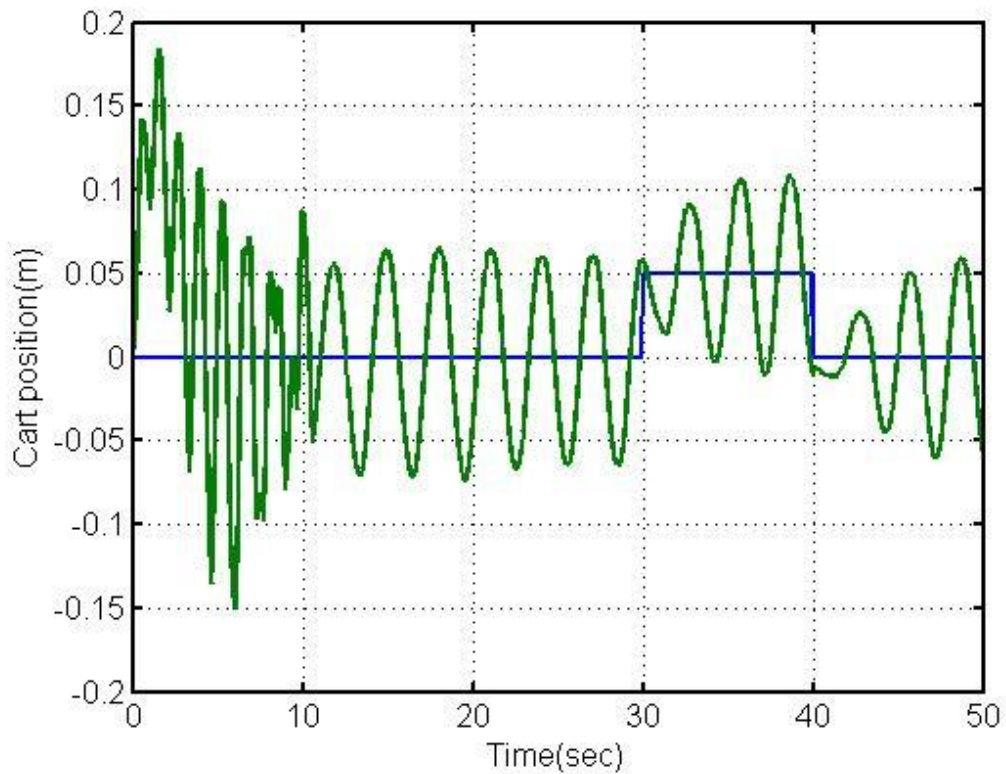


**Figure 5.29:** The cart position (green) plotted versus time in case of a mass of 894.63 gram and reference (blue) pulse change of 0.05 units for the cart position. The plots are obtained employing the  $C_{\text{cart\_position}}(s)$  and  $C_{\text{pend\_angle}}(s)$  controllers given in Equation (5.1) and Equation (5.2).

The results when the new controllers are used for the same application are shown in Figure 5.30.

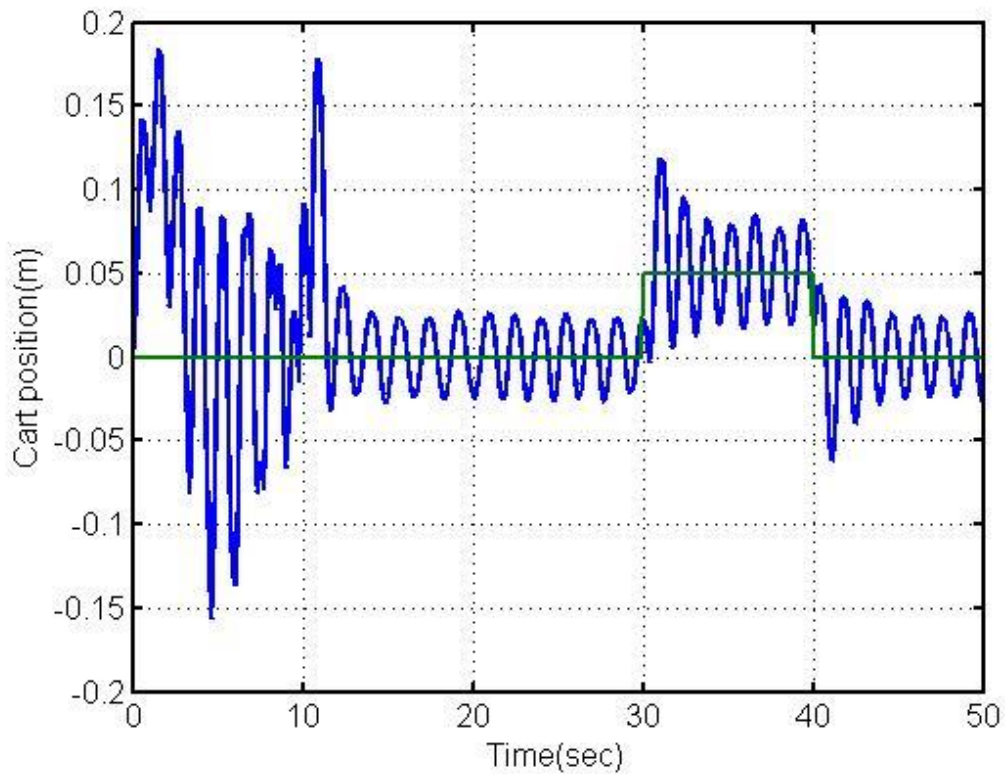


**Figure 5.30:** The cart position (blue) plotted versus time in case of a mass of 894.63 gram and reference (green) pulse change of 0.05 units for the cart position. The plots are obtained employing the  $C_{\text{cart\_position}}(s)$  and  $C_{\text{pend\_angle}}(s)$  controllers given in Equation (5.29) and Equation (5.20).

If we apply a pulse type reference change coupled with a mass type of disturbance, the new controllers track the reference signal more rapidly and settles down around the cart position set point a few level faster compared to the old controllers. However, increasing the amplitude of the pulse or increasing the mass further degenerate the system response more rapidly when new controllers are on duty. Thus although new controllers exhibit better steady state error values and settles around the cart position set point more rapidly, they are not as robust as the old controllers.

## CHAPTER 6

### CONCLUSION

In this thesis, the main aim is to design of PID controllers for a high dimensional non-linear system that is guided around an unstable equilibrium point. To complete the design, some complex procedures are carried out in an order one by one. Primarily, the system state is brought from an initial stable equilibrium point (state) close to an unstable equilibrium point by a previously defined swing up operation. Then a system identification operation is carried by means of previously defined controllers around the unstable equilibrium point. Finally, using the outputs of system identification step, new PID controllers are designed through using root locus method. By these procedures, the closed loop system with the designed controllers attains some specific characteristics pertaining to stability. Besides, improvements are also observed for various performance criteria. Speed of the system response is increased and steady state error is decreased. Besides, for some control application such as reference signal tracking (for cart position), the designed controllers are more successful than the preciously defined controllers in terms of speed and steady state error both for sinusoidal and pulse like reference inputs.

Despite the success of the designed controllers in many operations, it is also observed that they have some drawbacks. Primarily, reference signal tracking of suddenly applied signals such as pulses are a bit problematic. If the magnitude of the pulse like reference signal (for cart position) is so high no tangible problem is observed. However, if the magnitude is further increased, the designed controllers produce higher overshoots in the cart position and unfortunately after some extent, the overshoot increases radically and the closed loop system turns out to be unstable. The old controllers are more robust for such reference signal alterations although they began to trace longer trajectories. Another drawback is observed when extra

mass is exerted to the cart as a disturbance. Until some extent (nearly 1250 gram of extra mass), both old controllers and new controllers operate similarly: the performances are nearly same as the performances they have for unloaded cases. However, if the mass is further increased (nearly 2140 gram of extra mass), it is observed that the durability of the old controllers for such a disturbance is higher than the new designed controllers. The old controllers keep operating properly however, the new controllers began to produce increasing oscillations in the cart position and the system become unstable at the end.

Hence, as a future work, it is intended to deal with the drawbacks of the designed controllers. For this reason, the primary future work will be increasing the robustness of the designed controllers by parameter adjustment and optimization. Secondly, the developed controller structures will be used in order to design newer ones having unconventional structures such as neural networks and these controllers will be implemented in real time applications.



## REFERENCES

1. (2013) “33-936S Digital Pendulum Control Experiments Manual”, Feedback Instruments Ltd., United Kingdom.
2. **Betayeb M., Boussalem C., Mansouri R., Al-Saggaf U. M., (2014)**, “*Stabilization of an inverted pendulum-cart system by fractional PI-state feedback*”, ISA Transactions, vol. 4, pp.508-516.
3. **Udhayakumar K., Lakshmi P., (2007)**, “*Design of robust energy control for cart-inverted pendulum*”, International Journal of Engineering and Technology, vol. 53, pp.66-76.
4. **Nabanita Adhikary n, Chitralkha Mahanta (2013)** “ Integral backstepping sliding mode control for underactuated systems: Swing-up and stabilization of the Cart–Pendulum System”, ISA Transactions 52 870–880
5. **Tatsuya Kai, Kensuke Bito, (2014)** “A new discrete mechanics approach to swing-up control of the cart-pendulum system”, Commun Nonlinear Sci Numer Simulat 19 230–244.
6. **Sarit K. Das, Kaustav K. Paul, (2011)** “Robust compensation of a Cart–Inverted Pendulum system using a periodic controller” Experimental results, Automatica 47 2543–2547

7. **Ranjan Mukherjee.J.L, Khalil.H K, (2015)** “Output feedback stabilization of inverted pendulum on a cart in the presence of uncertainties”, *Automatica* 54 146–157.
8. **Gandhi.P.S, Pablo Borja, Romeo Ortega,** “ Energy shaping control of an inverted flexible pendulum fixed to a cart”, *Control Engineering Practice* 56 (2016) 27–36.
9. **Issa Amadou Tall, (2014)** “Linearization of control systems”A Lie series approach, *Automatica* 50 3310–3315
10. **Xiaoming Hu.D.C, Shen.T (2010)** “Analysis and Design of Nonlinear Control Systems”, Springer, Germany.
11. Congxu **Zhuş (2009)** “**Feedback** control methods for stabilizing unstable equilibrium points in a new chaotic system”, *Nonlinear Analysis* 71 2441–2446.
12. **Jia-Jun Wang, (2011)** “Simulation studies of inverted pendulum based on PID controllers, *Simulation Modelling Practice and Theory*” 19 440–449.
13. **Chang.W.D, Shih.S.P, (2010)** “PID controller design of nonlinear systems using an improved particle swarm optimization approach, *Commun Nonlinear Sci Numer Simulat* 15 3632–3639.
14. **Lua.H.C, Changa.M.H, Tsai.C.H, (2011)** “Adaptive self-constructing fuzzy neural network controller for hardware implementation of an inverted pendulum system”, *Applied Soft Computing* 11 3962–3975.
15. **El-Nagar.A.M, El-Bardini.M, EL-Rabaie.N.M, (2014)** “Intelligent control for nonlinear inverted pendulum based on interval type-2 fuzzy PD controller”, *Alexandria Engineering Journal* 53, 23–32.
16. **RAFİD İBRAHİM,(2015),** “*Desiging efficiant three phase brushless DC motor control systems*”*Gankay Univer.*

17. **Dorf R. C., Bishop R. H., (2005)**, *“Modern Control Systems”*, Pearson Prentice Hall, United States.
  
18. **Ogata K., (2010)**, *“Modern Control Engineering”*, Prentice Hall, United States.
  
19. **Sussmann H. J., (1972)**, “Controllability of Nonlinear Systems” *Journal of Differential Equations* 12, 95-116 (1972)
  
20. **Krastanov M.I., (1998)** “A Necessary Condition For Small Time Local Controllability, *Journal Of Dynamical And Control Systems”*, Vol. 4, No. 3, 425-458.

## Appendices 1

### Set Point Selection

```
function angle_set_point = fcn(angle)
if angle>=pi,
    angle_set_point=2*pi;
else
    angle_set_point=0;
end
```

## Appendices 2

### Applied force direction function

```
function force_direction = fcn(angular_velocity,zone_signal)
if angular_velocity>=0,
%the pendulum is returning in counterclockwise direction
    if zone_signal==1,
        force_direction=-1;
%the pendulum is at the upper region so applied_force should
%be in -x direction
    else
        force_direction=1;
%the pendulum is at the lower region so applied_force should
%be in x direction
    end
else %the pendulum is returning in clockwise direction
    if zone_signal==1,
        force_direction=1;
%the pendulum is at the upper region so
%applied_force should be in x direction
    else
        force_direction=-1;
%the pendulum is at the lower region so applied_force should
%be in -x direction
    end
end
```

## Appendices 3

### Lower zone-upper zone function

```
function zone_signal = fcn(angle)
if angle<=pi/2 | angle>=3*pi/2,
    zone_signal=1; %upper zone
else
    zone_signal=0; %lower zone
end
```

## Appendices 4

### Upright position detection function

```
function s_z_r = fcn(angle,angle_compare_val)
s_z_r=or((abs(angle-
2*pi)<=angle_compare_val),angle<=angle_compare_val);
%s_z_r is the stabilization zone region
```

## APPENDICES A

### CURRICULUM VITAE

#### PERSONAL INFORMATION

**Surname, Name:** Fidan SEDEEQ

**Date and Place of Birth:** 1st January 1983, Kirkuk/Iraq

**Marital Status:** Married

**Phone:** +905059715583

**Email:** [fidann2014@yahoo.com](mailto:fidann2014@yahoo.com)



#### EDUCATION

Degree	Institution	Year of Graduation
M.Sc.	Çankaya Univ., Electronic and Communication Engineering	2016
B.Sc.	Technology/Kirkuk. Electronic and Control Engineering Techniques	2004
High School	Kirkuk. High School. For girls	2000